Original

The Tectonic Evolution of Asia

Edited by

AN YIN T. MARK HARRISON

University of California, Los Angeles

CAMBRIDGE UNIVERSITY PRESS

20 A Phanerozoic palinspastic reconstruction of China and its neighboring regions

AN YIN AND SHANGYOU NIE

Abstract

A tectonic model is proposed for the Phanerozoic evolution of eastern Asia. The palinspastic implications of this model are shown in a series of maps indicating probable structural and sedimentologic relationships of various tectonic elements. The main features of this model are as follows: (1) The collision between the North Tarim–North China block and the Qaidam–South Tarim block occurred during the Devonian, following the early Paleozoic subduction of the Qaidam–South Tarim plate underneath the North Tarim–North China block. (2) The Permo–Triassic collision between the North Tarim–North China block and the South China block caused westward extrusion of the South Tarim–Qaidam block, which was located between the two. (3) The extrusion of the Qaidam block was accommodated by a left-slip fault system in the eastern Kunlun–southern Qinling region in the south and by a right-slip fault system in the Qilian Shan in the north. (4) The middle Paleozoic suture system between the North Tarim–North China block and South Tarim–Qaidam block has been offset by the late Cenozoic Altun Tagh fault for about 500 km left-laterally. The middle Paleozoic extrusion model provides a solution to an apparent paradox: whereas the collision of North China and Soutb China did not occur until the late Permian–Early Triassic, widespread middle Paleozoic deformation has been consistently documented along the southern margin of the North Tarim–North China block. It also explains why a late Paleozoic–early Mesozoic volcanic arc has not been observed in the Dabie and Shandong regions along the southern margin of North China: That arc was translated, together with the Qaidam block, to the west. In addition, right-slip faulting in the Qilian Shan area, required by the extrusion of Qaidam, not only accounts for the abrupt termination and bending of a north-striking Triassic–Jurassic thrust belt in the western Ordos at the Qilian suture but also provides a plausible connection in space to link the Triassic–Jurassic right-slip thrust faults in the central Tien Shan and northern Tarim with the Qilian Shan regions. Collision of the irregular northern margin of the South China block with the North China block resulted in initiation of the left-slip Tan Lu and right-slip Honam shear zones in eastern Asia and gave rise to the Huabei plateau north of the Dabie and Shandong regions in eastern North China. This topographically high region was further elevated and enlarged during the Yanshanian orogeny, which peaked in the late Jurassic. That orogeny was produced by the combination of several plate-boundary processes: (1) closure of the Mongol–Okhotsk ocean, (2) west-dipping subduction of the Pacific plate, and (3) continued collision of the North China and South China. The Huabei plateau began collapsing in the early Cretaceous, as expressed by widespread east–west extension and the development of North American Cordilleran–type core complexes and detachment faults (i.e., regional low-angle normal faults). The extension continued well into the Tertiary, as evidenced by the opening of the North China (Huabei) basin, Bohai Bay, and marginal seas along the eastern edge of Asia. That extensional event also reactivated the Tan Lu fault in Anhui and Shandong in east-central China. The tectonics of eastern Asia since 50 Ma have been dominated by both strike-slip faulting and crustal thickening produced by the Indo–Asian collision. As both the timing and magnitude of the Phanerozoic intracontinental deformation are yet to be systematically quantified, our reconstruction should be viewed as preliminary.

Introduction

The tectonic framework of Asia (Figure 20.1) was established over the past 500 m.y. by a number of collisional events among continental blocks and island-arcs (e.g., Klimetz, 1983; Zhang Liou, and Coleman, 1984; Watson et al., 1987; Şengör, 1987; Şengör, Natal'in, and Burtman, 1993). The impact of each new tectonic event on the older tectonic framework of Asia must be understood in order to reconstruct the tectonic history of Asia. Although the possible effects of the Indo–Asian collision in changing the shape of the Eurasian continent and in reactivating older structures during the Cenozoic are widely recognized (e.g., Molnar and Tapponnier, 1975; Tapponnier et al., 1982; Dewey et al., 1988; Peltzer and Tapponnier, 1988; Hendrix et al., 1992), how such processes operated throughout the Paleozoic and Mesozoic in Asia is less well understood. With a few exceptions (e.g., Tapponnier et al., 1981; Şengör et al., 1993; Yin and Nie, 1993), most tectonic reconstructions of Asia have assumed that

the present geometry of the sutures represents their original configurations at the time of formation (e.g., Klimetz, 1983; Zhang et al., 1984; Wang, 1985; Watson et al., 1987; Scotese and McKerrow, 1990; Enkin et al., 1992). Little consideration has been given in those reconstructions to the possibility that later tectonic events, particularly collisions between continents and subsequent strike-slip faulting, could have significantly modified the distribution and geometry of existing geologic features, such as suture zones, sedimentary-facies boundaries, and fold-and-thrust belts. In fact, the histories of Cenozoic and pre-Cenozoic deformations of Asia are inextricably linked. Understanding the Cenozoic tectonics of Asia will provide numerous insights into the processes operating during construction of the continent. These include the spatial associations between various geologic processes (Molnar and Tapponnier, 1975; Peltzer and Tapponnier, 1988; Harrison et al., 1992; Molnar, England, and Maritinod, 1993), the relationship between intraplate deformation and plate-boundary conditions (Harrison et al., Chapter 11, this volume; Houseman and England, Chapter 1, this volume; Kong and Bird, Chapter 2, this volume), and the roles of deep-crustal and mantle processes in mountain-building (Bird, 1991; Molnar et al., 1993; Davis et al., Chapter 5, this volume), to name a few. Also, understanding the nature of older tectonic features will provide clues to help identify strain markers that will allow quantitative restorations of Cenozoic deformation (e.g., Tapponnier et al., 1981; Peltzer and Tapponnier, 1988; Leloup et al., 1993). Thus, neotectonic and paleotectonic reconstructions must be carried out interactively. This chapter is the result of such an effort.

We first outline the geologic framework for selected areas of China that will constrain our tectonic reconstructions. This is based primarily on recently published Chinese provincial reports and detailed studies of oil-producing basins in China (Zai, 1987). The former will provide comprehensive descriptions of Chinese regional geology and stratigraphy, illustrated by accompanying geologic maps and cross sections on scales between 1 : 500000 and 1 : 2000000. The latter will offer systematic documentations of structure and sedimentology for many oil-producing basins in mainland China and in its offshore regions. In addition to synthesizing the existing Chinese geologic data and maps, we present the findings from our recent structural and thermochronologic studies of the Tien Shan in northwestern China, Anhui in east-central China, and Liaoning province in northeastern China. We highlight certain salient tectonic problems concerning eastern Asia and attempt to provide solutions through a step-by-step palinspastic reconstruction of eastern Asia during the Phanerozoic. Although this is a first-order reconstruction, it provides a framework of testable hypotheses that should aid in directing future research.

Geologic settings of selected areas

The formation of Asia over the past 500 m.y. has been accomplished by accretion of fragments of Gondwana onto the southern margin of the Eurasian continent (McElhinny et al., 1981; Tapponnier et al., 1981; Metcalfe, 1983; Allègre et al., 1984; Lin, Fuller, and Zhang, 1985; Şengör, 1987; Nie, Rowley, and Ziegler, 1990). Microcontinents and island-arcs in the Tethyan oceans also may have contributed significantly to that accretionary process (Şengör et al., 1988, 1993). These continental and oceanic fragments include the North China block, the South China block, the North Tarim block, the South Tarim–Qaidam block, the North Tien Shan, Central Tien Shan, and South Tien Shan, the Qiangtang block, the Lhasa block, the Mongolian island-arc systems, and Siberia (Figure 20.1). These blocks are separated by sutures, whose geometry and distribution have been significantly modified at various stages by later collisional and translational events. Our descriptions focus only on the geologic constraints that are relevant to our proposed tectonic model. Comprehensive reviews of Chinese geology can be found in publications by Huang et al. (1980), Wang (1985), and Yang, Cheng, and Wang (1986). We also refer readers to a milestone paper by C. Y. Li (1975), who first applied the principles of plate tectonics for a systematic interpretation of the geology of China. Despite new observations reported since that publication, many of Li's kinematic and tectonic concepts, such as recognizing the Tan Lu fault as a transform fault and describing occurrences of middle Paleozoic suturing in the Qinling, Qilian Shan, and Kunlun Shan areas, remain applicable to geologic research in eastern Asia today.

Geology of the North and South China blocks

The North China block, also known as the Sino–Korean craton or Sino–Korean platform, consists of metamorphic basement rocks as old as the early Archean (>3.8 Ga) (Liu et al., 1992). Archean ages for metamorphic basement rocks up to 3.8 Ga have also been inferred in the South China block (Zhou, 1994) and its northern extension in South Korea (Lan et al., 1995). Proterozoic unmetamorphosed sedimentary rocks are widely distributed in both North China and South China. Proterozoic stratigraphy in China is divided into four systems (Yang et al., 1986): the Changchengnian (1,850–1,400 Ma), the Jixianian (1,400–1,050 Ma), the Qingbaikouan (1,050–850 Ma), and the Sinian (850–570 Ma). The North China block (Figure 20.1) contains rocks of the first three systems, but Sinian strata are rare except along its marginal regions. In North China, the three older systems are best exposed in the Jixian area, about 100 km east of Beijing, where the total thickness of the sequence is in excess of 10 km. The Precambrian sequence is also distributed in a NE–SW-trending trough across the central part of the North China block (Hebei BGM, 1989). Its upper part consists of volcanic rocks. The great thickness, the linear trough geometry, and the presence of volcanics have all been interpreted to be the results of rifting (Hebei BGM, 1989). In many respects (i.e., shallow-water clastic and carbonate deposits, abundant volcanic clastics, great thickness, depositional age), this sequence is similar to that of the Belt–Purcell Supergroup in the northwestern United States and southwestern Canada (Winston, 1986). It is possible that North China could have been part of the late

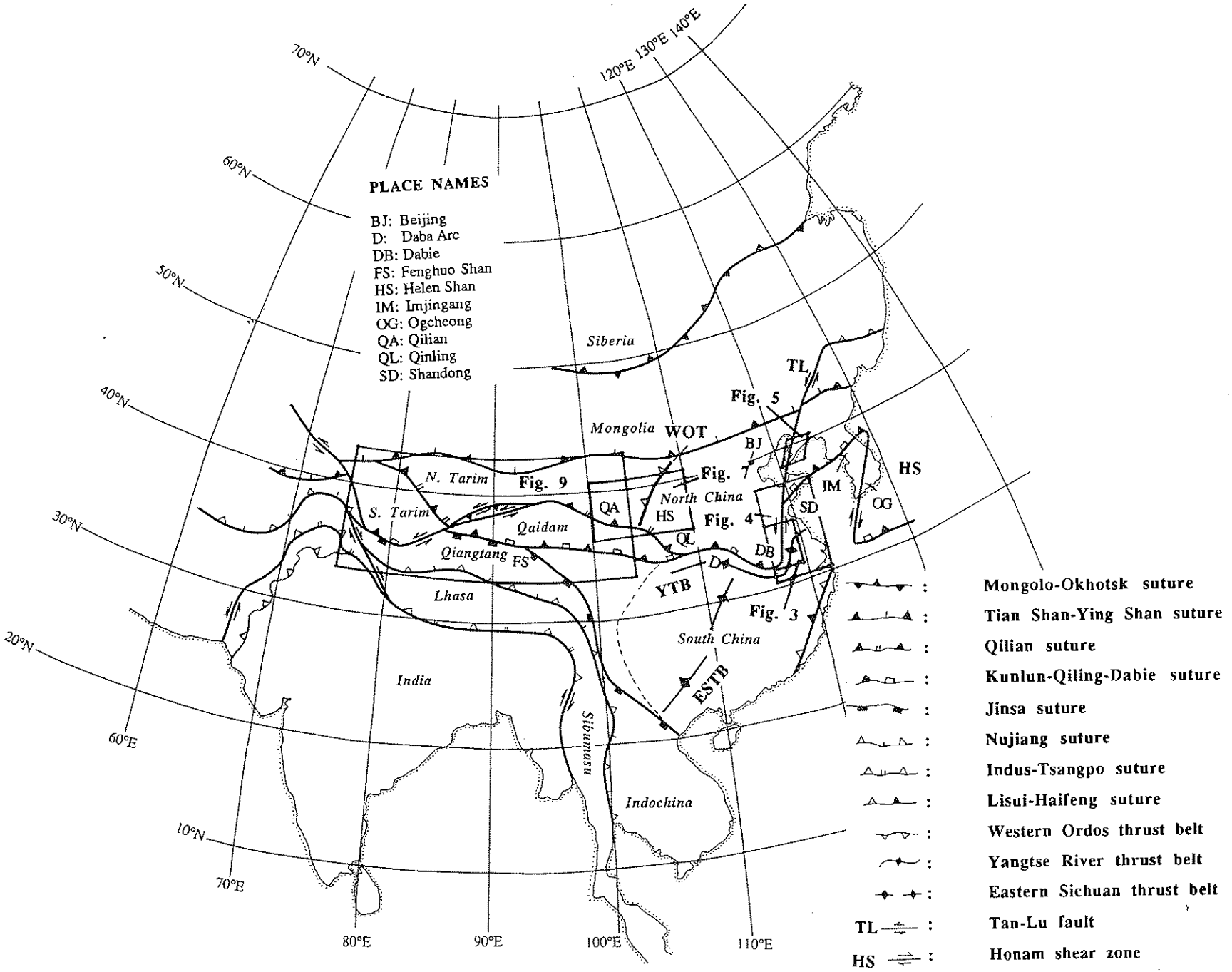
PLACE NAMES
BJ: Beijing
D: Daba Arc
DB: Dabie
FS: Fenghuo Shan
HS: Helen Shan
IM: Imjingang
OG: Ogcheong
QA: Qilian
QL: Qinling
SD: Shandong
70°N
60°N
50°N
40°N
30°N
20°N
10°N
60°E
70°E
80°E
90°E
100°E
110°E
120°E
130°E
140°E
Siberia
Mongolia
WOT
TL
Fig. 5
Fig. 7
Fig. 4
Fig. 3
Fig. 9
N. Tarim
S. Tarim
Qaidam
Qiangtang
Lhasa
India
Sibumasu
Indochina
South China
North China
QA
HS
QL
FS
D
DB
YTB
ESTB
BJ
SD
IM
OG
Mongolo-Okhotsk suture
Tian Shan-Ying Shan suture
Qilian suture
Kunlun-Qiling-Dabie suture
Jinsa suture
Nujiang suture
Indus-Tsangpo suture
Lisui-Haifeng suture
Western Ordos thrust belt
Yangtse River thrust belt
Eastern Sichuan thrust belt
Tan-Lu fault
Honam shear zone

Proterozoic supercontinent Rodinia (Dalziel, 1991; Moores, 1991) and could have been located close to western North America.

During the Paleozoic, the North China block was a stable craton, with shallow-marine carbonate sedimentation. Except along its marginal areas, that sedimentation was interrupted between the late Ordovician and late Carboniferous in the North China block, as marked by a regionally extensive disconformity between Upper Ordovician and Upper Carboniferous strata (e.g., Wang, 1985). As discussed by Yang et al. (1986), and in our tectonic model, that transition from marine to terrestrial deposition may be attributable to a combination of (1) northward subduction of the Qaidam block from the south, (2) southward subduction of an oceanic plate from the north beneath the North China block, and (3) a eustatic sea-level low following the Caledonian orogeny. Both the Qilian–Qinling and Helan regions of western North China are devoid of shallow-marine deposition. Instead, thick Lower Paleozoic strata consisting dominantly of deep-marine shale, chert, and volcaniclastic sediments have been documented (e.g., Wang, 1985; Yang et al., 1986; Gansu BGM, 1989). Based on the abrupt changes in stratigraphic thickness and depth of deposition, the early Paleozoic sedimentation in the Helan region may have been related to the development of an aulacogen (Ningxia BGM, 1989) following the breakup of the late Proterozoic supercontinent Rodinia (Bond, Nickerson, and Kominz, 1984; Moores, 1991).

The South China block (i.e., Yangtze craton or Yangtze platform) was separated from the North China block by intervening oceans in the Paleozoic. Sinian strata include several cycles of glacial deposition (Yang et al., 1986; Liu, 1991). In contrast to North China, pre-Sinian unmetamorphosed sedimentary sequences generally are absent from the South China block (Yang et al., 1986). After the amalgamation of the western South China (the Yangtze block) and eastern South China blocks (the Huanan block) in the latest Precambrian (Ji and Coney, 1985), northern South China was a passive continental margin, as expressed by continuous shallow- to deep-marine sedimentation (Yang et al., 1986).

Between the late Permian and the late Triassic, sedimentation patterns changed dramatically in South China. Dominantly shallow-marine deposition gave way to terrestrial clastic deposition. That change has been attributed to the initial collision between North China and South China (Şengör, 1985; Hsü et al., 1987) and has been used to infer a diachronous collisional history (Yin and Nie, 1993). The transition from marine to terrestrial deposition occurred earlier in the interior of the North China block, in the late Carboniferous (Yang et al., 1986), which could have been the result of (1) northward subduction of the South China plate beneath the North China plate in the late Paleozoic and (2) a eustatic sea-level low due to the late Paleozoic Gondwana glaciation (Hallam, 1992).

Figure 20.1. Tectonic map of Asia, showing major suture zones. Map symbols are explained in the legend. The locations of Figures 20.3–20.5 and 20.7–20.9 are also shown.

Correlation of Chinese and Korean geology

The Korean Peninsula is divided by the Imjingang and Ogcheon belts into three tectonic blocks (Figure 20.1). They are, from north to south, the Nangrim–Pyeongnam block, the Gyeonggi block, and the Ryeongnam block (Reedman and Um, 1975; Lee, 1987; Cluzel, Cadet, and Lapierre, 1990). In addition, the Gyeonggi block in central Korea has been correlated with South China, and the Nangrim–Pyeongnam and Tyeongnam blocks have been correlated with North China (Figure 20.1) That division and correlation are based principally on the distribution of Cambrian faunal affinities established by Kobayashi (1966). In this tectonic framework, the Imjingang belt is the eastern extension of the Shandong suture zone (Earnst, Cao, and Jiang, 1988; Hsü et al., 1990). This, in turn, connects with the Triassic Honam shear zone in the Ogcheon belt, thus separating the North China–Ryeongnam block from the South China–Gyeonggi block (Yin and Nie, 1993). The presence of late Permian–early Jurassic granites (276–200 Ma) in the Ogcheon belt, all deformed by the Honam shear zone (Choo and Kim, 1986; Choo and Chi, 1990; Cluzel et al., 1990; Kim, Park, and Kang, 1994), is consistent with the prediction of the Yin and Nie (1993) model and thus supports Kobayashi's division. Despite the foregoing tectonic speculations on how the Chinese blocks correlate with the Korean blocks, little detailed geologic work had been done to clarify the deformation history of the Ogcheon and Imjingang belts until recently. In fact, Choi (1994) disputed Kobayashi's paleobiogeographic division and believed that the whole Korean Peninsula was close to, or may have belonged to, the North China block in the middle Cambrian–early Odovician, during the deposition of the Joseon Group in the Ogcheon belt.

Because the Imjingang belt, with the exception of its southern part, is located in North Korea, its tectonic nature and detailed evolutionary history are still largely unknown to researchers outside of North Korea. Preliminary structural and metamorphic studies in the southernmost part of the Imjingang belt in northern South Korea suggest that the belt experienced Triassic deformation and metamorphism at pressure and temperature conditions of 0.7–1.1 GPa and 660–760°C (Ree et al., 1994). Ree et al. (1994) related that metamorphism to the Triassic collision between the Nangrim–Pyeongnam and Gyeonggi blocks and correlated the Imjingang belt with the Shandong suture zone in east-central China. In addition, a recent study in the central Gyeonggi block suggests a similar Triassic metamorphic event (Lee, Cho, and Kwon, 1994), implying that the Triassic deformation may have affected a much broader area of the Korean Peninsula than just the Imjingang and Ogcheon belts.

Timing and duration of the North China–South China collision

North China and South China are separated by the Qinling–Dabie–Shandong suture zone, which possibly extends to Kore (Figure 20.1). Its westward extension is somewhat uncertain Most workers believe that it connects with the suture zone in th

eastern Kunlun Shan along the southern margin of the Qaidam block, because it lies along the strike (e.g., Watson et al., 1987) (Figure 20.1). However, the Qinling region of the suture zone may instead connect with the middle Paleozoic Qilian Shan suture zone along the northern margin of the Qaidam block. This is possible because the Qinling and Qilian Shan areas share a middle Paleozoic collisional event (e.g., Li et al., 1978; Mattauer et al., 1985). As shown in Figure 20.1 and discussed in our tectonic model to be presented later, we believe that the western part of the Qinling suture zone was linked with the Qilian Shan suture zone in the middle Paleozoic and was significantly modified by strike-slip faulting in the Triassic and Jurassic, synchronous with indentation of the South China block into North China.

As summarized by Yin and Nie (1993) and Hacker et al. (Chapter 16, this volume), the time of the North China collision has been widely disputed in the past decade. The dispute arises from the incompleteness of the geochronologic data and, in some cases, from misconceptions and misinterpretations of the stratigraphic record and radiometric ages. For clarity, we first classify the chronologic data into four categories and discuss their geologic implications for the timing of initiation and the duration of the collision between the North China and South China blocks: (1) Chronostratigraphic data may indicate closure of the ocean(s) between North China and South China. This may be assessed by examining the first appearance of terrestrial clastic rocks on the northern margin of South China that were derived from North China, implying proximity of the two blocks and thus the time of their initial collision. (2) Radiometric dates for metamorphic and plutonic rocks may constrain our estimations of the timing of deformation, metamorphism, and denudation along the suture zone. This data set could be ambiguous in terms of its implications for the age and duration of collision. Without information on the age relationships between deformation and arc magmatism, which is the case along most of the Qinling–Dabie–Shandong suture zone because the magmatic arc is missing, such data could be interpreted to represent pre-collisional intra-arc deformation, syn-collisional metamorphism, or post-collisional intracontinental deformation (Yin and Nie, 1993). (3) Paleomagnetic data may constrain our estimations of the time of post-ocean-closure convergence of the two continents. That age could be significantly younger than the age of the ocean closure itself, if significant intracontinental deformation, similar to that in the Indo–Asian collision, was accommodated during the North China–South China collision (Molnar and Tapponnier, 1975; Harrison et al., 1992; Nie and Rowley, 1994). (4) The youngest age of arc magmatism may provide the youngest limit for subduction, and thus the time of ocean closure. Following this classification, we review each of the four data sets and summarize the geologic implications of these ages (Figure 20.2).

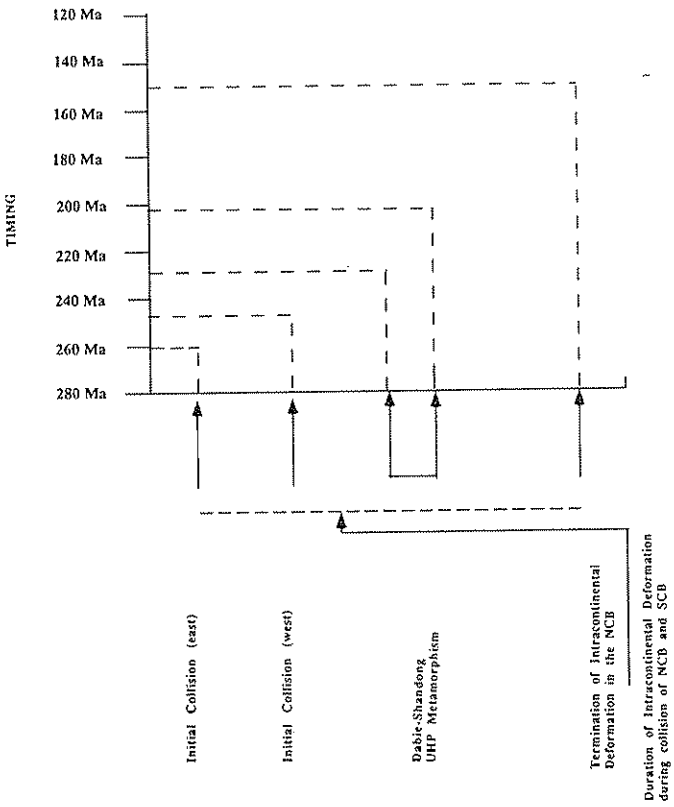

Figure 20.2 Summary of various geologic data sets that constrain our estimations of the times of the initial collision and termination of collision between the North and South China blocks.

1. **Sedimentologic data:** On the basis of the timing of the final disappearance of marine sedimentation along the northern margin of the South China block in the Qinling region, Wang, Xu, and Zhou (1982) and Hsü et al. (1987) concluded that the collision between North China and South China occurred in the late Triassic. Yin and Nie (1993) reviewed the stratigraphic record along the entire northern passive margin of the South China block, as well as the sedimentologic and structural characteristics of central Korea. Based on the timing of the first appearance of clastic input from a northern source onto the northern margin of the South China block, they concluded that the ocean closure between North China and South China had been diachronous, initiated first in the late Permian in Korea and Shandong, and progressing westward to the Qinling region in the late Triassic. A similar inference of a diachronous collision between North China and South China in that general time window was made by Watson et al. (1987), although they did not provide data in support of their speculation. It is important to note that the sedimentologic data summarized by Hsü et al. (1987) and Yin and Nie (1993) provide only the timing of ocean closure and thus the age of initial contact between the North and South China continents. The data have no implications for when the collision of the two continents, accommodated by large-scale intracontinental deformation, ceased.

2. **Ages of deformation along the suture zone:** The collision of North China and South China was inferred by Mattauer et al. (1985) to have been middle Paleozoic, on the basis of (1) the age of contractile deformation in the northern Qinling orogenic belt

of the Qinling region and (2) a widespread nonconformity between the Devonian terrestrial clastic sediments, interpreted as molasse deposits (Li et al., 1978), and the underlying Qinling metamorphic complex. The Devonian nonconformity has been interpreted by Chinese geologists (e.g., Huang et al., 1977) as marking the end of the Caledonian (early Paleozoic) orogenic event. Mattauer et al. (1985) further suggested that the Mesozoic and Tertiary deformations of the southern Qinling suture zone had been entirely intracontinental phenomena. In contrast to that interpretation, and in light of new geochronologic data derived from the Tongbai region (between the Qinling and Dabie mountains), Zhang et al. (1989) and Kröner, Zhang, and Sun (1993) suggested that the middle Paleozoic deformation in the Qinling orogenic belt had been related to a collision between the North China block and a magmatic arc to the south, with the former being subducted southward underneath the arc. Okay, Şengör, and Satir (1993) disputed those dates as representing the age of a magmatic arc. Instead, they suggested early Paleozoic granulite-facies metamorphism in the Tongbai region. As the restoration of the younger strike-slip faults in the region was not considered by Zhang et al. (1989) and Kröner et al. (1993), the arc–continent collision model is yet to be tested.

Such ultra-high-pressure metamorphism has been interpreted to have been related to the collision between North China and South China because of large-scale involvement (several tens of kilometers across the orogenic belt) of the continental crust (Okay and Şengör, 1992; Liou et al., Chapter 15, this volume). The amount of geochronologic data on the age of ultra-high-pressure metamorphism in the Dabie–Shandong region has increased rapidly in the past few years (e.g., Li et al., 1989, 1993; Chen et al., 1992; Ames, Tilton, and Zhou, 1993; Okay et al., 1993; Ames, 1994; Hacker et al., Chapter 16, this volume). The age range for that metamorphism, constrained by U-Pb, $^{40}Ar/^{39}Ar$, Rb-Sr, and Sm-Nd dating techniques, is between 246 Ma and 179 Ma. Those ages for the metamorphism provide a general upper limit for the initial contact between the North and South China continents and imply that North China and South China did not begin to collide prior to the late Permian and early Triassic in the Dabie and Shandong regions. Furthermore, if the late Triassic deposition in the Songpan–Ganzi region (Figure 20.1) was the result of rapid denudation of the Dabie and Shandong regions (Yin and Nie, 1993; Nie et al., 1994b; Zhou and Graham, Chapter 14, this volume), then it implies that the rapid late Triassic cooling of the ultra-high-pressure metamorphic rocks in the Dabie and Shandong regions (Liou et al., Chapter 15, this volume; Hacker et al., Chapter 16, this volume) was primarily the result of erosion, not tectonic denudation by normal faulting. That process of thrust-induced denudation may have been similar to that of the Himalaya and the southern Tibetan plateau during the Cenozoic Indo–Asian collision, when significant erosion of the Himalaya and Gangdese Shan was caused by the development of the Main Central Thrust and the Gangdese thrust system (Harrison et al., 1992; Yin et al., 1994).

Radiometric dates for single zircons between 210 Ma and 202 Ma were obtained by the U-Pb method for the Dabie and Shandong ultra-high-pressure eclogites (Ames, 1994). Because of the similar ages in the two regions, Ames (1994) suggested that the collision between North China and South China had occurred synchronously along the entire suture zone. We would like to call particular attention to a potential interpretive misconception by using an example from the Himalayan orogen and the southern Tibetan plateau. The collision between India and Asia occurred diachronously, beginning first in northern Pakistan at about 60 Ma in the west, progressively suturing to the east in Tibet (e.g., Searle, Chapter 7, this volume; Le Fort, Chapter 6, this volume). However, significant and detectable crustal thickening and denudation did not occur in southern Tibet until about 27–20 Ma (Hubbard and Harrison, 1989; Burchfiel et al., 1992; Harrison et al., 1992; Yin et al., 1994). In the Himalaya, however, compression along the Main Central Thrust and extension along the South Tibet detachment system occurred between 24 Ma and 18 Ma and produced a metamorphic event along the entire length of the Himalaya (Copeland, Harrison, and Le Fort, 1990; Harrison et al., 1992, in press; Le Fort, Chapter 6, this volume). These ages of metamorphism imply that the collision between India and Asia occurred neither synchronously nor during the early Miocene. Because of this possible complexity, the new age dates of Ames (1994) for the ultra-high-pressure metamorphism do not provide unambiguous constraints on when and how the North China–South China collision occurred.

3. **Paleomagnetic data:** The existing paleomagnetic data from North China and South China seem to suggest that their final amalgamation did not occur until the late Jurassic (e.g., Enkin et al., 1992), because the paleomagnetic poles older than the Cretaceous do not coincide. That age (~150 Ma) is about 110 m.y. younger than the time of the earliest ocean closure (~260 Ma), as inferred from the sedimentologic data (Yin and Nie, 1993; Nie and Rowley, 1994). The two sets of data can be interpreted in a consistent manner if the North China block was extensively deformed after the initial contact by post-collisional convergence between the North China and South China continents. This would require significant internal deformation (crustal thickening, strike-slip faulting, and relative rotation) in North China between the early Triassic and the late Jurassic. The widespread late Triassic–late Jurassic north–south crustal shortening in Anhui (Anhui BGM, 1987), Liaoning (Liaoning BGM, 1989), northern Hebei (Hebei BGM, 1989; Davis et al., Chapter 13, this volume), and western Inner Mongolia (Zheng, Wang, and Wang, 1991) may have been a manifestation of that continued convergence.

4. **Dating the youngest arc magmatism along the suture zone:** It is difficult to document arc magmatism, because pre-Triassic arc-related plutons have been swept away by denudation (Nie et al., 1994b; Zhou and Graham, Chapter 14, this volume), strike-slip faulting (Mattauer et al., 1985), or a combination of the two. A few Triassic granites, possibly related to arc magmatism, are present in the Qinling region. The crystallization age for one such granite was determined by U-Pb zircon analysis to be about 211 Ma (Reischmann et al., 1990). That age, if the granite was

the product of a magmatic arc, indicates that the collision in the Qinling region did not begin before the late Triassic, consistent with the sedimentologic evidence.

In the Ogcheon belt of South Korea, Permian–Triassic granites and granodiorites have been reported (Kim et al., 1994). Those granites are distributed along the Ogcheon belt and were deformed by the Honam shear zone, which was in turn intruded by late Jurassic and Cretaceous plutons. Because the origin of those granites (subduction-related melting versus post-orogenic thermal relaxation) remains unknown, the age of initial collision in that belt is not well established.

Deformation related to the North China–South China collision

Intracontinental deformation was widespread in both North China and South China in the early Mesozoic, during the collision between North China and South China. In North China, Mesozoic deformation traditionally has been classified as the result of the Indosinian orogeny, between the late Triassic and early Jurassic, and the Yanshanian orogeny, between the late Jurassic and early Cretaceous (Figure 20.1) (e.g., Yang et al., 1986). The structures related to that period of deformation are characterized by E–W-trending folds and thrusts in the northern part of North China, and by N–S-trending folds and thrusts in the western margin of North China (Figure 20.1). The South China block experienced extensive deformation in the Triassic and Jurassic along the Yangtze River in the Anhui region (Figure 20.3), as expressed by the development of a fold-and-thrust belt. From east to west, the fold-and-thrust belt changes its trend from the E–W direction south of the Dabie Shan to the N–S direction along the Tan Lu fault, and again to the E–W direction south of the Shandong suture zone (Chen, 1989; Yin and Nie, 1993). Additionally, a late Jurassic–early Cretaceous fold-and-thrust belt developed in South China along the eastern margin of the Sichuan basin (Figure 20.1) (Chen, 1989). That belt merges to the north with the Yangtze River fold-and-thrust belt. It is difficult to relate its development to the subduction of the Pacific plate, as it does not extend north of the Qinling–Dabie–Shandong suture system, despite its apparent younger age.

Although the age and spatial distribution of the late Mesozoic deformation ("Yanshanian orogeny") are well documented, it has been difficult to account for its mechanical cause (Yang et al., 1986). As discussed later, this difficulty may be due to the fact that the North China block in the early Mesozoic was bounded by three active plate boundaries: (1) a west-dipping subduction along its eastern margin, (2) a south-dipping subduction zone and/or convergence zone along the Okhotsk ocean on its northern margin, and (3) a collisional boundary between North China and South China along its southern margin. Thus the Yanshanian deformation in North China could be attributable to the North China–South China collision (Yin and Nie, 1993), to closure of the Mangol–Okhotsk ocean (Nie and Rowley, 1994), or to subduction of the Pacific plate beneath Asia (Xu et al., 1993). Despite the uncertainty of its mechanical cause, the magnitude and kinematics of deformation in North China can be linked quantitatively to processes along individual plate boundaries.

Two contrasting models have been proposed for the ocean closure and subsequent convergence between North China and South China. Zhao and Coe (1987), on the basis of a synthesis of paleomagnetic data, suggested that the North China–South China collision involved nearly 70° of relative rotation (i.e., the South China block rotated clockwise with respect to the North China block). In contrast, Yin and Nie (1993) proposed that the collision was accomplished by indentation of the South China block into the North China block and involved no significant rotation. [A model similar to that of Yin and Nie (1993) was independently proposed by Mattauer et al. (1991). However, they suggested that the collision of North China and South China occurred in the middle Paleozoic.] Although both models predict a diachronous collision from east to west, they differ in predicting the distribution of intracontinental deformation in North China during the collision. The Zhao and Coe (1987) model requires that (1) at least the southern part of the Tan Lu fault was in existence prior to the Permo–Triassic collision, and (2) the region presently east of the Tan Lu fault and south of the Shandong suture zone experienced syn-collisional Permo–Triassic extension, as demanded by the proposed rotation. However, the Yin and Nie (1993) model predicts that the Tan Lu fault initiated a subduction zone that was progressively modified and rotated during the North China–South China collision into its present configuration. Furthermore, Yin and Nie's model (1993) requires significant Triassic north–south shortening and/or left-slip faulting north of the Shandong region, which would have accommodated about 500 km of northward indentation of South China. Thus, the age and kinematics of the Tan Lu fault and the extent, magnitude, and style of deformation in eastern Asia during the collision of the two continents are keys to selecting between the two models. With this particular purpose in mind, we review the geology of three regions: Anhui, Liaoning, and Qilian Shan.

1. **Anhui region:** Dating the age of the Tan Lu fault is difficult, as it has been reactivated numerous times since its initiation (Tan-Lu Fault Working Group, 1987; Chen et al., 1988; Xu et al., 1993). Thus, an understanding of the younger deformational events associated with the Tan Lu fault is required to understand its past. Geomorphologic evidence, seismicity, and crosscutting relationships between the Tan Lu fault and Neogene strata suggest that the fault has been an active right-slip system throughout the late Cenozoic (Ma, 1986; Tan-Lu Fault Working Group, 1987). The ages of fault movements are also suggested by the age of the fault gouge collected in the Shandong region. Dating of that material by K-Ar and Rb-Sr methods has yielded model ages of 110–90 Ma and 106.8 ± 2.8 Ma, respectively (Chen et al., 1988). Because faults in the Tan Lu system bound numerous Cretaceous basins, Xu (1985) suggested that the Tan Lu fault was a Cretaceous normal-fault system. The Cretaceous normal-faulting history along the Tan Lu fault can be inferred from the geologic map of Anhui Province (Anhui BGM, 1987), which covers the southern

part of the Tan Lu fault. That fault is presently SE-dipping, with westward-tilted Cretaceous–Paleogene strata in its hanging wall and the Dabie ultra-high-pressure metamorphic rocks in its footwall (Figure 21.3A-B).

The original configuration of the Tan Lu fault cannot be reconstructed with confidence, as the present fault trace has been intensely modified since its initiation (Figure 20.3A). However, the following lines of evidence suggest that the Tan Lu fault was active prior to the normal and right-slip faulting: First, the normal and right-slip-faulting history of the Tan Lu fault in the Cretaceous to the present cannot explain the large offset of the ultra-high-pressure metamorphic rocks in the Shandong and Dabie Shan regions. Second, the normal and right-slip-faulting history cannot account for the formation of the Triassic–Jurassic fold belt that follows the E–W-trending Qinling–Dabie Shan suture belt and bends abruptly along the NNE-trending Tan Lu fault in the eastern Dabie Shan (Figure 20.1). We suggest that the Tan Lu fault was initiated in the Permian as a left-slip system, based on the sedimentologic record discussed by Yin and Nie (1993). Left-slip faulting was occurring along the Tan Lu fault until the late Jurassic. That termination age for the left-slip faulting is based on stratigraphic age constraints from the Yangtze River fold-and-thrust belt (Jiangsu BGM, 1984; Anhui BGM, 1987; Chen, 1989). The curved geometry of the fold-and-thrust belt is most likely to have formed as an orocline/drag-fold system related to the lift-slip motion along the Tan Lu fault. The age of the fold-and-thrust belt is well defined by the stratigraphic relationships in eastern Anhui province, as well as thrusting-related denudation ages along the Tan Lu fault (Anhui BGM, 1987) (Figure 20.3). That fold-and-thrust belt deforms a continuous sequence of Paleozoic–Triassic sedimentary rocks along the northern margin of the South China block. The folds are unconformably overlain by Upper Jurassic volcanic rocks in many places (Figure 20.3). Thrusting related to the oroclinal bending of the Yangtze River fold-and-thrust belt was active during the Triassic (~ 244–212 Ma), as indicated by $^{40}Ar/^{39}Ar$ biotite and muscovite ages derived from the Archean and Proterozoic rocks in the Zhangbaling region and the eastern foothills of the Dabie Shan east of the Tan Lu fault (see the $^{40}Ar/^{39}Ar$ dates from this study summarized in Figure 20.3A). Note that the early Triassic age of motion along the Tan Lu fault is consistent with the prediction of Yin and Nie's model (1993). The $^{40}Ar/^{39}Ar$ samples were collected from the hanging walls of the major thrusts in the region. Thus, their cooling ages likely are related to denudation during thrusting. Note that mylonitic fabrics, with sub-horizontal lineations and nearly vertical foliations, were also observed in the Zhangbaling region in the metamorphosed Archean and Proterozoic units where the Triassic cooling ages were obtained (Xu, 1993; Zhang et al., 1994; Wang et al., 1994); left-slip kinematic indicators have been reported by those studies. Those ductile fabrics likely are related to the Triassic left-slip history of the Tan Lu fault. The distribution of blueschist-facies metamorphic zones has been documented along the southern Tan Lu fault between the Dabie and Shandong suture zones (Sun et al., 1993) (Figure 20.4), suggesting that the Tan Lu fault could have been the locus of subduction. This relationship is consistent with the prediction of the Yin and Nie (1993) model that the Tan Lu fault was originally a subduction zone and subsequently was bent and stretched by the indentation of South China. Note that Permo–Triassic E–W extension, as predicted by the Zhao and Coe model (1987), has not been observed along or east of the Tan Lu fault.

2. **Southern Liaoning region:** Structural and stratigraphic relationships suggest that the Liaoning peninsula experienced significant N–S shortening between the late Permian and the late Jurassic, as the Paleozoic–Triassic strata are extensively deformed, as expressed by E–W-trending folds and thrusts (Liaoning BGM, 1989) (Figure 20.5 and 20.6A). That deformed sequence is unconformably overlain by Upper Jurassic–Lower Cretaceous volcaniclastic deposits. The upper age limit for the E–W-trending folds and thrusts has been independently determined by dating the regionally extensive Liaonan detachment fault, which cuts the older contractional structures (Figure 20.5). The trace of the detachment fault outlines the peninsula and exhibits a south-plunging half-domal geometry, with the fault dipping to the east, south, and west. It juxtaposes the unmetamorphosed Proterozoic–Paleozoic sedimentary rocks in its hanging wall and the metamorphic Archean–Proterozoic rocks in its footwall. Cretaceous plutons and north-trending dike swarms are also common in the footwall (Figure 20.5). A mylonitic shear zone below the detachment fault is at least several hundred meters thick. Kinematic indicators observed from the footwall mylonitic gneisses suggest a top-to-the-west sense of shear (Figures 20.6B-C). Samples collected from the footwall of that detachment fault yield $^{40}Ar/^{39}Ar$ ages between the late Jurassic (~150 Ma) and late Cretaceous (~110 Ma) for muscovite and biotite directly below the fault, and middle Proterozoic ages away from the fault. As the mylonitic fabrics die out and the cooling ages get older northward in the footwall (Liaoning BGM, 1989) (Figure 20.5), we interpret that displacement along the Liaonan detachment fault decreases northward.

The N–S shortening in the southern Liaoning region could have been induced by (1) the North China–South China collision in the Triassic (Yin and Nie, 1993), (2) the early Cretaceous closure of the Mongol–Okhotsk ocean between Siberia and North China (Nie et al., 1990; Zhao et al., 1990; Enkin et al., 1992; Nie and Rowley, 1994), and (3) late Jurassic oblique subduction of the Pacific plate (Xu et al., 1987; Okay and Şengör, 1992). The key to differentiating these causes is to determine the upper age limit for the shortening event and the kinematic history of the deformation. We exclude the closure of the Mongol–Okhotsk ocean as a cause because it did not occur until the Cretaceous (Zonenshain, Kuz'min, and Natapov, 1990; Nie and Rowley, 1994). It is also difficult to attribute the formation of those E–W folds and thrusts to subduction of the Pacific plate, because the structures and the subduction zone were nearly perpendicular to one another. Another key prediction of the Yin and Nie (1993) model is that the total magnitude of shortening and strike-slip faulting should be on the order of 500 km east of the Tan Lu fault and north of the Shandong suture

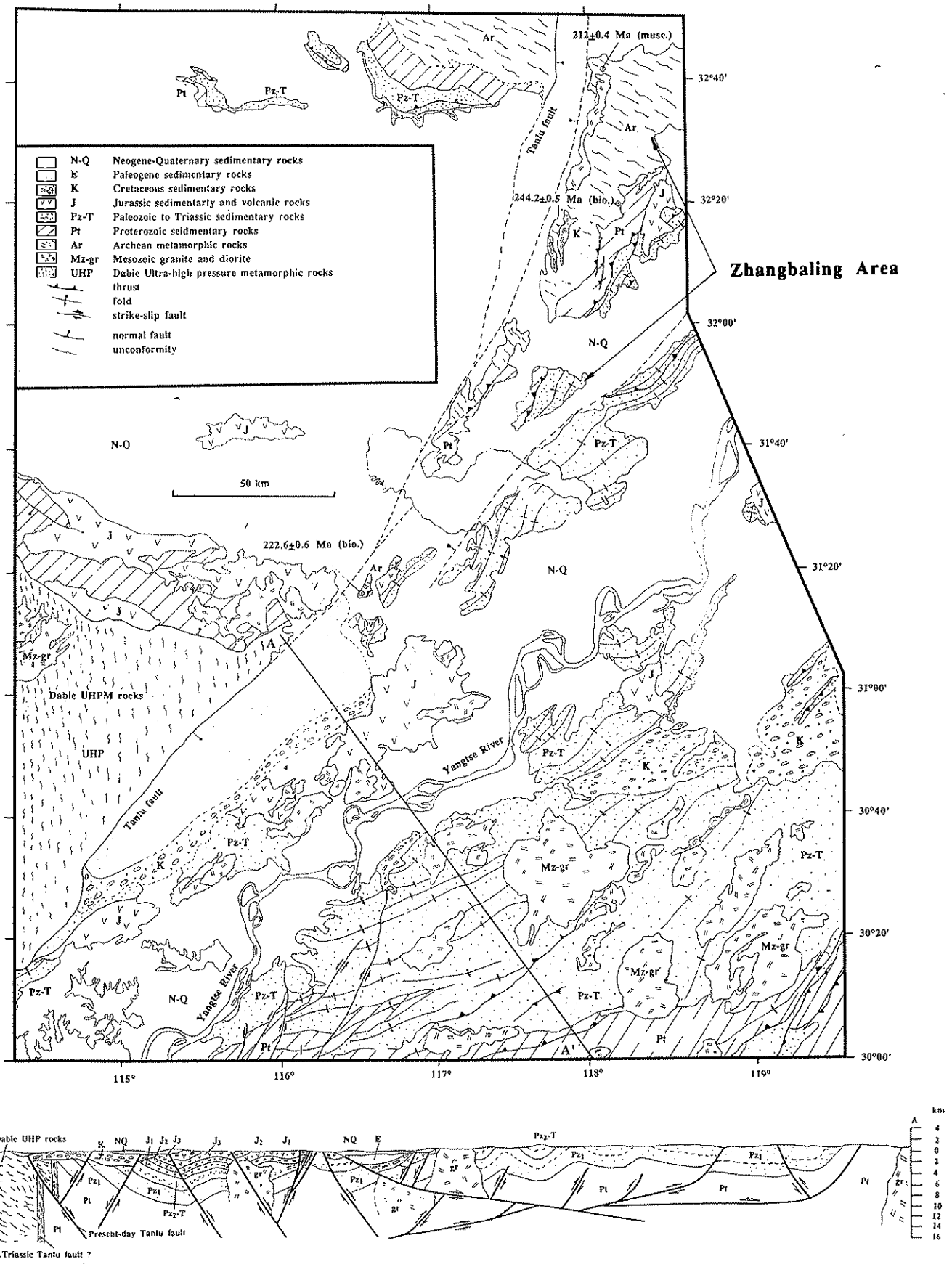
N-Q Neogene-Quaternary sedimentary rocks
E Paleogene sedimentary rocks
K Cretaceous sedimentary rocks
J Jurassic sedimentarty and volcanic rocks
Pz-T Paleozoic to Triassic sedimentary rocks
Pt Proterozoic seidmentary rocks
Ar Archean metamorphic rocks
Mz-gr Mesozoic granite and diorite
UHP Dabie Ultra-high pressure metamorphic rocks
thrust
fold
strike-slip fault
normal fault
unconformity
212±0.4 Ma (musc.)
244.2±0.5 Ma (bio.)
222.6±0.6 Ma (bio.)
Zhangbaling Area
Tanlu fault
Yangtse River
Dabie UHPM rocks
50 km
32°40'
32°20'
32°00'
31°40'
31°20'
31°00'
30°40'
30°20'
30°00'
115°
116°
117°
118°
119°
A
A'
Present-day Tanlu fault
Triassic Tanlu fault ?

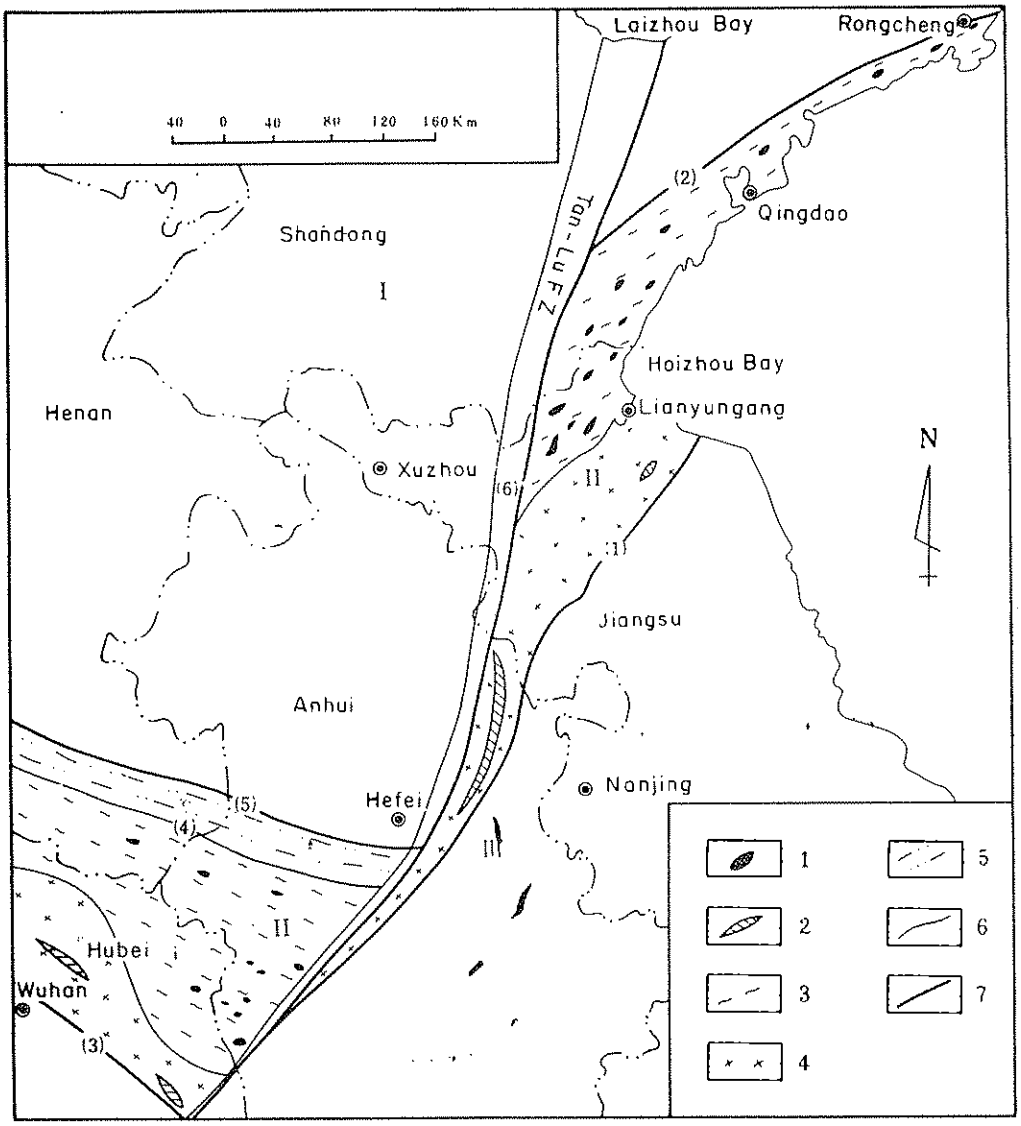

Figure 20.4 Simplified geologic map of the southern Tan Lu fault system and major rocks units. Numbers in the inset box: 1, eclogites; 2, blueschist-facies metamorphic zone; 3, distribution of the Dabie and Shandong ultra-high-pressure metamorphic rocks; 4, distribution of the Hongan–Susong Group and the Zhangbaling–Haizhou Group; 5, Paleozoic metamorphic series; 6, boundaries between geologic units; 7, major faults. Number on the map: (1) Xuyi–Ziangshui fault; (2) Zhucheng–Qingdao fault; (3) Xiangfan–Guanji fault; (4) Fuziling–Xiaotien fault; (5) Queshan–Feidong fault; (6) Tan Lu fault. Major tectonic units: I, North China; II, Qinling orogenic belt; III, South China block. (Adapted from Sun et al., 1993.)

zone. Although about 100 km of left-slip along the Tan Lu fault and an equivalent amount of N–S shortening east of the Tan Lu fault can be inferred from the existing Chinese geologic maps at scales of 1 : 200,000 and 1: 50,000 in the Liaoning region, the total amount of shortening in the Bohai region remains poorly known, as the structures between Liaoning and Shandong lie beneath the Bohai sea. Triassic N–S shortening may be inferred in the Bohai Bay region, as a widespread unconformity between Jurassic–Cretaceous strata on top and highly deformed E–W-trending Paleozoic strata has been revealed by seismic-reflection profiles and drill-hole data (Gong, 1987). This observation at least qualitatively conforms to the prediction by Yin and Nie (1993) that N–S shortening occurred beyond the Shandong belt.

3. **Qilian–Qinling–Kunlun regions:** A N–S-trending fold-and-thrust belt lies along the western Ordos region (Figure 20.7A). That fold belt involves Paleozoic–Jurassic strata and changes its trend to an E–W direction to the south as it approaches the middle Paleozoic Qilian Shan suture zone between North China

Figure 20.3 (A) Simplified geologic map of eastern Anhui region, based on the geologic map of Anhui province, scale 1 : 500000 (Anhui BGM, 1987), showing the present traces of the Tan Lu fault and the Yangtze fold belt and the locations for $^{40}Ar/^{39}Ar$ samples. Although the Jurassic rocks in many places unconformably overlie Paleozoic–Triassic folded strata, they are locally involved with folding. (B) Geologic cross section across the Tan Lu fault and the Yangtze fold-and-thrust belt. Note that the present-day trace of the Tan Lu fault is marked by a normal fault. The Triassic Tan Lu fault probably was cut and is now buried beneath a Cretaceous–early Tertiary basin. The mylonitic fabrics observed in the Archean and Proterozoic metamorphic rocks in the Zhangbaling area (Xu, 1993) may have been part of the Triassic left-slip Tan Lu fault zone, because those rocks experienced Triassic cooling, as indicated by the 245–210-Ma $^{40}Ar/^{39}Ar$ cooling ages. Note that folding in the Yangtze belt involves rocks whose ages as young as the late Jurassic. Cretaceous rocks are clearly related to the late Cretaceous extension, as they are restricted in the extensional basins and unconformably lie on top of the Paleozoic–Jurassic folded sequence. The symbols in the cross section are same as those on the map. (Adapted from Anhui BGM, 1987.)

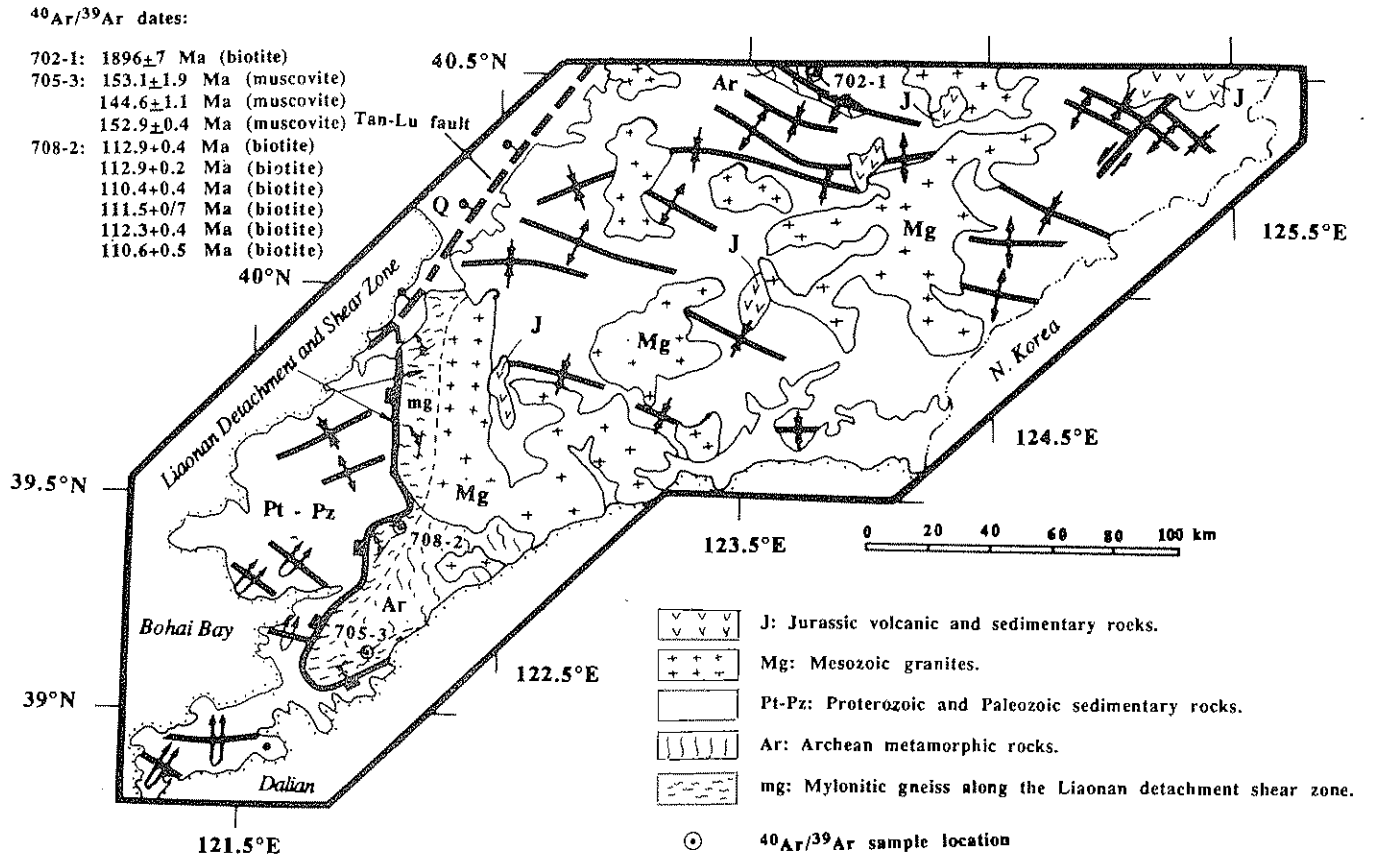

Figure 20.5A. Simplified geologic map of southern Liaoning, based on the geologic map of Liaoning province, scale 1 : 500000 (Liaoning BGM, 1989), showing the Liaonan detacbment and E–W-trending thrusts and folds in the hanging wall of the detachment. Sample locations for $^{40}Ar/^{39}Ar$ dating are also shown. The thermochronologic data corresponding to the numbers shown on the map are summarized at the upper left.

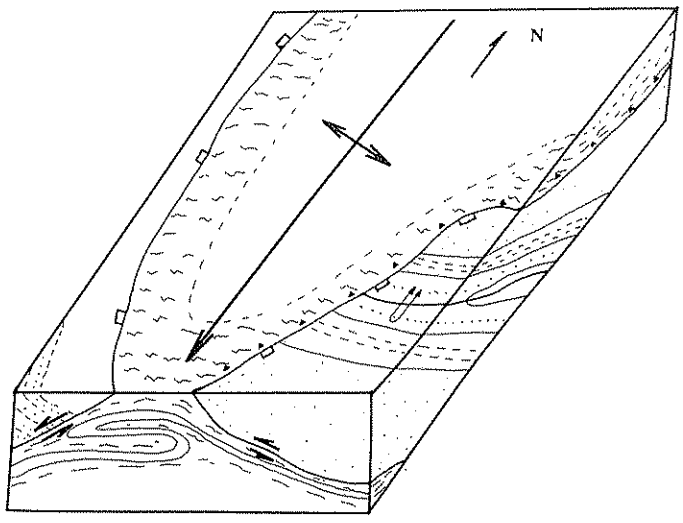

Figure 20.5B. Block diagram showing relationships between the warped Liaonan detachment fault and the hanging wall of the Triassic–early Jurassic fold-and-thrust belt. Note that ductile nappes in the footwall of the nappe verge toward the west, consistent with the kinematic indicators suggesting a top-to-the-west sense of shear.

and Qaidam (Li et al., 1978). The apparent offset of the Proterozoic–Triassic contact in the Qilian Shan region and the oroclinal geometry of the fold-and-thrust belt suggest that right-lateral strike-slip movement occurred along the Qilian suture system in the Jurassic. The western Ordos fold-and-thrust belt may have been initiated in the late Triassic, as indicated by an abrupt change from dominantly lacustrine deposition to dominantly coarse alluvial-fluvial deposits derived from the west (Sun, Xie, and Yang, 1989). The thicknesses of the late Triassic basal conglomerate are 3·km along the western margin and 1.5 km along the eastern margin of the Ordos basin, respectively (Figure 20.7B). That change in thickness may be attributable to loading of the east-directed thrust system in the western Ordos, which was in turn controlled by the collision between North China and South China, as suggested by Sun et al. (1989). Because the Cretaceous strata are not involved with the folding and thrusting in the western Ordos (Ningxia BGM, 1989) (Figure 20.7A), the development of the western Ordos thrust belt ceased by the end of the Jurassic. The timing and geometric relationships between the thrust belt and the E–W-trending faults in the Qilian Shan region require that the right-slip deformation could also have been initiated in the Triassic and lasted to the Jurassic.

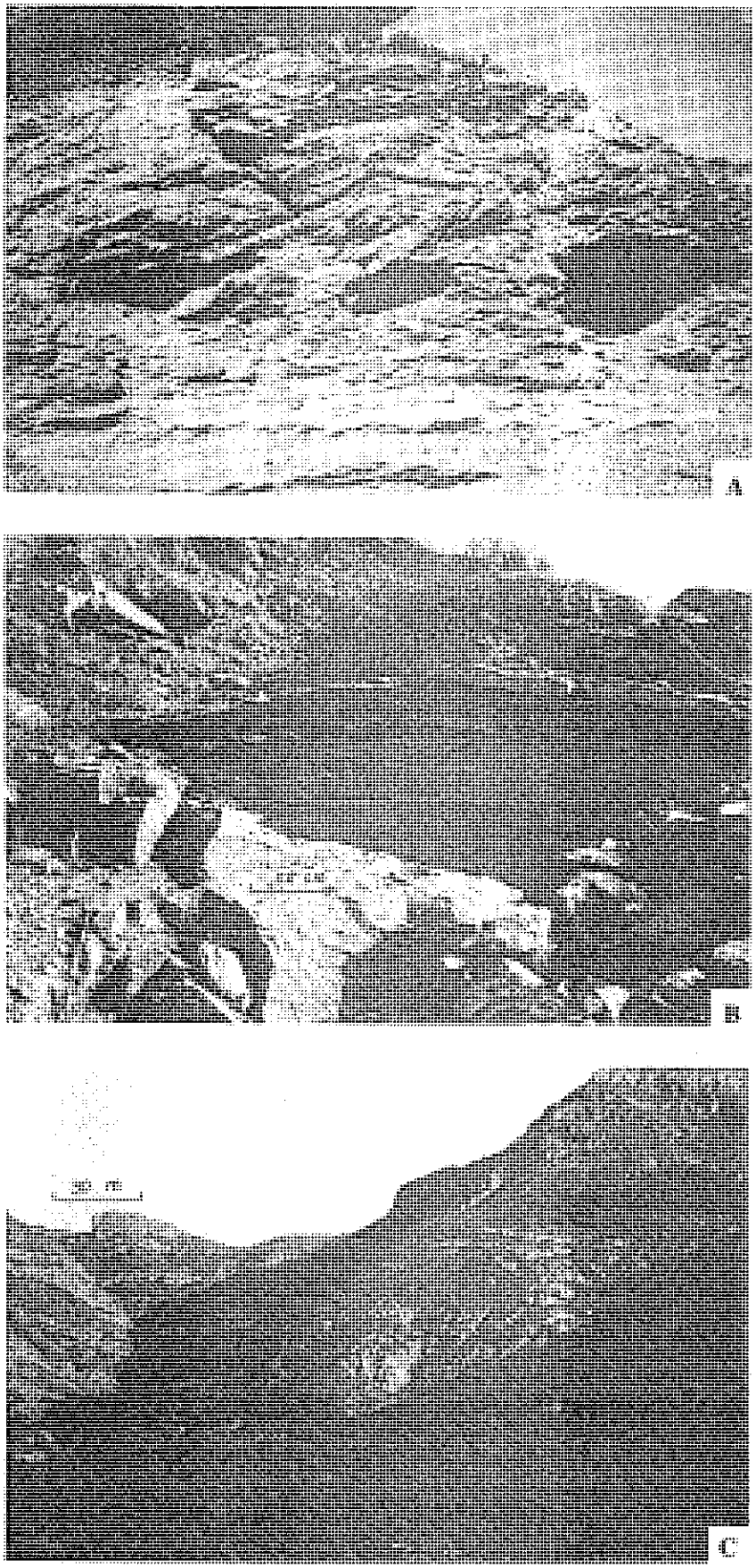

Figure 20.6A. E–W-trending overturned folds of the Paleozoic strata in southern Liaoning. This structure is located in the hanging wall of the Liaonan detachment fault. (B) Asymmetric boudinage observed from the mylonitic gneisses in the footwall of the Liaonan detachment fault, indicating a top-to-the-west sense of shear. (C) Overturned west-verging ductile nappe in the footwall of the Liaonan detachment fault.

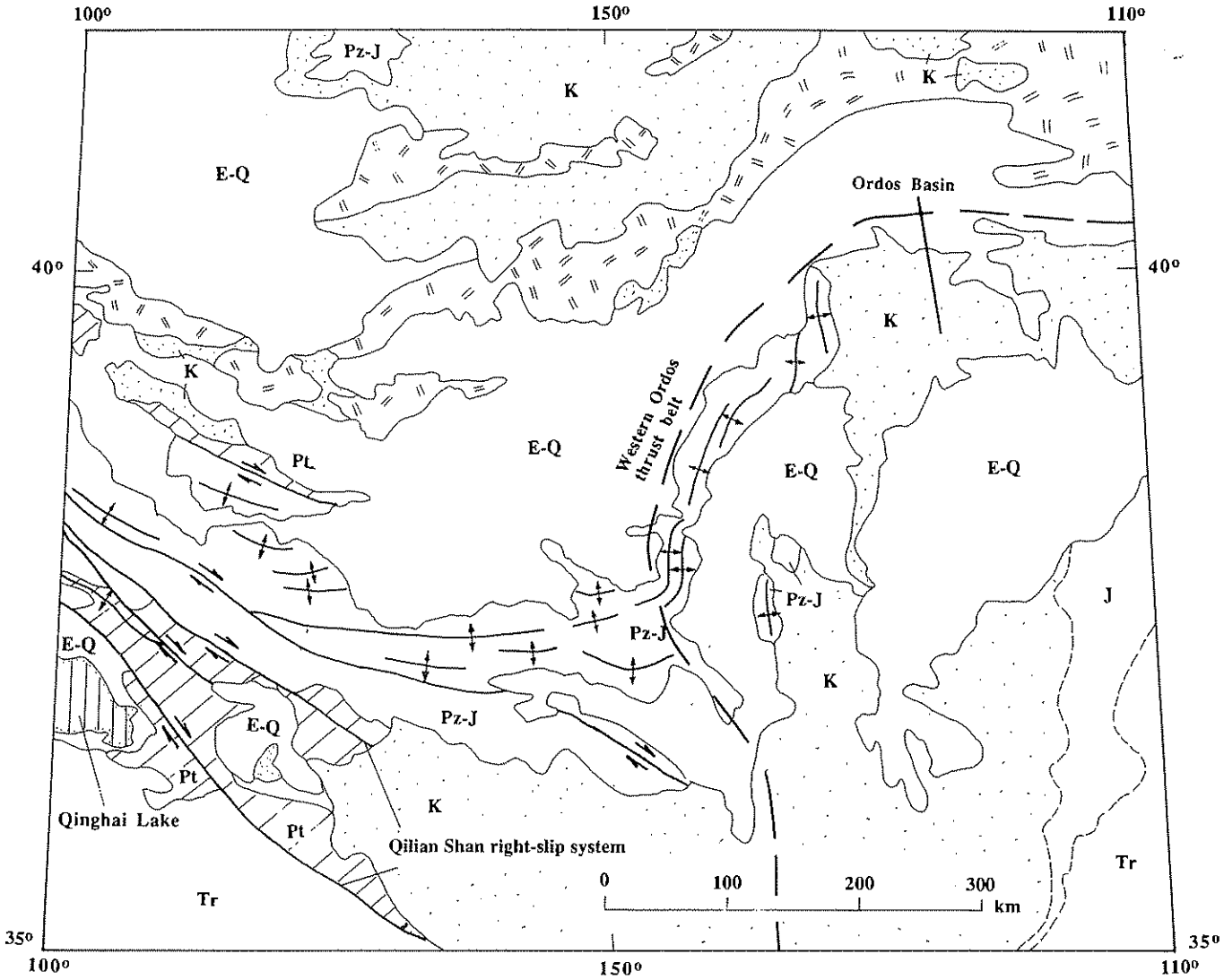

Figure 20.7A. Simplified geologic map of the Qilian and western Ordos region (Ningxia BGM, 1989). Note that folds involving Paleozoic–Jurassic strata make a sharp turn as they approach toward the Qilian suture zone. The bent fold belt is interpreted as an orocline developed during the Triassic–Jurassic right-slip faulting along the middle Paleozoic Qilian suture zone.

Southeast of the Qilian Shan region is the Qinling suture zone, where Triassic left-slip motion has been documented and extended to the eastern Kunlun Shan, which bounds the Qaidam block to the north (Mattauer et al., 1985). Based on the geometric relationships of the strike-slip faults in the Qilian Shan, Qinling, and eastern Kunlun Shan, we speculate that the Qaidam block was extruded westward during the Triassic–Jurassic. The strike-slip faulting was, in turn, induced by the collision between the North and South China blocks. If the late Paleozoic batholith belt in the eastern Kunlun Shan was the southern active margin of the North China block in the Dabie Shan and Qinling regions prior to the collision of North China and South China (Mattauer et al., 1985), then the magnitude of westward extrusion of the Qaidam block in the middle Paleozoic should have been at least 600 km.

A middle Paleozoic collision in the Qinling and Qilian regions was first proposed by Li et al. (1978) (Figure 20.8) and supported by later studies (e.g., Zhang ef al., 1984; Mattauer et al., 1985; Kröner et al., 1993). The spatial distribution of the western suture zone is unclear, because it abruptly terminates at the Altun Tagh fault, which is a major Cenozoic strike-slip fault that developed during the collision between India and Asia (Molnar and Tapponnier, 1975; Tapponnier et al., 1982; Burchfiel et al., 1989; Altun Tagh Working Group, 1992). The magnitude of left-slip along that fault is estimated to be about 500 km, as measured by the offset of the late Paleozoic magmatic arc (Peltzer and Tapponnier, 1988) (Figure 20.9). This implies, if it is the same arc, that the western extension of the Qilian suture should lie underneath the Tarim basin and be covered by Cenozoic sediments.

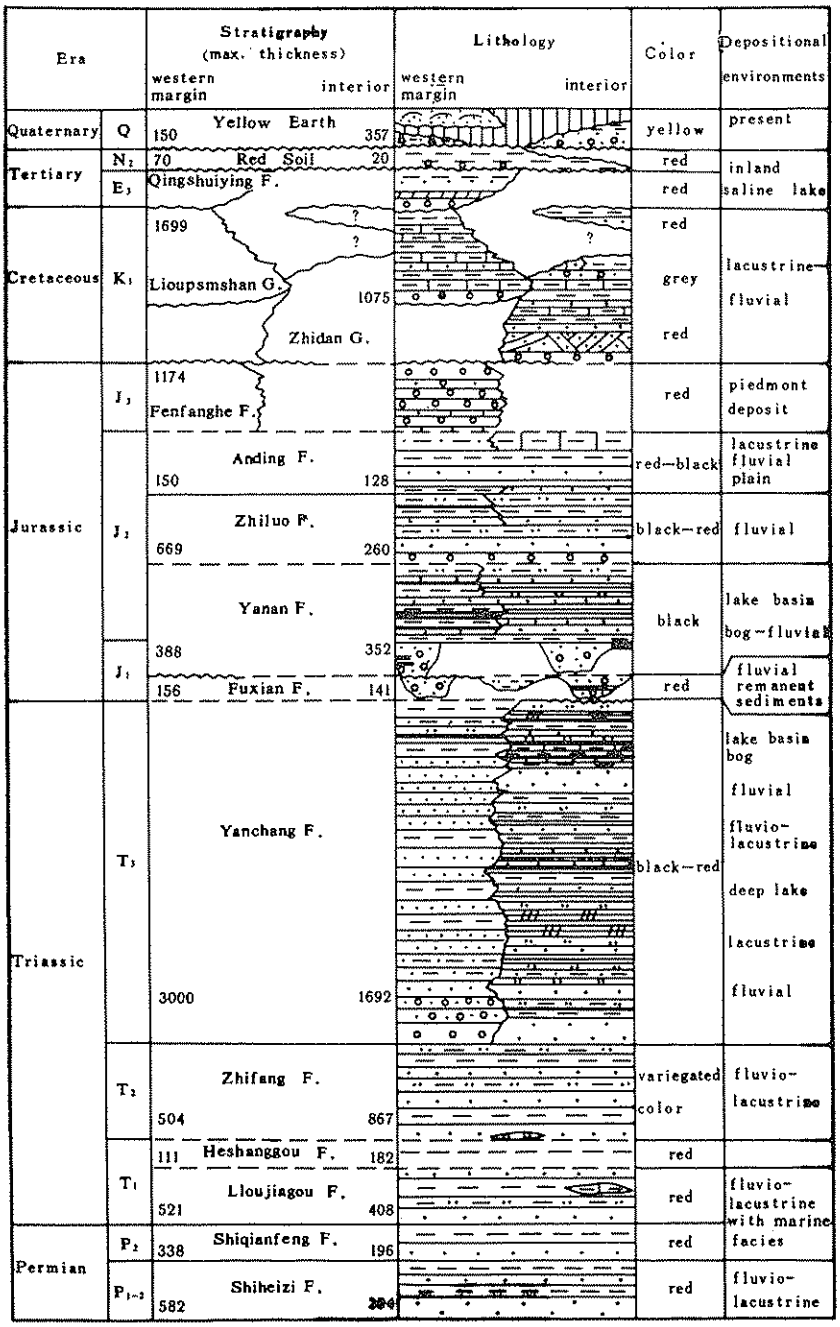

Figure 20.7B. Stratigraphic section of the Permian–Jurassic in the western Ordos region (Sun et al., 1989). The appearance of clastics and the rapid sedimentation rate in the Triassic are interpreted as signaling the initiation of the western Ordos fold-and-thrust belt.

Geology of the Tarim basin

The present Tarim basin is a late Cenozoic feature, as it is covered by Neogene sediments (Zhou and Chen, 1990; Jia et al., 1991) (Figure 20.9). Recent drilling, seismic-reflection profiles, and field studies in the basin suggest that it has had a protracted history of deformation since the late Precambrian (Jia et al., 1991; Hendrix et al., 1992; Carroll et al., 1995). The Precambrian stratigraphy in Tarim and the southern Tien Shan is exposed in the Keping (NW Tarim) and Kuruk Tagh (NE Tarim) regions (Figure 20.10). The Keping sequence is assigned to the upper Qingbaikouan and Sinian systems. Upper Qingbaikouan strata consist dominantly of sandstone, whereas the Sinian strata are dominantly conglomerate, sandstone, shale, and carbonate. The conglomerate is interpreted to be a glacial deposit (Zhou and Chen, 1990), although some of it may be alluvial (S. A. Graham, personal communication, 1995). In the Kuruk Tagh region, the Qingbaikouan sequence is mostly stromatolite carbonate. The Sinian strata lie conformably above the Qingbaikouan system and consist of multiple layers of glacial deposits, volcanic deposits, sandstone, and carbonate. Those sediments are concentrated in a trough, the Manjiaer depres-

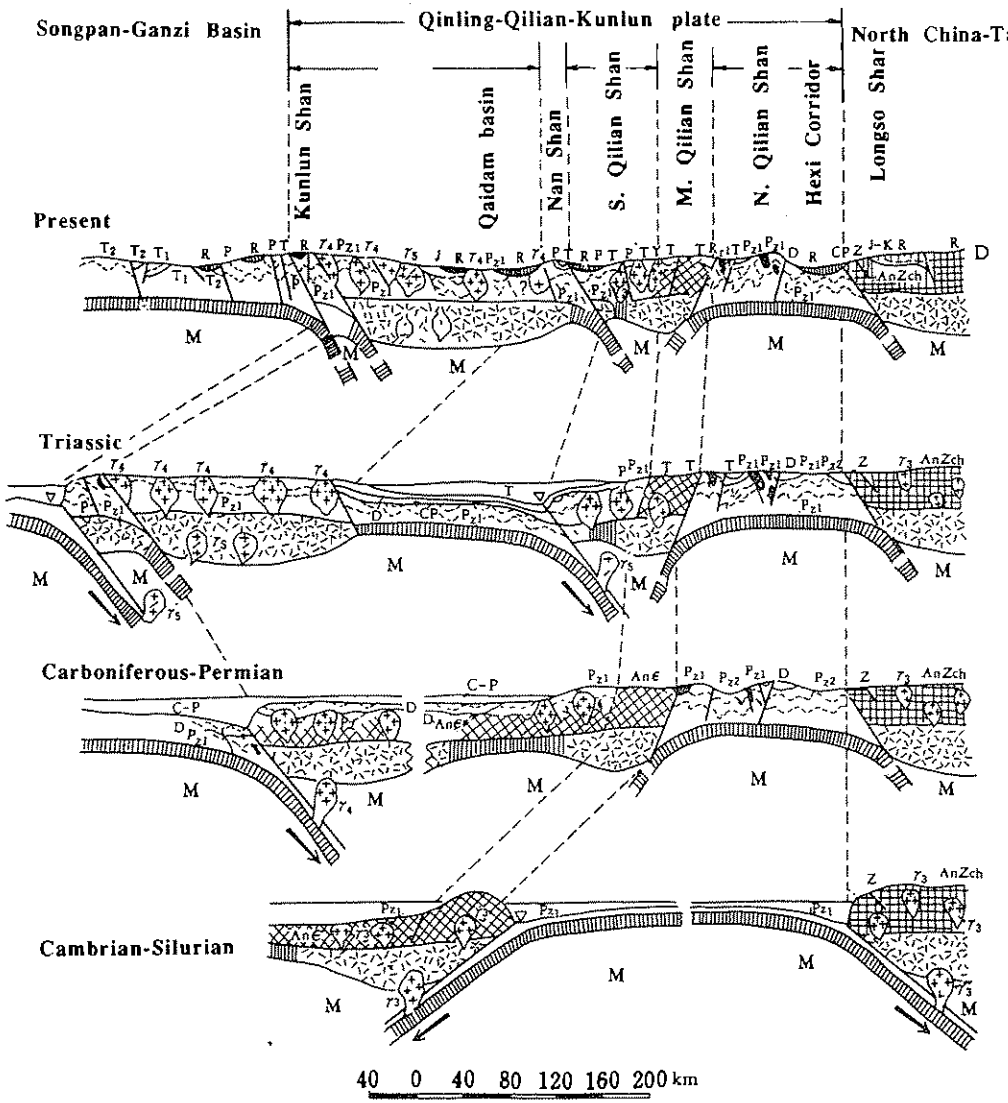

1. Cenozoic terrestrial basins
2. fold belt
3. pre-Changchengian basement rocks
4. pre-Sinian basement rocks
5. Precambrian basement rocks
6. melange complex
7. ophiolite
8. early Paleozoic granite and granodiorite
9. late Paleozoic granite
10. early Mesozoic granite and granodiorite
11. late Mesozoic granite
12. fault
13. contact
14. nonconformity
15. nonconformity in the intracontinental basins
16. continental crust
17. oceanic crust
18. subduction direction

R: Cenozoic
J-K: Cretaceous-Jurassic
T: Triassic
P: Permian
C: Carboniferous
Pz1: early Paleozoic
Pz2 late Paleozoic
Z: Sinian
An€: Precambrian
AnZch: Pre-Sinian
M: mantle

Figure 20.8 Schematic cross sections showing the evolution of the Qilian suture system. (Adapted from Li et al., 1978.)

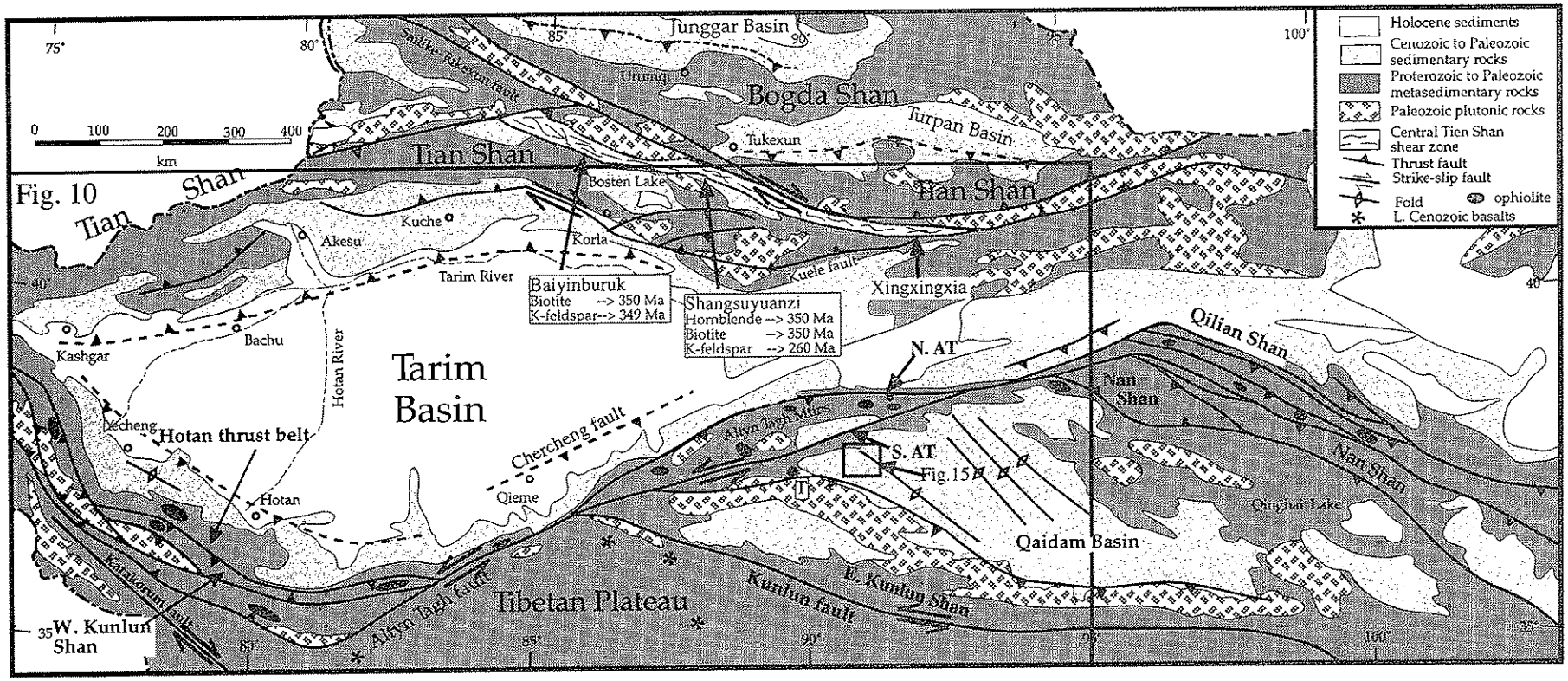

Figure 20.9 Simplified geologic map of the Chinese Tien Shan, Altun Tagh, Kunlun Shan, Tarim, Qaidam, and Qilian Shan regions; data from Chen (1989), with our own tectonic interpretations. The map shows locations for $^{40}Ar/^{39}Ar$ samples and their ages in the central Tien Shan ductile shear zone.

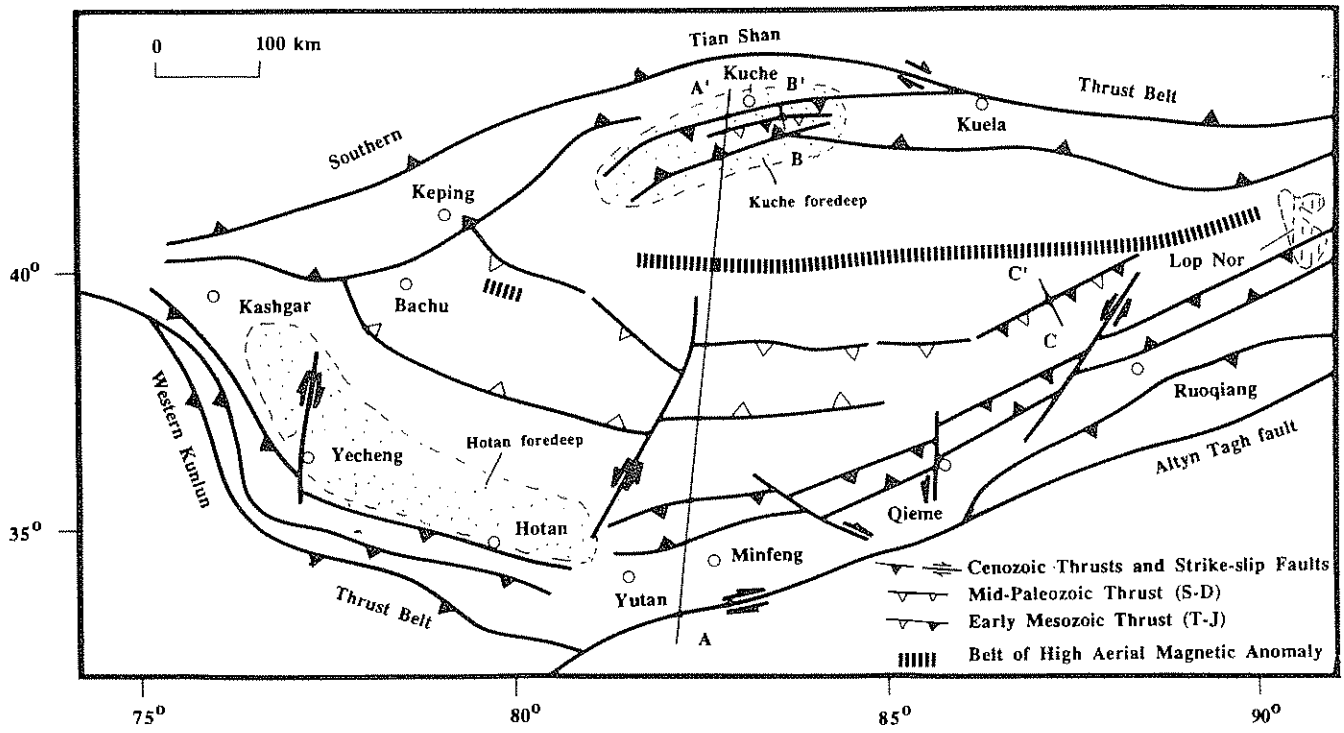

Figure 20.10A. Simplified tectonic map of the Tarim basin, showing locations of geologic cross sections. (Adapted from Zhou and Zheng, 1990.)

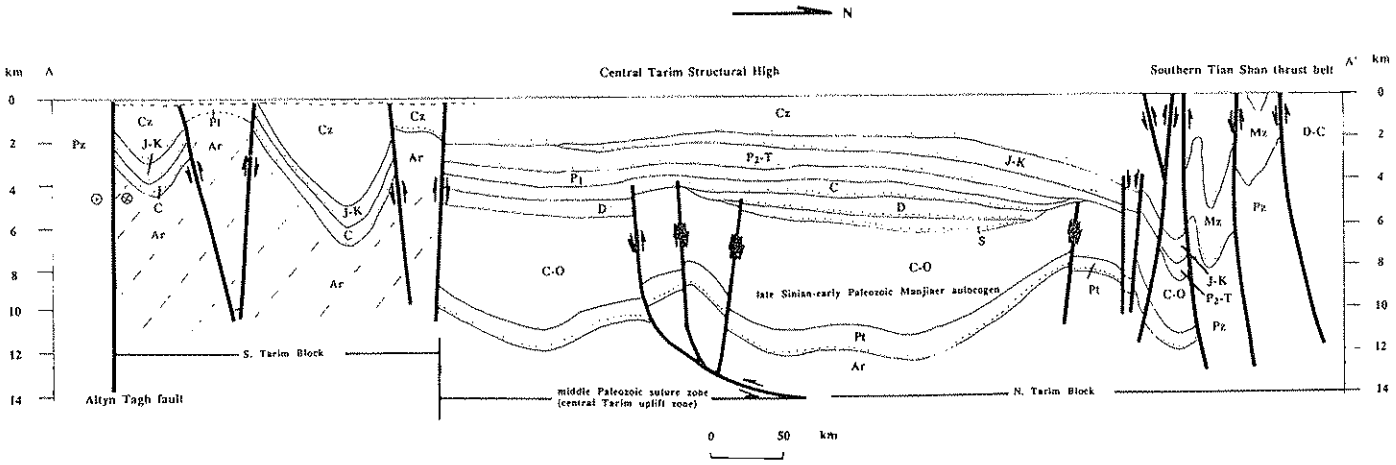

Figure 20.10B. Schematic geologic cross section across the Tarim basin. See part A for location. (Adapted from Jia et al., 1991.)

sion, in the northeastern Tarim and are interpreted to be the result of rifting in the late Precambrian (Jia et al., 1991) (Figure 20.10).

We consider the North and South Tarim blocks as continental blocks separated by an intervening ocean prior to the middle Devonian. This division is based on the geometric requirement for the offset late Paleozoic magmatic belt between the eastern and western Kunlun Shan on both sides of the Altun Tagh fault (Figure 20.9), which requires the offset Qilian Shan suture zone north of the Altun Tagh fault in central Tarim (Figure 20.10A). We warn the reader, however, that this tectonic scheme is not universally accepted. In fact, Carroll et al. (1995) proposed that the central Tarim uplift zone formed as a consequence of collision between the Tarim block and the central Tien Shan arc of Windley et al. (1990) in the middle Paleozoic. Both the North and South Tarim blocks contain carbonates and sandstone of Cambrian and Ordovician age. During the Silurian, the tectonic settings of both North Tarim and South Tarim changed – from

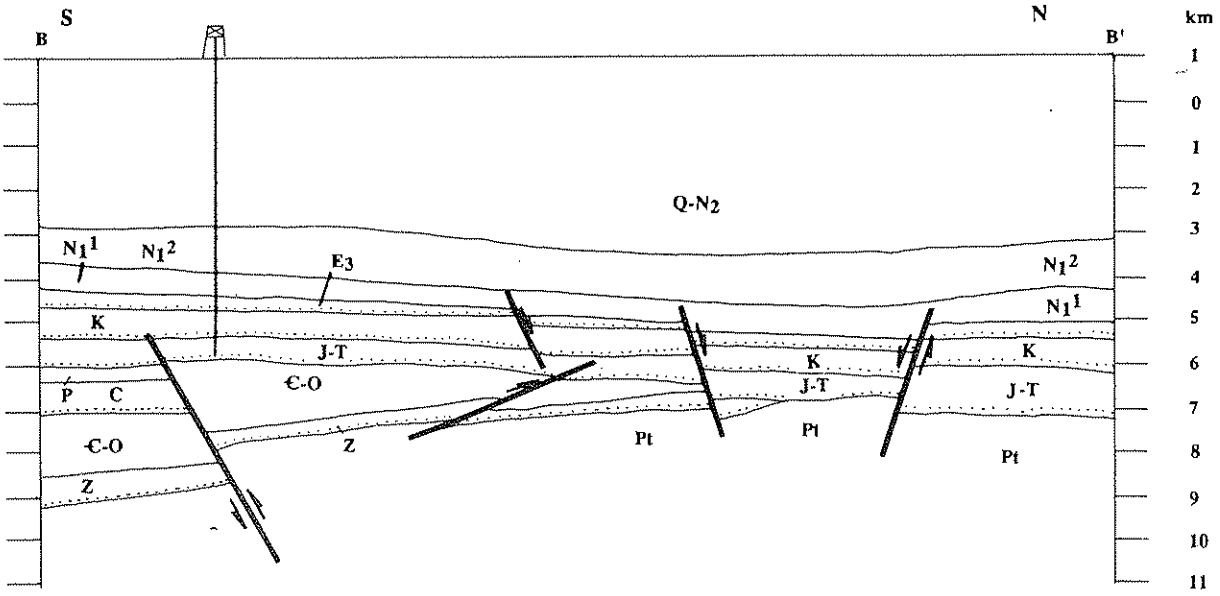

Figure 20.10C. Geologic cross section of north-central Tarim. See part A for location.

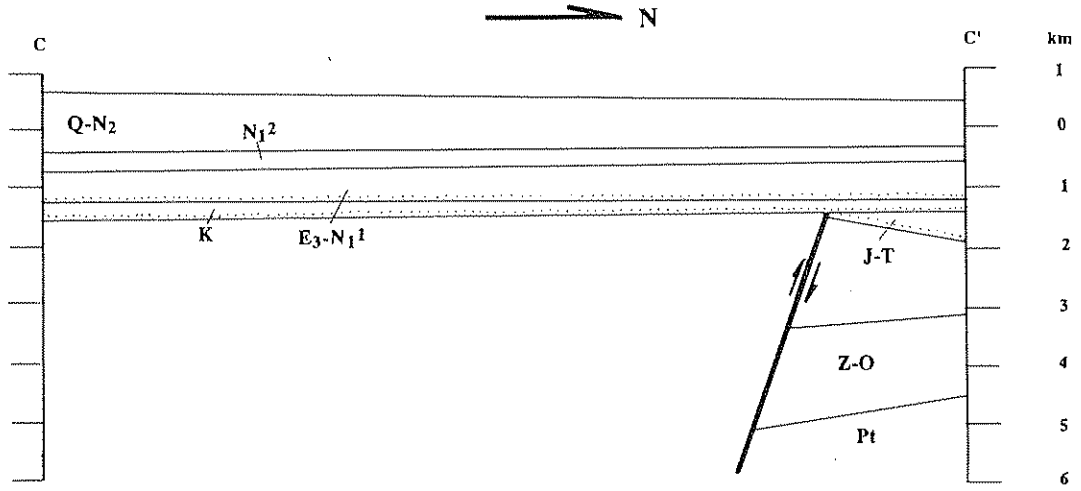

Figure 20.10D. Geologic cross section of eastern Tarim. See part A for location.

passive-margin continental-shelf deposition to a volcanic-arc setting in North Tarim and regional uplift in South Tarim. This is suggested by the absence of Silurian sedimentation in the South Tarim block south of the central Tarim uplift zone (Figure 20.10A) and the widespread deposition of a thick sequence of flysch and volcaniclastics in the North Tarim block (Zhou and Chen, 1990). We interpret the Silurian sequence in the North Tarim block as having been deposited in an arc and/or fore-arc setting when the South Tarim block was subducting beneath the North Tarim block. During the Devonian, both the North and South Tarim blocks were areas of fluvial deposition (Zhou and Chen, 1990). Sedimentologic studies of the Devonian and Lower Carboniferous strata in tbe Aksu region between Keping and Kuche (Figure 20.10A) suggest that the source region for the sediments was to the south (Carroll et al., 1995). Seismic-reflection studies suggest that the central Tarim uplift zone is a middle Paleozoic contractional belt (Figure 20.10B) (Jia et al., 1991). Because the late Paleozoic magmatic arc may be offset for about 500 km along the Altun Tagh fault (Peltzer and Tapponnier, 1988), it is possible that the uplift zone represents the western extension of the middle Paleozoic Qilian suture zone (Figures 20.9 and 20.10). This is implied by the geometric relationship between the late Paleozoic magmatic arc across the Altun Tagh fault system with respect to the Qilian suture zone (Figures 20.9 and 20.10). This interpretation suggests that Devonian terrestrial sedimentation in the soutbernmost Tien

Tertiary Stratigraphic Section of Kuche Area, Northern Tarim (after Ye and Huang, 1992)

Age	Fm.	Thick	Lithology	Description	Fossil Content
Pliocene	Xiyu	50 - 606m		dark gray conglomerate, with brown sandy mudstone interbeds. maximum thickness: 1366m	no fossil reported
	Kuche	300 - 700 m		grey, brown conglomerates interbeded with grey sandstone maximum thickness: 2670m	Charophyta, Ostracod
Miocene	Kangcun	300 - 800 m		upper: gray, brown sandstone & siltstone; lower: gray sandstone and brown mudstone, with greenish siltstone interbeds	Charophyta, Ostracod
	Jidike	600 - 800 m		red, grayish green sandstone and mudstone interbeds, with minor amount of conglomerates and gypsym-bearing siltsone.	Charophyta, Ostracod
	Suweiyi	200 - 400 m		dark red conglomerates, sandstone and mudstone interbeds, with gypsum and salt	Charophyta, Ostracod
				unconformity (Oligocene missing)	
Paleocene - Eocene	Awate	239 m		upper: rock salt with mudstone lower: purple and greenish mudstone, siltstone and tuffaceous interbeds	no fossil reported
	Xiaokuziba	230 m		red, purple sandy mudstone, siltstone, and thin gypsum, carbonate rocks	Foramnifera, (marine) Ostracod, Gastrapod
	Dalake	209 m		top: gypsum, siltstone, and calcareous mudstone; middle: multi-colored fine grain clastics with dolomite; bottem: mostly conglomerates, clast-bearing limestone	(marine) Ostracod, Clams, Fastrapods
				unconformity (no L. Paleocene)	
Upper Cretaceous	Dalake	62 - 200 m		upper: pink and purple sandstone siltstone and mudstone; lower: purple conglomerate	(fresh water) Ostracod

Figure 20.11A. Stratigraphic section of the Kuche area. (Adapted from Ye and Huang, 1992.)

Tertiary Stratigraphic Section of Hotan Area, Southwest Tarim (after Ye and Huang, 1992)

Age	Fm.	Thick	Lithology	Description	Fossil Content
Pliocene	Xiyu	100 - 3000 m		dark gray thick conglomerate, with occasional conglomatic sandstone	Ostracod
	Atushi	670 - 3400 m		upper: gray, red conglomerate, sandstone with siltstone & mudstone lower: gray, red sandstone and conglomerate	Chaophyta, Ostracod
Miocene	Wuqia Group Pokabulake	1100 - 2168 m		thick brown, red sandy mudstone and gray sandstone, siltstone interbeds	Foramnifera, Ostracod
	Wuqia Group Anquan	468 - 668 m		upper: multi-colored mudstone, sandstone; middle: mainly mudstone, w/ sandstone & gypsum; lower: gray, black mudstone with sandstone and siltstone (mud cracks preserved in siltstone)	Foramnifera, Ostracod
	Wuqia Group Kezhiluoyi	422 - 451 m		upper: gray sandstone, with red mudstone and conglomerate; lower: red sandstone and siltstone, with several horizons of gypsum	Foramnifera, Ostracod
Oligocene	Kashi Group Bashibulake	341 - 801 m		red mudstone, and fine grain sandstone, with gypsum nodules in lower parts	Foramnifera, Clamnifera, Ostracod, Gastropod
	Kashi Group Wulagan	120 m		upper: red mudstone, green sandstone; lower: gray, green mudstone, with thin limestone	Foramnifera, Clamnifera, Ostracod, Gastropod
Eocene	Kashi Group Kalataer	112 m		upper: limestone lower: red gypsum mudstone, gypsum, gray limestone, and yellow mudstone	Foramnifera, Clamnifera, Ostracod
Paleocene	Kashi Group Qimugan	194 m		upper: purple mudstone, and gypsum; lower: gray, green mudstone with thin limestone	Foramnifera, Clamnifera, Ostracod
	Kashi Group Aertashi	413 m		upper: gray sandy & muddy limestone; lower: white gypsum layers	Clamnifera, Ostracod
U. Cretaceous	Tulukeyi	< 67 m		red mudstone, gypsum mudstone, with few thin limestone beds	

Figure 20.11B. Stratigraphic section of the Hotan area. (Adapted from Ye and Huang, 1992.)

Shan resulted from the middle Paleozoic collision and that the central Tarim high aeromagnetic anomaly (Figure 20.10A) may represent either the remnant north-dipping oceanic slab of South Tarim underneath North Tarim or the Silurian volcanic rocks in North Tarim. This is in contrast to the interpretations that the aeromagnetic anomaly represents a trapped back-arc oceanic basin (Hsü, 1988) or a late Precambrian–early Paleozoic aulacogen (Jia et al., 1991).

In addition to the middle Paleozoic deformation in the central Tarim basin, widespread Triassic–Jurassic deformation has been documented in eastern Tarim (Jia et al., 1991) (Figure 20.10C-D). Those structures are variably interpreted as contractional (Jia et al., 1991) or transpressional structures (Yan, 1991). The latter interpretation is based on the observation that those faults commonly exhibit flower structures (Yan, 1991). The Triassic–Jurassic structures in eastern Tarim could have been connected with the Triassic–Jurassic right-slip fault system in the Qilian Shan (Figure 20.1). If this interpretation is valid, it implies that the collision of the North and South China blocks affected a much larger region than previously considered (Yin and Nie, 1993).

On the basis of isopach patterns and the sedimentation rates, Hendrix et al. (1992) proposed that the Triassic–Cretaceous sedimentation in the Tien Shan occurred in foreland basins produced by N–S compression. They further suggested that the Mesozoic pulses of coarse clastic sedimentation in the Tien Shan were correlated with successive collisional events between the southern margin of Eurasia and the Qiangtang and Lhasa blocks and Kohistan arc. Because the Triassic–Jurassic faults have not been directly studied in the field, the kinematics of the faults imaged by seismic profiles in the Tarim basin remain unknown.

Two regions of the Tarim basin received thick (75 km) Cenozoic sediments: the Kuche and Hotan foredeeps (Figure 20.10A). Their development was interpreted to be related to the southern Tein Shan and western Kunlun thrust belts, respectively (Figure 20.10A) (Zhou and Zheng, 1990; Zhou and Chen, 1990). The ages of initiation of the foredeep basins can constrain the ages of initial thrusting in both thrust belts. Generalized stratigraphic columns of the Kuche and Hotan areas are shown in Figure 20.11. On the basis of biostratigraphic constraints (Ye and Huang, 1992), we plotted the sedimentation rates as functions of time for both

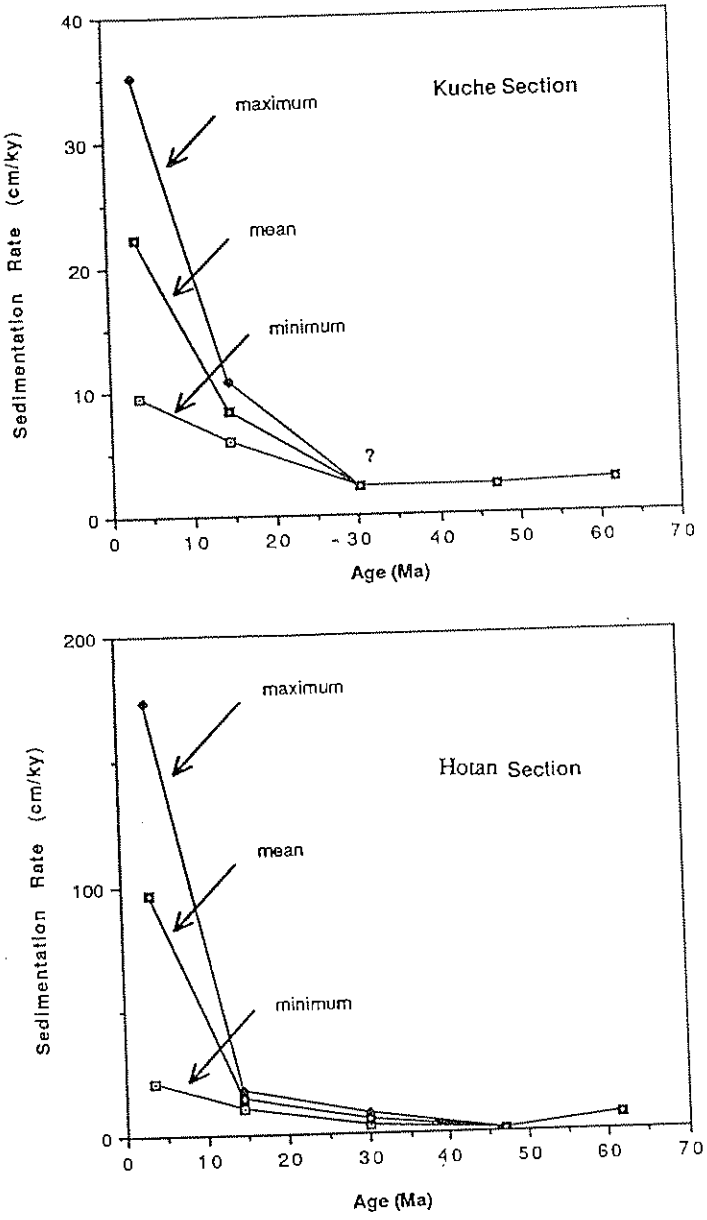

Figure 20.12 Inferred Cenozoic sedimentation rates in (A) the Kuche area and (B) the Hotan area, based on biostratigraphic information of Ye and Huang (1992).

areas (Figure 20.12). It is apparent that the sedimentation rate increased rapidly between about 20 Ma and 15 Ma in both areas. That abrupt jump in sedimentation rate suggests that the southern Tien Shan and Hotan thrust belts were initiated in the mid-Miocene, about 30 m.y. after the collision between India and Asia began. As the Hotan thrust belt is interpreted to be geometrically and kinematically linked with the Altun Tagh strike-slip system to the east and the Pamir thrust system–Chanman strike-slip fault to the west (Yin et al., 1993), the Altun Tagh fault can be inferred to have been initiated in the mid-Miocene. This conclusion is similar to that of Avouac and Peltzer (1993), based on extrapolation of the current rate and total magnitude of shortening in the Tien Shan. Note that the lower part of the biostratigraphy of the Hotan section is well constrained on the basis of foraminifera and other marine fossils from the Upper Cretaceous to Lower Oligocene (Hao, 1983; Tang, 1990). The Kuche section consists entirely of alluvial and fluvial deposits, and thus its age is more problematic. However, preliminary results from recent magnetostratigraphic studies (Craig et al. 1994), fission-track cooling ages in the Tien Shan (Hendrix, Dumitra, and Graham, 1994), and inferences about the duration of Cenozoic shortening in the Tien Shan, based on the current slip rate and the total amount of shortening (Avouac and Peltzer, 1993), are consistent with the age assignment of the Kuche section by Ye and Huang (1992) and the interpretation that thrusting in the southern Tien Shan began at about 20 Ma.

Geology of the Tien Shan

The Tien Shan, one of the longest mountain belts in the world, with an average elevation of about 3,500 m, extends east–west for more than 2,500 km across Central Asia (Figure 20.9). Its western part is located in the former USSR and connects with the Pamir syntaxis. Its eastern part, approximately 1,700 km long (that nearly equals the total length of the U.S. Cordillera) and 300 km wide, is located in northwestern China. The geology of the western Tien Shan and the Pamir region has been described in detail by Burtman and Molnar (1993). On the basis of paleomagnetic analysis, sedimentologic studies, and structural investigations, Burtman and Molnar (1993) suggested that the south-dipping thrusts in the Pamir region originated as straight traces in the Neogene and became curved because of development of the Pamir syntaxis. Those south-dipping thrusts in the Pamir are geometrically linked with the thrust system along the northern foothills of the western Kunlun Shan (i.e., the Hotan thrust system) (Figure 20.16). Together, the thrusts in the Pamir and the western Kunlun have accommodated the southward subduction of the Tarim block underneath the western Kunlun Shan and Pamir and have produced seismicity at depths greater than 200 km. The Neogene initiation of the Pamir thrust system suggested by Burtman and Molnar (1993) is consistent with the inferred age of initiation of the Hotan thrust system.

The development of the Tien Shan orogenic belt was related to arc–continental collision (Windley et al., 1990) in the middle Paleozoic, followed by reactivation due to successive collisions of island-arc systems onto the southern margin of Asia (Hendrix et al., 1992), and has been rejuvenated in the late Cenozoic because of the Indo–Asian collision (Burchfiel and Royden, 1991). The Tien Shan is flanked by E–W-trending active thrust systems on both sides (Molnar and Tapponnier, 1975; Tapponnier and Molnar, 1979; Burchfiel and Royden, 1991; Molnar et al., 1994; Burchfiel et al., 1994; Nie et al. 1994a). The axial part of the mountain range is transected by the WNW-trending Sailimu–Tukexun fault system, or the central Tien Shan fault system of Hendrix et al., (1992). The Sailimu–Tukexun fault system was recognized from Landsat images by Tapponnier and Molnar

(1979) as a right-lateral strike-slip fault. That fault bounds the Turpan basin to the north and Boston basin to the south. Both basins are also bounded by thrusts that merge with the Sailimu–Tukexun fault system (Figure 20.9). That relationship and the fact that both the strike-slip and thrust systems are presently active suggest that the two systems have been kinematically linked: Strike-slip faulting transfers shortening from one thrust system to another. Our estimation of the time of initiation of the Sailimu–Tukexun fault system can be constrained on the basis of a time of rapid subsidence and drastic increase in the input of coarse clastic sediments in the early Miocene in the Turpan and Boston basins (Xinjiang BGM, 1993).

The relationships between the Paleozoic–Mesozoic structures and Cenozoic tectonics in the Tien Shan have been discussed by Windley et al. (1990) The Mesozoic sedimentary history and its relationship to regional tectonics has been discussed by Graham et al. (1991), Hendrix et al., (1992), and Carroll et al. (1995). Hendrix et al. (1992) related episodic foreland-basin sedimentation in the Tien Shan region in the Mesozoic to successive collisional events between the southern margin of Eurasia and the Qiangtang and Lhasa blocks and Kohistan arc.

During the summers of 1992, 1993, and 1994, we undertook preliminary studies along three highways (the Dushanzi–Kuche, Urumuqi–Korla, and Hami–Dunhuang) across the Tien Shan. A ductile shear zone of at least several hundred meters was recognized in all three transects, at Bayinburuke, Shangsuyuanzi, and Xingxingxia, respectively (Figure 20.9). Subhorizontal lineations, asymmetric boudinage, and *S-C* mylonitic fabrics suggested that it is a rigbt-lateral strike-slip system (Figure 20.14). Where the ductile shear zone was observed during that study, the age of the mylonitic gneiss in the shear zone was assigned as either Proterozoic or Silurian in the geologic map of Xinjiang (Chen, 1985). Hornblende $^{40}Ar/^{39}Ar$ ages and field observations of the shear zone suggest that those Proterozoic and Silurian rocks consist not only of metasedimentary rocks, but also of mylonitic granite and granodiorite of Carboniferous age. Based on the distribution of those rocks and the geologic map of Xinjiang, we interpret the "basement" rocks in the central Tien Shan to be part of the same central Tien Shan ductile shear zone (Figure 20.9). We are not certain how far the shear zone extends to the east and west. The observed ductile shear zone coincides with the Nikolaev line of Burtman (1975) and Şengör et al. (1993), who interpreted that tectonic boundary to be Permian and to indicate left-lateral strike slip. Allen, Şengör, and Natal'in (1994) related that proposed left-slip system in the central Tien Shan to the opening of the Junggar basin in the Permian. The kinematic indicators observed in our studies are inconsistent with the left-slip interpretation, but that does not preclude possible reactivation along the fault system, as detailed mapping is yet to be conducted.

The ductile shear zone in the central Tien Shan has been dated in two places, one near Shangsuyuanzi along the Urumuqi–Kuala highway and one along the Dushanzi–Kuche highway near Bayinburuke (Figure 20.9). In Shangsuyuanzi, $^{40}Ar/^{39}Ar$ cooling ages for hornblende, biotite, and K-feldspar from a deformed granodiorite (samples TS-0 and TS-1; Figures 20.9 and 20.13) are 350 Ma, 350 Ma, and 260 Ma, respectively. We interpret 350 Ma as the time of granite emplacement; similar ages for hornblende and biotite are results of conductive cooling during pluton emplacement. This implies that the ductile shear zone was initiated after 350 Ma. The K-feldspar age spectrum is consistent with the ambient temperature having dropped below about 200°C by 250 Ma (Lovera, Richter, and Harrison, 1989, 1991). Because that is well below the temperatures associated with the brittle–ductile transition, this implies that the exposed part of the ductile shear zone probably stopped moving in the late Permian. Although this does not preclude possible continuation of ductile deformation at deep-crustal levels and brittle deformation at shallow levels along the same shear zone, cataclastic deformation in the fault zone has not been observed. The shear zone near Bayinburuke has also been dated. The $^{40}Ar/^{39}Ar$ ages for K-feldspar and biotite are essentially the same (~350 Ma), indicating that the shear zone postdates the early Carboniferous. The ductile shear zone could have been active during and after the late Permian. More detailed structural mapping and geochronologic work will be needed to decipher the origin and timing of the shear zone. Considering the suggestion that the Triassic–Jurassic faults in the northern Tarim basin could have been related to strike-slip faulting, as indicated by the development of flower structures (Yan, 1991), the central Tien Shan ductile shear zone could have been synchronous with and related to strike-slip faulting in the northern Tarim.

Geology of the Qaidam basin

The Qaidam basin is located between the Qilian Shan and the Tibetan plateau, and its present configuration began to develop in the Cenozoic (e.g., Song and Wang, 1993). Because it contains Upper Cenozoic strata, its subsurface geology has been inferred from seismic-reflection profiles and drill-hole data (Song and Wang, 1993), as well as from the exposed rocks to the north, along the southern flank of the Qilian Shan, and to the south, along the eastern Kunlun Shan (Qinghai BGM, 1989). Lower Proterozoic–Sinian metamorphic rocks are exposed together with highly deformed Lower Paleozoic deep-marine and volcanic rocks (Cambrian–Silurian) along the southern flank of the Qilian Shan (Qinghai BGM, 1989). Deformation of the Lower Paleozoic rocks is interpreted to have been the result of the early Paleozoic subduction of an oceanic plate consisting of the Qaidam block, which could have been an island-arc or accretionary complex, underneath the North China block (Li et al., 1978) (Figure 20.8). Devonian clastic rocks are exposed along the southern flank of the Qilian Shan, marking the end of suturing between the Qaidam and North China blocks (Li et al., 1978). In the Carboniferous and Permian, the Qaidam region was the site of shallow-marine deposition of limestones (Qinghai BGM, 1989). During the late Carboniferous and Permian, a magmatic arc developed along its southern edge because of northward subduction of the Paleo-Tethys, resulting in the eastern Kunlun Shan magmatic belt.

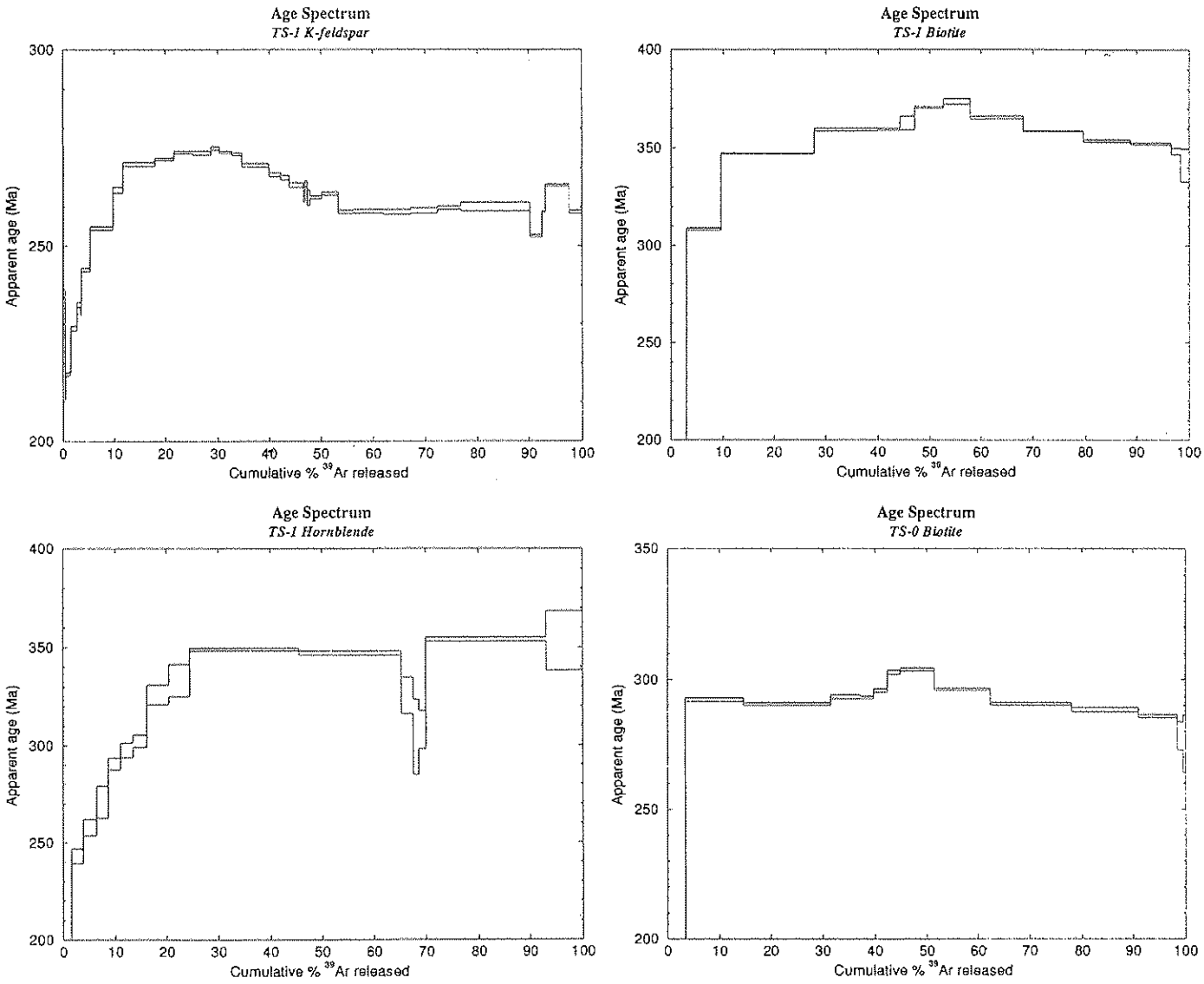

Figure 20.13. $^{40}Ar/^{39}Ar$ spectra of biotite, hornblende, muscovite, and k-feldspar from the central Tien Shan region.

Because Mesozoic sedimentary rocks are sparsely exposed in the Qaidam region, their deformational history is not well understood. Seismic-reflection profiles obtained from the southern part of the basin suggest that the Mesozoic strata are only several hundred meters thick, much thinner than Cenozoic strata (Figure 20.14) (Song and Wang, 1993). The Cenozoic sequence is, on average, between 4 and 5 km thick and locally exceeds 10 km (Song and Wang, 1993). Three major unconformities, Paleogene–Eocene, early Pliocene, and early Quaternary, are recognized in the Cenozoic sequence of the Qaidam basin (Figure 20.15). An influx of conglomerates in the late Paleocene and early Eocene is consistent with observations from the Fenghuo Shan region in northern Tibet (Figure 20.1), where Eocene foreland-basin sedimentation related to thrusting has been reported by Leeder, Smith, and Yin (1988). We interpret the southern margin of the Qaidam and the northern Tibetan plateau as having experienced late Paleocene–early Eocene N–S compression, possibly related to an early phase of the Indo–Asian collision (Harrison et al., 1992); the profound early Pliocene unconformity in the Qaidam basin may have been produced by initiation of the second phase of thrusting, possibly linked with the eastward propagation of the Altun Tagh fault. Because sedimentary facies of Mesozoic strata in the Tarim and Qaidam basins have not been investigated in detail, when and how the two basins were partitioned remain unknown.

Cenozoic tectonics of Asia

There have been numerous publications regarding the Cenozoic tectonic evolution of Asia (e.g., Tapponnier and Molnar, 1979;

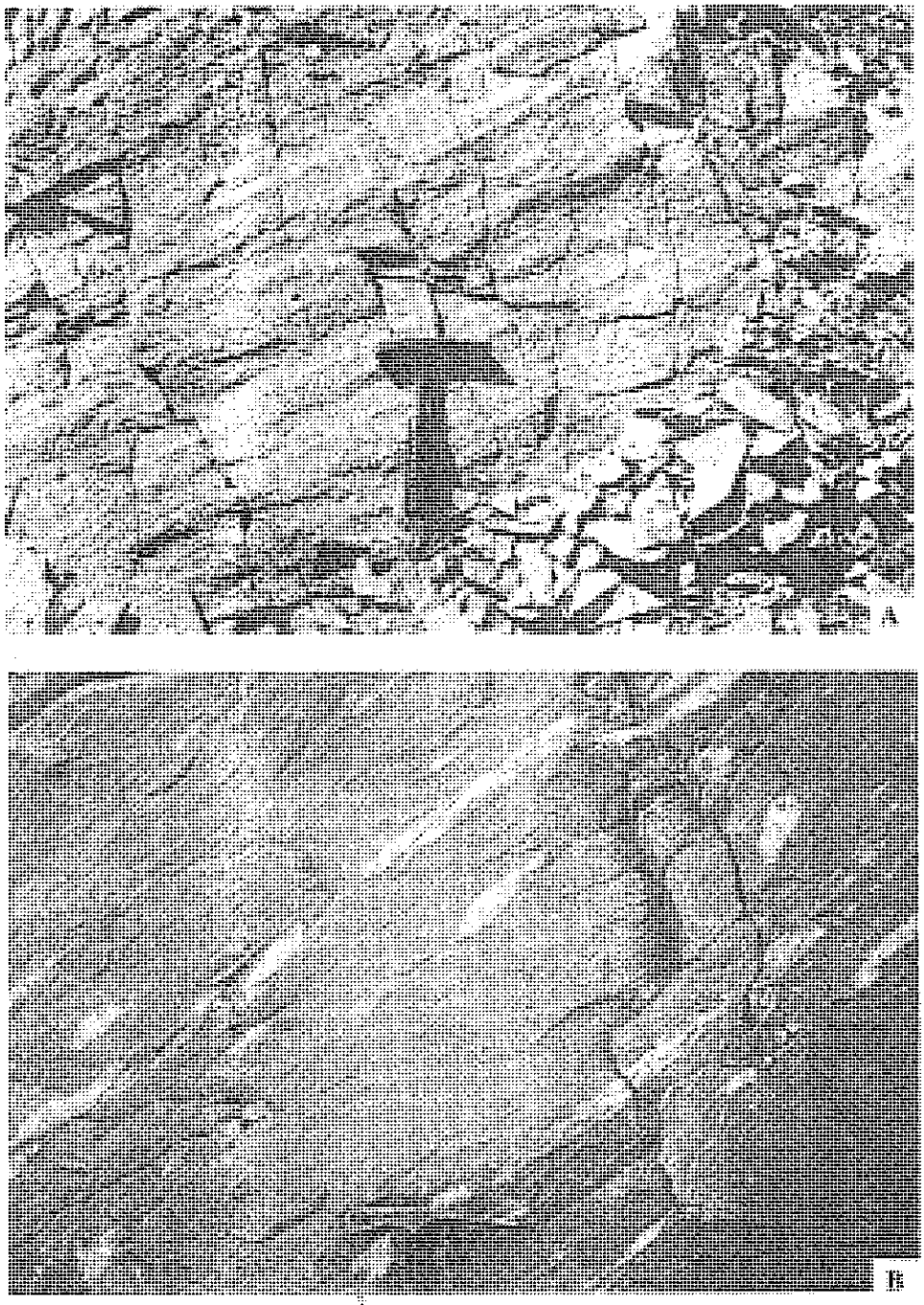

Figure 20.14(A) Mylonitic granodiorite in the central Tien Shan ductile shear zone, Shangsuyuanzi (see Figure 21.9 for location), in the central Tien Shan. (B) Asymmetric boudinage in the central Tien Shan ductile shear zone, indicating right-slip sense of shear, Shangsuyuanzi (see Figure 21.9 for location), in the central Tien Shan.

Peltzer and Tapponnier, 1988; Burchfiel and Royden, 1991). However, the timing and magnitudes of deformation along major tectonic boundaries remain poorly understood. Increasing efforts have been made in the past few years to investigate these issues (e.g., Altun Tagh Working Group, 1992; Harrison et al., 1992; Leloup et al., 1993; Molnar et al., 1994; Yin et al., 1994). Some of the basic aspects of that work, though controversial, are summarized next.

Red River fault system

The Red River fault can be traced from eastern Tibet through the Yunnan province in China to the South China Sea, for a distance of more than 1,000 km (Figure 20.16), and it has had a complex history during the Indo–Asian collision. It was a left-slip fault between 35 Ma and 17 Ma, with a displacement greater than 80 km, and possibly as large as 550 km, as suggested by the

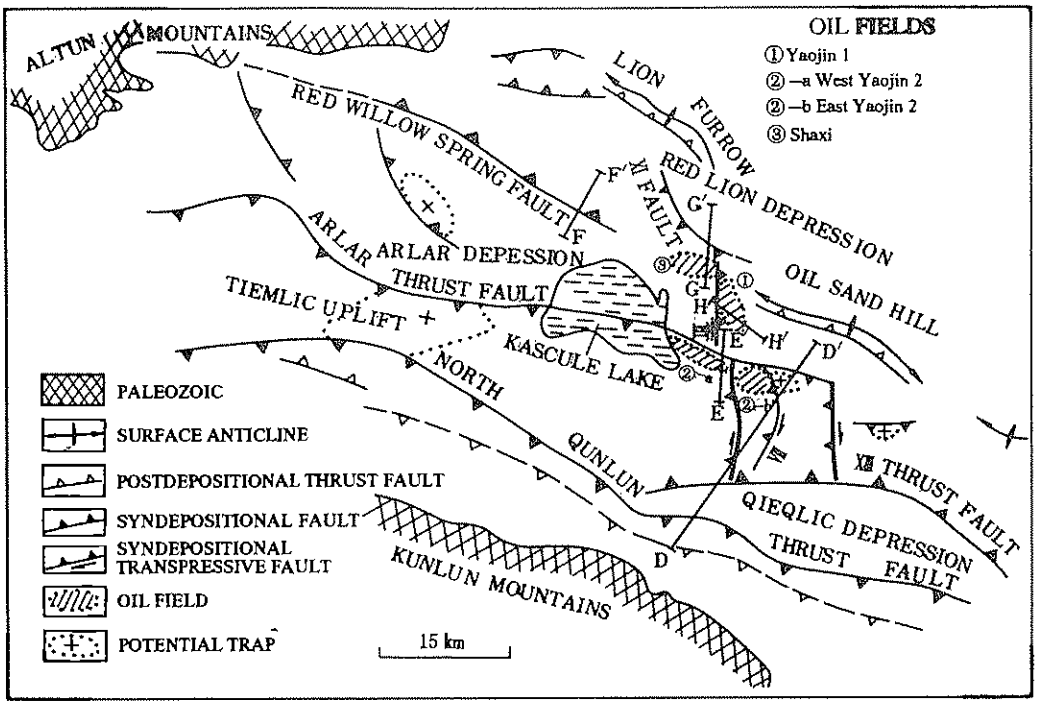

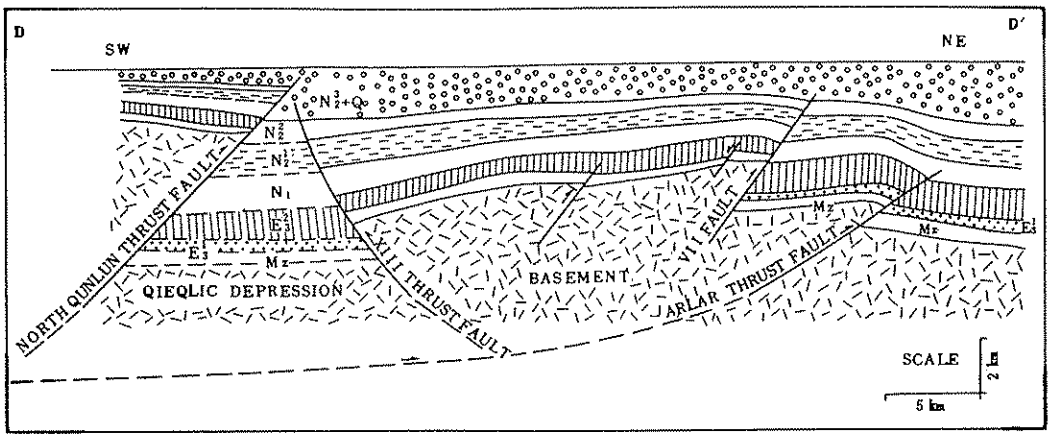

System/Series		Abbreviation		Lithology	Reference
QUATERNARY		Q		alluvium conglomerates	
				UNCONFORMITY	
PLIOCENE	UPPER	N_2^3		conglomerates, sandstones and shales with evaporite	
	MIDDLE	N_2^2		sandstones, shales, conglomerates	
	LOWER	N_2^1		red shales and sandstones	reservoir
				UNCONFORMITY	
MIOCENE	UPPER	N_1	N_1^2	mainly shales with sandstones	
	LOWER		N_1^1	mainly shales with calcareous shales and sandstones	source rocks
OLIGOCENE	UPPER	E_3	E_3^2	mainly shales with sandstones	major source rocks
	LOWER		E_3^1	mainly sandstones with shales	major reservoir
EOCENE AND PALEOCENE		E_{1+2}		conglomerates and sandstones	
				UNCONFORMITY	
MESOZOIC		Mz			

Figure 20.15(A) Cenozoic tectonic map of the Qaidam basin. (Adapted from Song and Wang, 1993.) (B) Geologic cross section of the southern Qaidam basin. (Adapted from Song and Wang, 1993.) (C) Simplified Cenozoic stratigraphic section of the Qaidam basin. (Adapted from Song and Wang, 1993.)

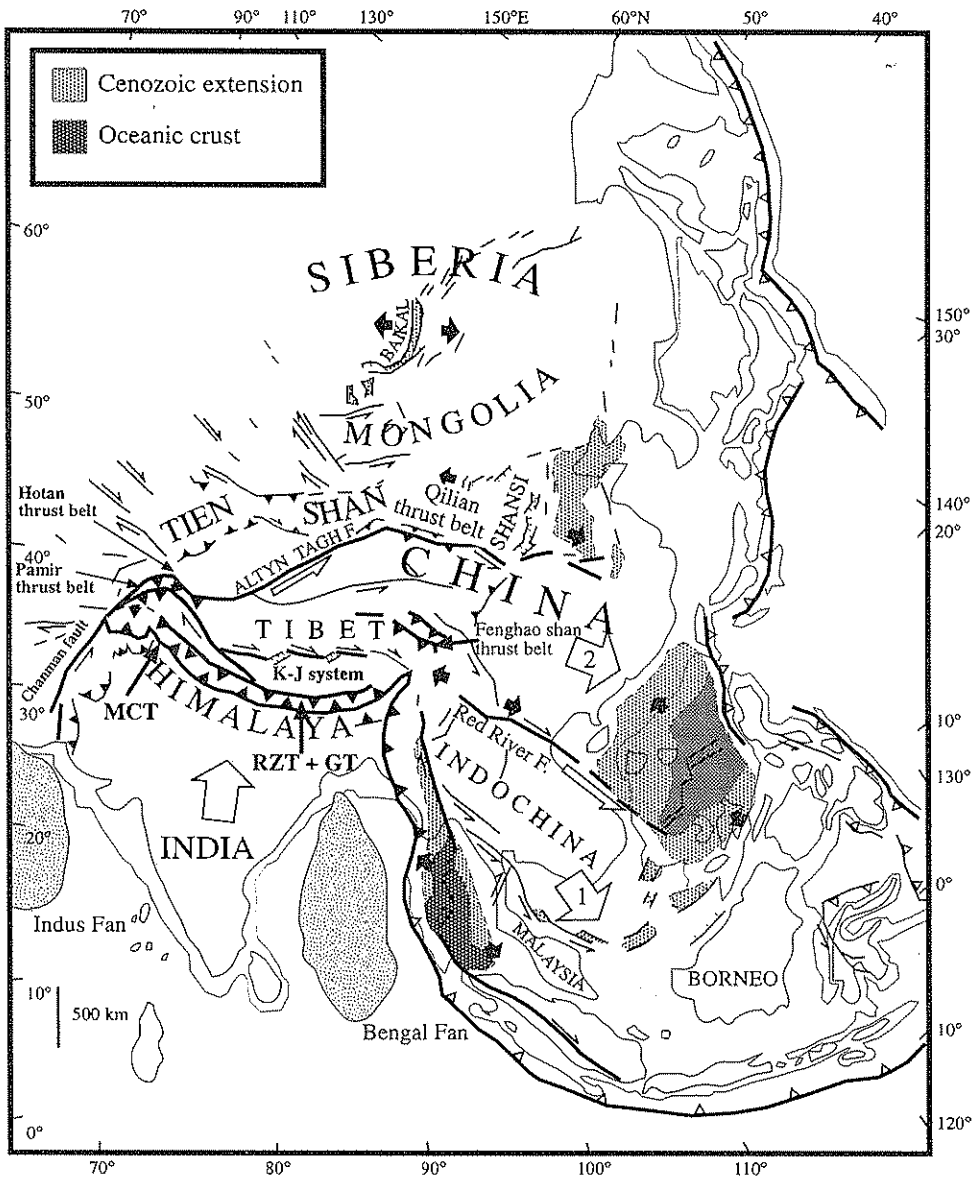

Figure 20.16 Cenozoic tectonic map of Asia. Major tectonic features discussed in the text are the Red River fault, the Gangdese thrust (GT), the Renbu–Zedong thrust (RZT), the Altun Tagh fault, the Fenghuo Shan thrust belt, the western Kunlun thrust belt, the Qilian thrust belt, the Chaman fault, the Tien Shan fault system, the Main Central Thrust (MCT), and the Karakoram–Jiali fault system (K-J). (Adapted from Peltzer and Tapponnier, 1988.)

opening of the South China Sea (Briais, Patriat, and Tapponnier, 1993) and by finite-strain analysis across the fault zone (Lacassin, Leloup, and Tapponnier, 1993). The direction of motion on the Red River fault system reversed at about 5 Ma (Leloup et al., 1993) and it became a right-slip fault, with normal-slip components in places (Allen et al., 1984; Leloup et al., 1993). The later stage of the left-slip history of the Red River fault system was associated with transtensional tectonics, which were initiated diachronously from the south at 25 Ma in Vietnam to the north at 17 Ma in the Ailao Shan of Yunnan (Harrison et al., Chapter 11, this volume). The change in slip direction along the Red River fault could have been related to the rotation of the fault itself during the collision.

In contrast to the extrusion hypothesis (Peltzer and Tapponnier, 1988; Leloup et al., 1993), slip along the Red River fault has been attributed, alternatively, to accommodation of the rotations of rigid blocks about the eastern syntaxis of the Himalaya orogenic belt (Cobbold and Davey, 1988; England and Molnar, 1990). In that view, the magnitude of slip is much less than that suggested for eastward extrusion of the Indochina block during the collision of India and Asia (e.g., Peltzer and Tapponnier, 1988). The timing of initiation of transtensional tectonics along the Red River fault and the kinematic history of the Red River fault inferred from the seafloor magnetic-reversal history in South China sea are consistent with the extrusion hypothesis of the Indochina block in the middle Tertiary (Harrison et al., Chapter 11, this volume).

Altun Tagh fault system

Estimates of the Quaternary slip rate along the Altun Tagh fault have varied from 2–3 cm/a (Peltzer, Tapponnier, and Armijo,

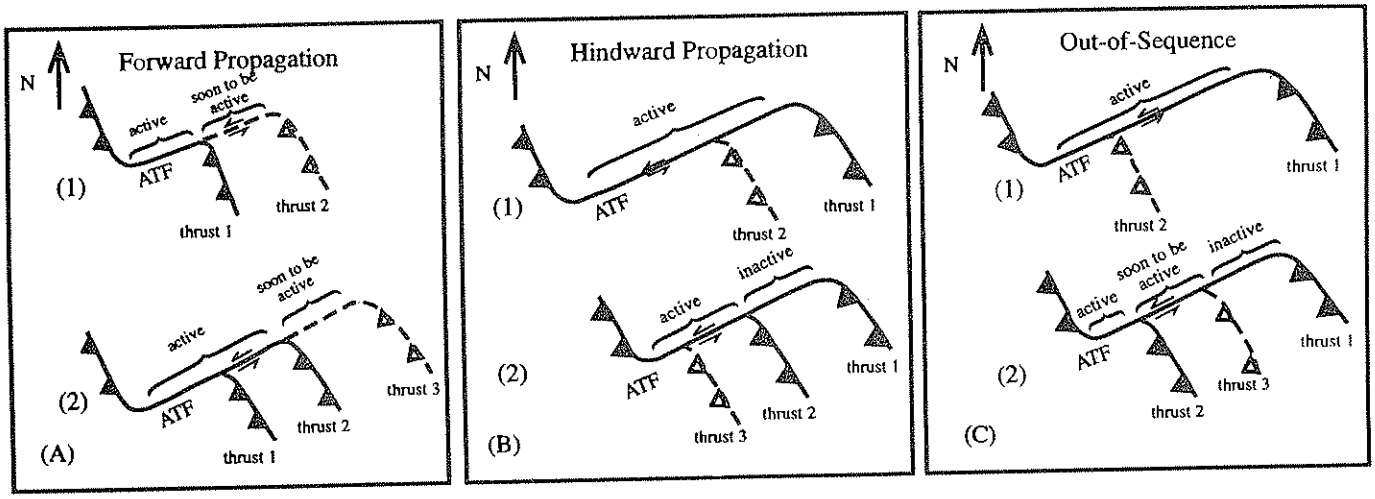

Figure 20.17(A) Forward propagation of thrusting in Tibet and lengthening of the Altun Tagh fault (ATF). (B) Hindward propagation of thrusting in Tibet and shortening of the Altun Tagh fault. (C) Out-of-sequence thrusting, requiring various initiation and termination ages for different thrusts.

1989) to about 0.5 cm/a (Altun Tagh Working Group, 1992). Estimates of its total left-slip have varied widely: (1) 1,200 km on the basis of the offset of the Qilian Shan suture zone and the western Kunlun Shan (Figure 20.9) (Altun Tagh Working Group, 1992); (2) about 500 km, on the basis of comparing the offsets of the late Paleozoic magmatic belts in the western and eastern Kunlun Shan (Peltzer and Tapponnier, 1988) and matching the Qilian Shan suture zone with the central Tarim uplift zone (this study); (3) about 200 km, based on inferences from the measured Pliocene–Quaternary slip rate as a constant along the Altun Tagh fault and the duration of the Indo–Asian collision (Burchfiel and Royden, 1991; Altun Tagh Working Group, 1992). As noted by both Tapponnier et al. (1990) and Burchfiel et al. (1989), the Altun Tagh fault is currently a transfer fault linking thrusts in the Tibetan plateau and Qilian Shan (= Nan Shan) (Figure 20.9). This kinematic model requires that the slip history along the Altun Tagh fault be related to the sequence of thrusting in Tibet and in the Nan Shan. Because the magnitude of deformation in Tarim is much less than that in Tibet and the Nan Shan, the total left-slip along the Altun Tagh fault should have decreased northeastward along the strike. If thrusting in the plateau propagated from south to north (e.g., Molnar et al., 1987; England and Houseman, 1988), then the Altun Tagh fault would progressively have lengthened since its initiation (Figure 20.17A). Although the initiation age of the Altun Tagh system would have decreased northeastward in this model, each segment of the fault would have been continuously active once formed. Alternatively, thrusting could have propagated from north to south in Tibet and the Nan Shan (e.g., Harrison et al., 1992), which would imply that the active length of the Altun Tagh fault would have decreased since its initiation and that slip along the Altun Tagh fault would have terminated sequentially from northeast to southwest (Figure 20.17B). If the thrusting sequence was not unidirectional, then both the length and the active portion of the Altun Tagh fault would have varied with time (Figure 20.17C). The preliminary age constraints on the Altun Tagh fault, as inferred from the sedimentologic record in the Hotan foredeep (Figure 20.10) (Ye and Huang, 1992), are consistent with the first model (Figure 21.17A), permissive with the third model (Figure 21.17C), but incompatible with the second model (Figure 21.17B). We thus propose that the Altun Tagh fault was initiated in the west near Hotan in the middle Miocene, at about 20 Ma (Figure 21.9), and subsequently propagated eastward to link thrusts in the southern Qaidam and Nan Shan at about 6 Ma (Burchfiel and Royden, 1991; Song and Wang, 1993). This interpretation implies that the Altun Tagh fault propagated eastward at a rate of 60 mm/a from Hotan to the Nan Shan after 20 Ma.

As Paleozoic(?) ophiolitic fragments are distributed along the entire length of the Altun Tagh fault (Figure 21.9), the fault trace has been categorized as a Paleozoic suture zone that was reactivated in the Cenozoic (Altun Tagh Working Group, 1992). However, the ophiolitic fragments could have been dragged into the Altun Tagh fault zone and then displaced for a long distance. Because there have been no detailed studies to correlate the ophiolitic fragments in the Altun Tagh fault zone and those in the Qilian Shan and eastern Kunlun Shan (Figure 21.9), the origin of these ultramafic rocks in the Altun Tagh system is unknown.

The junction point of the eastern Kunlun and Altun Tagh faults divides the Altun Tagh system into eastern and western segments. The eastern segment is transpressional, as indicated by a series of folds and thrusts that involve Neogene strata and are parallel to the Altun Tagh fault (Burchfiel et al., 1989) (Figure 21.9). The western segment is transtensional, as expressed by Altun Tagh–parallel normal faults both north (Avouac and Peltzer, 1993) and south (Zhao and Zhu, 1980; Altun Tagh Working Group, 1992) of the Altun Tagh fault. As reported by the Altun Tagh Working Group (1992), late Neogene volcanic centers in western Tibet (e.g., Arnaud et al., 1992; Turner et al., 1993) are mostly distributed within pull-apart basins along the

Table 20.1. *Timing and magnitude of late Cenozoic deformation in Asia*

Name of structure	Magnitude of slip	Age and Duration	References
South Himalayan thrust systems (MCT, MBT, MFT)	>150 km, ~500 km	25 Ma to present	Lyon-Caen & Molnor (1985), Coward & Burtler (1985)
Tethyan Himalayan thrust system	~250 km	50–17.5 Ma	Ratschbacher et al. (1994)
Renbu–Zedong thrust	Unknown	17.5–8.0 Ma	Yin et al., (1994)
Gangdese thrust	>50 km	27–20 Ma	Yin et al. (1994)
Fenghuo Shan thrust system	Unknown	~50–25 Ma	Leeder et al., (1988), Coward et al., (1988), Qingha; BGM (1989)
Red River fault	80 km, ~500 km	~35–17 Ma	Leloup et al., (1993), Harrison et al. (Chapter 11, this volume)
Altun Tagh fault	~500 km	~ 20 Ma–present	Peltzer & Tapponnier (1988); cf. Burchfiel & Royden (1991) and Altun Tagh Working Group (1992)
Tien Shan fault system	100–200 km	~20 Ma–present	Avouac & Peltzer (1993), McKnight & Graham (1994); cf. Burchfiel & Royden (1991) and Altun Tagh Working Group (1992)
Kunlun fault	Unknown	Active in Quaternary	Peltzer et al. (1985)
Qinling fault	~150 km	Active in Quaternary	Tapponnier & Molnar (1977)
Haiyuan fault	<15 km	Active since Pliocene	Burchfiel & Royden (1991), Zhang et al. (1991)
Karakoram–Jiali fault system	>160 km[a]	Active at 8.0 Ma and since	Peltzer et al., (1985), Armijo et al., (1989)

[a]Inferred from the slip rate of 20 mm/a (Armijo et al., 1989) and a minimum duration of 8.0 m.y.; 8 Ma was the time of peak activity of the N–S-trending rifts in southern Tibet (Harrison et al., in press-a).

western Altun Tagh fault system. The change from strike-perpendicular contraction to strike-perpendicular extension along the Altun Tagh system implies that the Tarim basin has rotated clockwise with respect to the Tibetan plateau in the late Cenozoic. We thus propose that the Neogene volcanism in western Tibet may have been related to the late Cenozoic clockwise rotation of the Tarim basin. Such a clockwise rotation of Tarim has been proposed to explain a decrease in shortening from west to east in the Tien Shan (Avouac and Peltzer, 1993). This interpretation is in contrast with earlier models, holding that the Neogene volcanism in western Tibet was related to (1) convective removal of a thickened lithospheric mantle (England and Houseman, 1988) or (2) subduction of the Tarim basin beneath the Tibetan plateau (Arnaud et al., 1992) Neither interpretation requires spatial and temporal associations between surface structures and the locations of the volcanic centers.

Crustal shortening in the Himalaya, Tibet, and Tien Shan

Several large Cenozoic thrust systems have been recognized in the Lesser Himalaya (Gansser, 1964; Lyon-Caen and Molnar, 1983, 1985), the Tethyan Himalaya (Burg, 1983; Liu, 1988; Ratschbacher et al., 1994), the Gangdese Shan in southern Tibet (Yin et al., 1994), the Fenghuo Shan in northern Tibet (Liu, 1988; Leeder et al., 1988), and the Tien Shan (Chen, 1985; Avouac and Peltzer, 1993). From south to north, the major thrust systems are the Main Frontal Thrust (MFT), the Main Boundary Thrust (MBT), the Main Central Thrust (MCT), the Tethyan thrust system, the Renbu–Zedong thrust, the Gangdese thrust system, the Fenghuo Shan thrust system, the Nan Shan thrust system, and the Tien Shan thrust system. Their ages and magnitudes of shortening are summarized in Table 20.1. The total amount of shortening is on the order of 600 km across the Himalaya and southern Tibet, and 120–200 km across the Tien Shan. However, estimation of shortening across the interior of the Tibetan plateau is less well constrained.

The inferred Eocene thrusting in northern Tibet and the southern Qaidam is particularly interesting, because it would have been located near the northern tip of the Indochina block if the total slip along the Red River fault were restored. Considering the possibility that the Fenghuo Shan thrust belt and the left-slip on the Red River fault could have overlapped, in both time and space, it is likely that the Fenghuo Shan thrust belt

developed as a result of eastward extrusion of the Indochina block (Figure 20.16). This kinematic interpretation, illustrated in detail in our tectonic model discussed later, suggests that the South China Sea and the Fenghuo Shan thrust system marked the southern and northern termini of the Red River fault, respectively, during extrusion of the Indochina block. This model not only solves the space problem related to eastward movement of the Indochina block between the late Eocene and Oligocene but also explains why deformation occurred in northern Tibet, but not in southern Tibet, during the early stage of the Indo–Asian collision, a problem raised by Leeder et al. (1988) and Harrison et al. (1992).

Important Tectonic problems and possible solutions

In order to address these problems and to explain the newly acquired geologic data presented here, we propose a tectonic hypothesis for the Phanerozoic evolution of China and its neighboring regions. This model, in particular, addresses the following important questions:

1. Where is the western extension of the Devonian suture zone in the Qilian Shan?
2. Where did Tarim come from originally?
3. Where is the colliding block that produced pronounced middle Paleozoic deformation in the Qinling?
4. Where is the late Paleozoic magmatic arc along the southern margin of eastern North China?
5. What caused Triassic–Jurassic left-slip faulting in the Qinling region and the western Ordos thrust system along the western margin of the North China block?
6. What caused the extensive Silurian–Devonian disconformity in the North China suture system?
7. What is the nature of the central Tarim aeromagnetic high and the central Tarim uplift belt?
8. What caused Triassic east-directed thrusting along the western margin of the Ordos basin in western North China?

Tectonic reconstruction

In contrast to earlier geologic reconstructions of eastern Asia, which commonly emphasized regional geologic evolution on vertical sections (e.g., Li et al., 1978; Zhang et al., 1984; Hsü et al., 1990), we present a map reconstruction of eastern Asia. We divide the tectonic reconstruction of China in the Phanerozoic into 15 time slices, to be described sequentially. Note that the kinematic solutions provided here are not unique. The uncertainty can be judged from the quality of the available geologic observations, as outlined earlier. The numerical ages are from Harland et al. (1990).

Stage 1 (630–438 Ma): During the late Proterozoic–early Paleozoic, the North Tarim–North China block was characterized by passive continental margins on all sides (Figure 20.18A). Two deep depositional troughs developed in the northern corner and south-central part of the block: the Manjiaer aulacogen in the northeastern Tarim basin and the Helan aulacogen in the Ningxia region of North China. Note that the Tarim basin was divided into two pre- middle Paleozoic plates the North and South Tarim blocks (Figure 20.1), by the central Tarim uplift zone (Figure 20.10A).

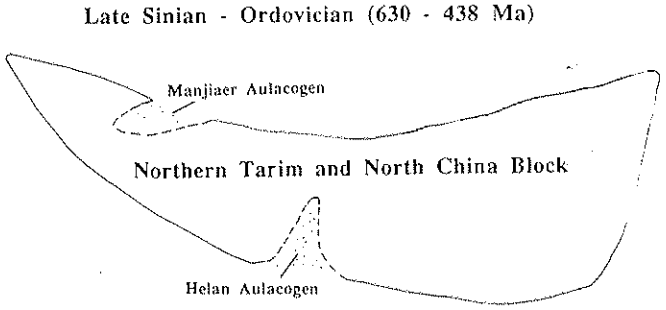

Figure 20.18 Tectonic model for the Phanerozoic evolution of China and its neighboring regions. Tectonic blocks and structures: NCB, North China block; SCB, South China block; ICB, Indochina block; ST, South Tarim block; NT, North Tarim block; QB, Qaidam block; LS-SM, Lhasa–Sibumasu block; QT, Qiangtang block; TLF, Tan Lu fault; ATF, Atlun Tagh fault. (A) Stage 1: late Sinian–Ordovician (630–438 Ma). The North Tarim–North China block was characterized by passive continental margins on all sides. The Manjiaer and Helan aulacogens were developed during rifting.

Stage 2 (438–421 Ma): During the early Silurian, the southern margin of the North Tarim–North China block was marked by a north-dipping subduction zone, along which a plate combining a part of the Pamir region (Burtman and Molnar, 1993), South Tarim, and Qaidam as its continental portion was subducted beneath the North Tarim–North China block in the Qinling and Qilian regions (Figure 20.18B). Simultaneously, an oceanic plate was subducting southward beneath the North China block (Yang et al., 1986). The synchroneity of initiation of the two active margins and the widespread disconformity in the North China block suggest that North China could have been raised above the sea level because of advection of heat from below related to the two subduction zones (Yang et al., 1986). Alternatively, sea-level changes due to other causes could have produced the unconformity in North China (e.g., Hallam, 1992). Because no middle Paleozoic deformation has been reported in the Dabie, Shandong, and Imjingang regions east of the Qinling area, the tectonic regime may have been partitioned by a transform fault that connected with the subduction zone to the east (Figure 20.18B). During that time interval, the North Tarim was marked by the deposition of flysch sediments and volcaniclastics (Zhou and Chen, 1990) in a fore-arc or intra-arc setting, possibly related to north-dipping subduction of South Tarim below North Tarim.

Stage 3 (421–387 Ma): During the late Silurian–early Devonian, the Pamir–South Tarim–Qaidam continental block collided into the North Tarim–North China block (Figure 20.18C). The diachronous collision is shown schematically to suggest a possibly complex history.

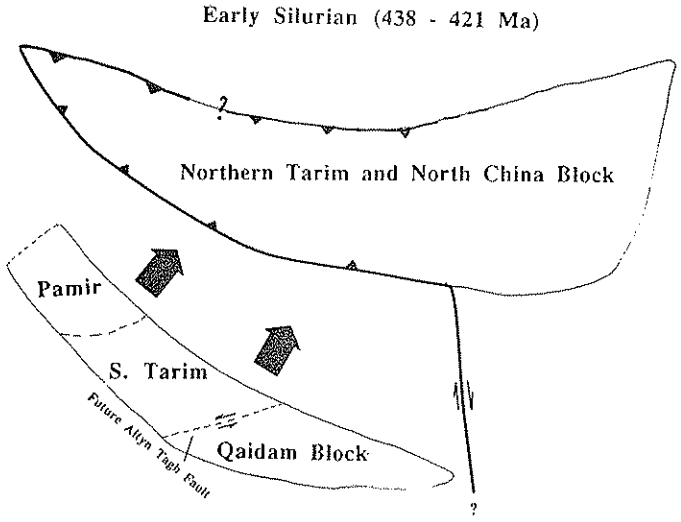

Figure 20.18 (B) Stage 2: early Silurian (438–421 Ma). The southern margin of the North Tarim–North China block was marked by a north-dipping subduction zone, along which a plate combined a part of the Pamir region, South Tarim, and Qaidam as its continental portion, subducted beneath the North Tarim–North China block in the Qinling and Qilian regions. Simultaneously, the Mongolian plate was subducting southward beneath the North China block. Because of those two active margins, the North China block was raised because of advection of heat from below, related to two subduction zones.

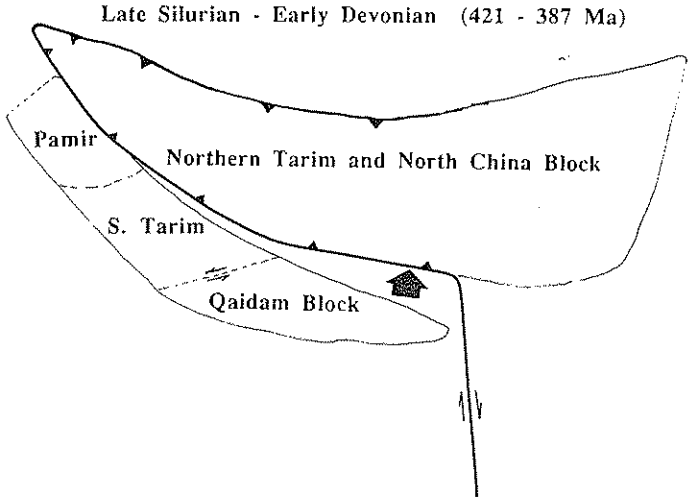

Figure 20.18 (C) Stage 3: late Silurian–early Devonian (421–387 Ma). The Pamir–South Tarim–Qaidam continental block collided into the North Tarim–North China block. The diachronous collision is shown schematically to suggest a possibly complex geologic history.

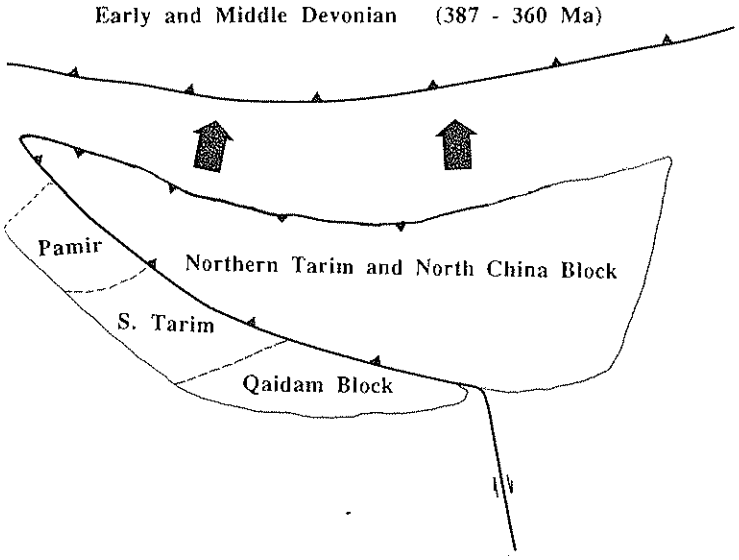

Figure 20.18 (D) Stage 4: early–middle Devonian (387–360 Ma). The collision between the Pamir–South Tarim–Qaidam microcontinent and the North Tarim–North China block was finished, as marked by the development of the Devonian molasse along the suture system. The southerly derived Devonian clastic sediments in the southern Tien Shan were derived from that collisional system to the north, along the central Tarim uplift zone. The middle Paleozoic suture zone extended from the Qinling region to the Pamir region across the central part of the future Tarim basin. At the same time, the North Tarim–North China plate began subducting beneath the southern margin of the Siberia–Kazakhstan plate.

Stage 4 (387–360 Ma): Between the early and middle Devonian, the collision between the Pamir–South Tarim–Qaidam microcontinent and the North Tarim–North China block ceased, as marked by deposition of Devonian molasse along the suture system (Figure 20.18D). The southerly sourced Devonian clastic sediments in the southern Tien Shan (Carroll et al., 1995) were derived from that collisional system to the north along the central Tarim uplift zone. The middle Paleozoic suture zone extended from the Qinling region to the Pamir region across the central part of the future Tarim basin. At the same time, the North Tarim–North China plate began subducting beneath the southern margin of the Siberia–Kazakhstan plate. The western part of the subduction zone formed the middle Paleozoic ophiolites in the central Tien Shan region (Chen, 1985) and incorporated a magmatic arc (not shown in Figure 20.8D), the central Tien Shan arc, between the North Tarim and the southern margin of the Eurasia continent (Windley et al., 1990; Carroll et al., 1995).

Stage 5 (360–258 Ma): During the late Carboniferous and early Permian, the North Tarim–North China block began colliding

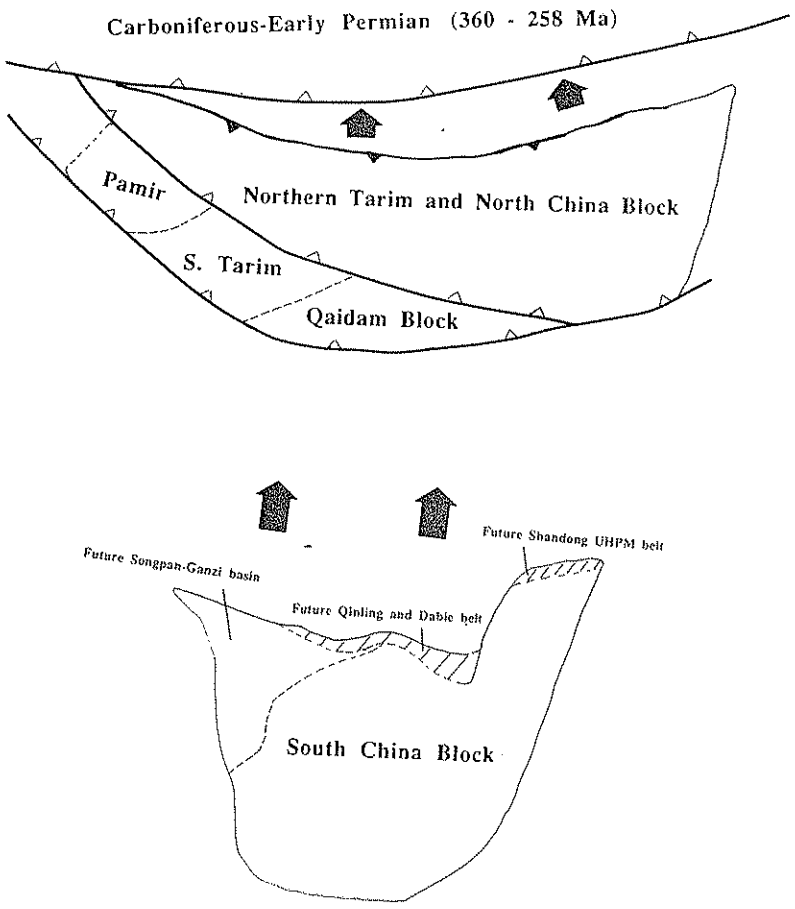

Figure 20.18 (E) Stage 5: Carboniferous–early Permian (360–258 Ma). The North Tarim–North China block began colliding with the Siberia–Kazakhstan microcontinent. The South China plate began subducting underneath the combined North China–Qaidam plate, and as a result, a late Paleozoic magmatic arc developed along the southern margin of Qaidam.

with the Siberia–Kazakhstan microcontinent and Mongolian arcs (e.g., Carroll et al., 1995) (Figure 20.18E). The South China plate began subducting underneath the combined North China–Qaidam plate, and as a result a late Paleozoic magmatic arc developed along the southern margin of the North China block.

Stage 6 (258–253 Ma): During the late Permian, South China began colliding with the North China block. The collision was initiated from the east and progressively migrated to the west (Figure 20.18F). Meanwhile, the South China plate was subducting underneath the Qiangtang– Indochina block.

Stage 7 (253–245 Ma): During the latest Permian, the initial collision of the eastern suture zone produced deposition of northerly derived clastics along the northern margin of the South China block (Figure 20.18G). Simultaneously, the collision between the North and South China blocks reactivated the middle Paleozoic suture system between the Qaidam and North China blocks and produced right-slip along it. Left-slip along the eastern Kunlun region, as documented by Mattauer et al. (1985), may have been the conjugate set that facilitated the westward extrusion of the Qaidam block from its original position.

Stage 8 (245–208 Ma): During the Triassic, the collision of North China and South China continued (Figure 20.18H). The collision of the two blocks squeezed the Qaidam farther to the west and produce the West Ordos thrust belt, which terminates at the Qilian right-slip fault zone. The relationship between the Qilian Shan right-slip faults and the West Ordos thrust belt suggests that the magnitude of right-slip decreased westward west of the Qilian Shan region.

The final collision of the northwestern corner of the South China block reversed the slip sense in the Qinling region from right-slip to left-slip. That was due to the departure of the Qaidam block and the local indentation of the northwestern corner of the South China block that formed the Daba Shan arc (Figure 20.1). The western part of the arc was formed by left-slip, as observed by Mattauer et al. (1985), in the Qinling, whereas the eastern part of the arc was formed by right-slip, as reported by Liu and Hao (1989), in the Dabie Shan.

Stage 9 (220–208 Ma): During the late Triassic (Figure 20.18I), sediments eroded from the Triassic ultra-high-pressure metamorphic terranes of the Dabie Shan and Shandong region were deposited in a remnant ocean basin (Graham, Dickinson, and Ingersoll, 1975; Ingersoll, Graham, and Dickinson, 1995) between the North and South China blocks in the Songpan–Ganzi region (Yin and Nie, 1993; Nie et al., 1994b; Ingersoll et al., 1995; Zhou and Graham, Chapter 14, this volume). Indentation of South China into North China created the Tan Lu fault in eastern China and the Honam shear zone in South Korea. Associated with the indentation was an extensive region of North China that experienced N–S crustal shortening. A consequence of that intracontinental deformation was the

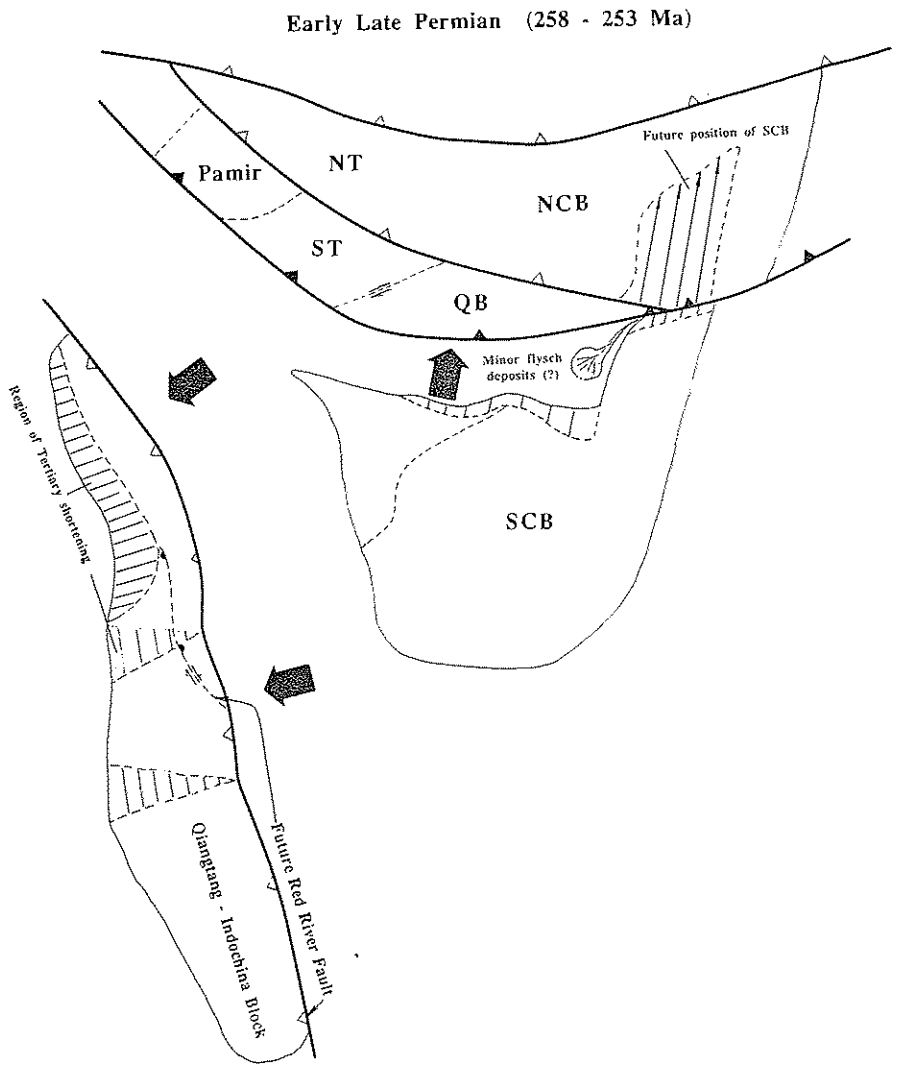

Figure 20.18 (F) Stage 6: late Permian (258–253 Ma). The South China block began colliding into the North China block. The collision was initiated from the east and progressively migrated to the west. Meanwhile, the South China plate was subducting underneath the Qiangtang–Indochina block.

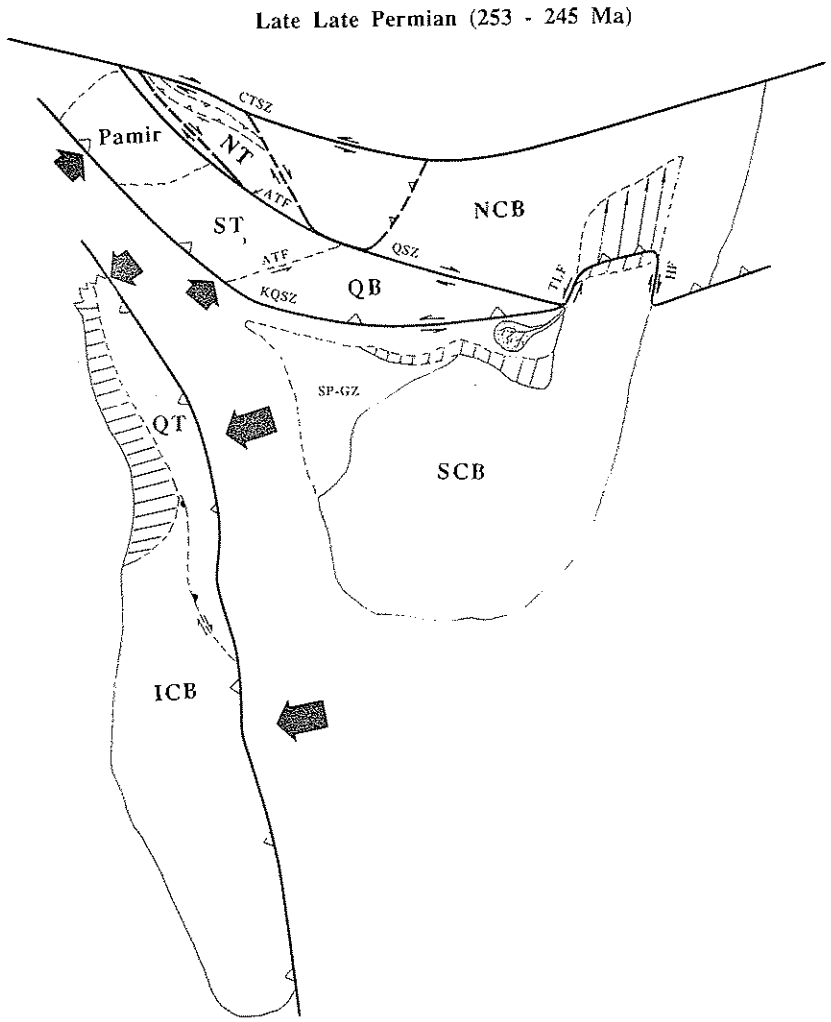

Figure 20.18 (G) Stage 7: latest Permian (253–245 Ma). The initial collision of the eastern suture zone produced terrestrial deposits along the northern margin of the South China block. Simultaneously, the collision between the North and South China blocks reactivated the middle Paleozoic suture system between the Qaidam and the North China and the produced right-slip along it. The left-slip along the eastern Kunlun region may be the conjugate set that facilitated the westward extrusion of the Qaidam block from its original position.

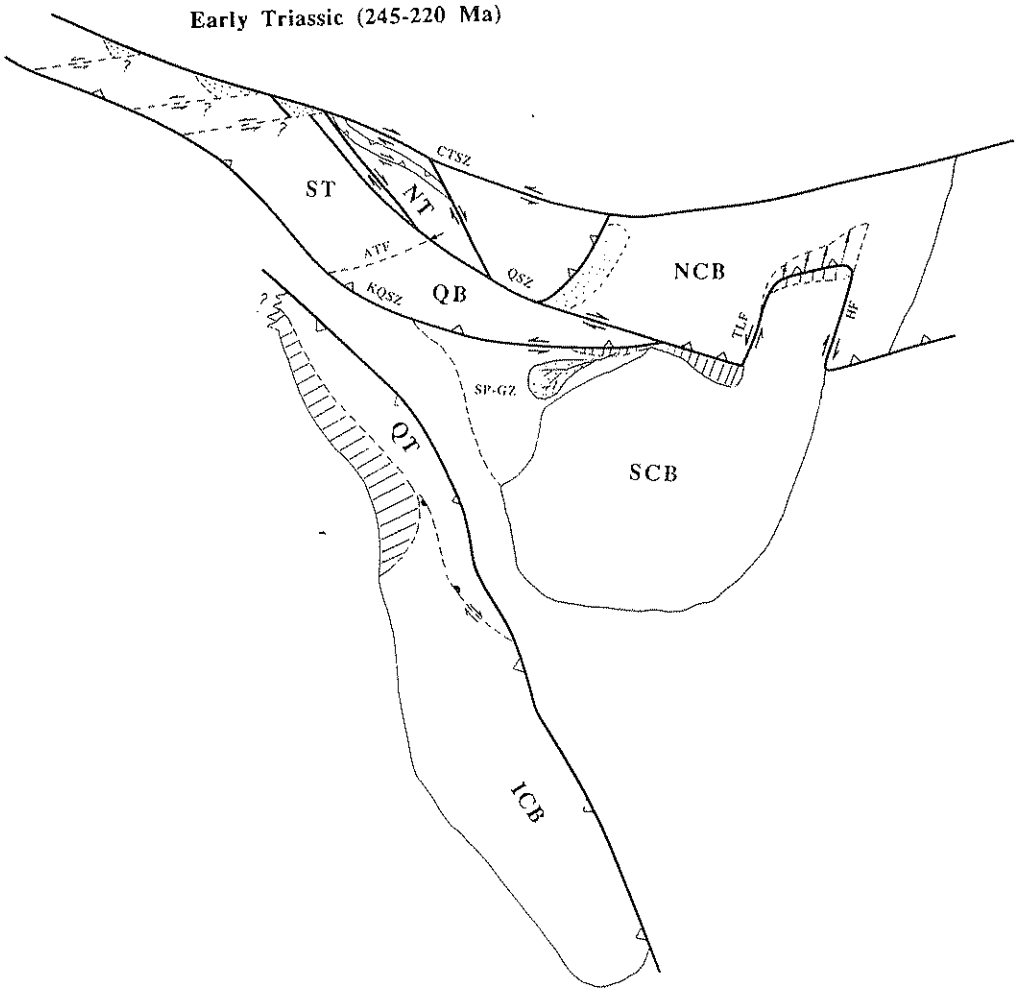

Figure 20.18 (H) Stage 8: early Triassic (245–220 Ma). The collision between the North and South China blocks was occurring. The collision of the two blocks squeezed the Qaidam farther to the west and produced the West Ordos thrust belt, which terminated at the Qilian right-slip fault zone. The relationship between the Qilian Shan right-slip faults and the West Ordos thrust belt suggests that the magnitude of right-slip decreased westward west of the Qilian Shan region. The final indentation of the northwestern corner of the South China block reversed the slip sense in the Qinling region from right-slip to left-slip. That was due to the departure of the Qaidam block and the local indentation of the northwestern corner of the South China block that formed the Daba Shan arc (D in Figure 20.1). The western part of the arc was formed by left-slip faulting in the Qinling, whereas the eastern part of the arc was formed by right-slip faulting in the Dabie Shan.

formation of a topographically high region, the Huabei plateau in eastern North China, where little Triassic sediment was deposited (Gong, 1987; Hebei BGM, 1989; Shandong BGM, 1989). Synchronously, the Mongol–Okhotsk ocean was opening, and the Okhotsk ocean began subducting to both the north and south (Zonenshain et al., 1990; Khain, 1993).

The late Triassic was also when the Qiangtang–Indochina block collided with the southern margin of the Eurasian continent (Chang et al., 1986; Şengör, 1987). The Qiangtang block and the Indochina block formed a continuous microcontinent in the Triassic (Metcalfe, 1988); it was dismantled by strike-slip and thrust faulting in late Cenozoic time (Peltzer and Tapponnier, 1988). The collision could have reactivated late Paleozoic suture zones in the Tien Shan region and produced paleo – Tien Shan and associated foreland basins (Hendrix et al., 1992). Alternatively, the late Triassic deformation in the Tien Shan and the northern Tarim basin could have been caused by strike-slip faulting, which was in turn induced by the continuous convergence of North China and South China and the associated westward extrusion of the Qaidam block (Figure 20.18I).

Stage 10 (208–98 Ma): During the early and middle Jurassic, convergence between the North and South China blocks could have continued, as indicated by paleomagnetic studies (Enkin et al., 1992; Nie and Rowley, 1994) and by the age of the Yangtze River fold-and-thrust belt (Figure 20.18J).

The late Jurassic E–W-trending fold-and-thrust belt can be traced from the Liaoning region to the eastern Tien Shan (e.g., Liaoning BGM, 1989; Zheng et al., 1991; Davis et al., Chapter 13, this volume). That contractional deformation was both spatially and temporally associated with emplacement of plutons and was followed in many places by early Cretaceous extension (Zheng et al., 1991; Davis et al., Chapter 13, this volume). That fold-and-thrust belt may have been generated by (1) southward subduction of the Mongol–Okhotsk plate beneath North China, (2) collision between North China and South China, (3) subduction of the Pacific plate beneath eastern Asia, or (4) a combination of the three (Figure 20.18I). That belt of deformation has traditionally been associated with the Yanshanian orogeny (e.g., Yang et al., 1986), the plate-tectonic setting of which has never been explicitly formulated. It is well known that the Cenozoic deformation of Asia has been the result of the combined effects of the Indo–Asian collision and Pacific subduction (e.g., Molnar and Tapponnier, 1975). Thus, assigning an exact cause for the late Jurassic intracontinental deformation

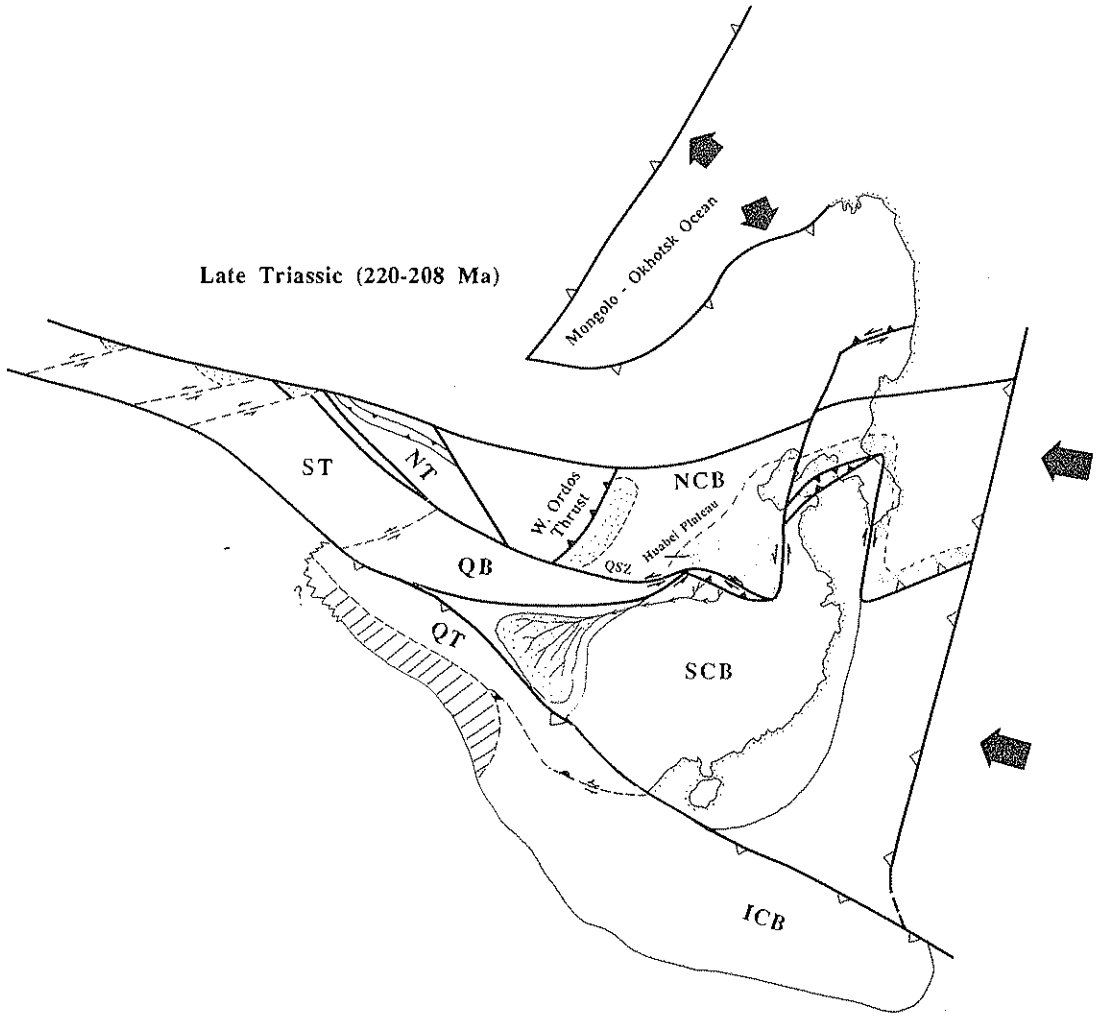

Figure 20.18 (I) Stage 9: late Triassic (220–208 Ma). Sediments eroded from the Triassic ultra-high-pressure metamorphic terranes of the Dahie Shan and Shandong region were deposited in a remnant ocean basin between the North and South China blocks in the Songpan–Ganzi region. Indentation of South China into North China created the Tan Lu fault in eastern China and the Honam shear in South Korea. Associated with the indentation was an extensive region of North China that experienced N–S crustal shortening. A consequence of that intracontinental deformation was the formation of a topographically high region, the Huabei plateau, where little Triassic sediment was deposited. During the same period of time, the Mongol–Okhotsk ocean was opening, and the Okhotsk plate began subducting to both the north and south. The late Triassic was also the time when the Qiangtang–Indochina block collided with the southern margin of the Eurasian continent. The Qiangtang block and the Indochina block formed a continuous microcontinent in the Triassic that was dismantled by strong strike-slip and thrust faulting in late Cenozoic time. The collision reactivated late Paleozoic suture zones in the Tien Shan region and produced paleo–Tien Shan and associated foreland basins.

in North China could oversimplify the complexity of plate-boundary interactions. However, the general E–W trend of the Yanshanian fold-and-thrust belt indicated N–S shortening. Thus, it implies that closure of the Mongol–Okhotsk ocean, or the collision of North China and South China, could be the primary cause for its development.

In addition to the closure of the Okhotsk ocean to the north, the Lhasa block was colliding with the Eurasian continent in the late Jurassic (Allègre et al., 1984; Chang et al., 1986). The Lhasa block was connected with the Sibumasu block of Metcalfe (1988) in southeast Asia. Similar to the Qiangtang–Indochina block, the Lhasa–Sibumasu block has been fragmented and bent during the Indo–Asian collision.

Immediately following the late Jurassic N–S shortening was E–W extension in the Cretaceous in southern Liaoning (Figure 20.5) and the Yunmeng Shan region (Davis et al., Chapter 13, this volume), as well as NE–SW extension in western Inner Mongolia (Zheng et al., 1991). That extensional event marked the collapse of the Huabei plateau and the formation of numerous Cretaceous extensional basins in North China. That event also reactivated and modified the trace of the Triassic left-slip Tan Lu fault (Figure 20.3).

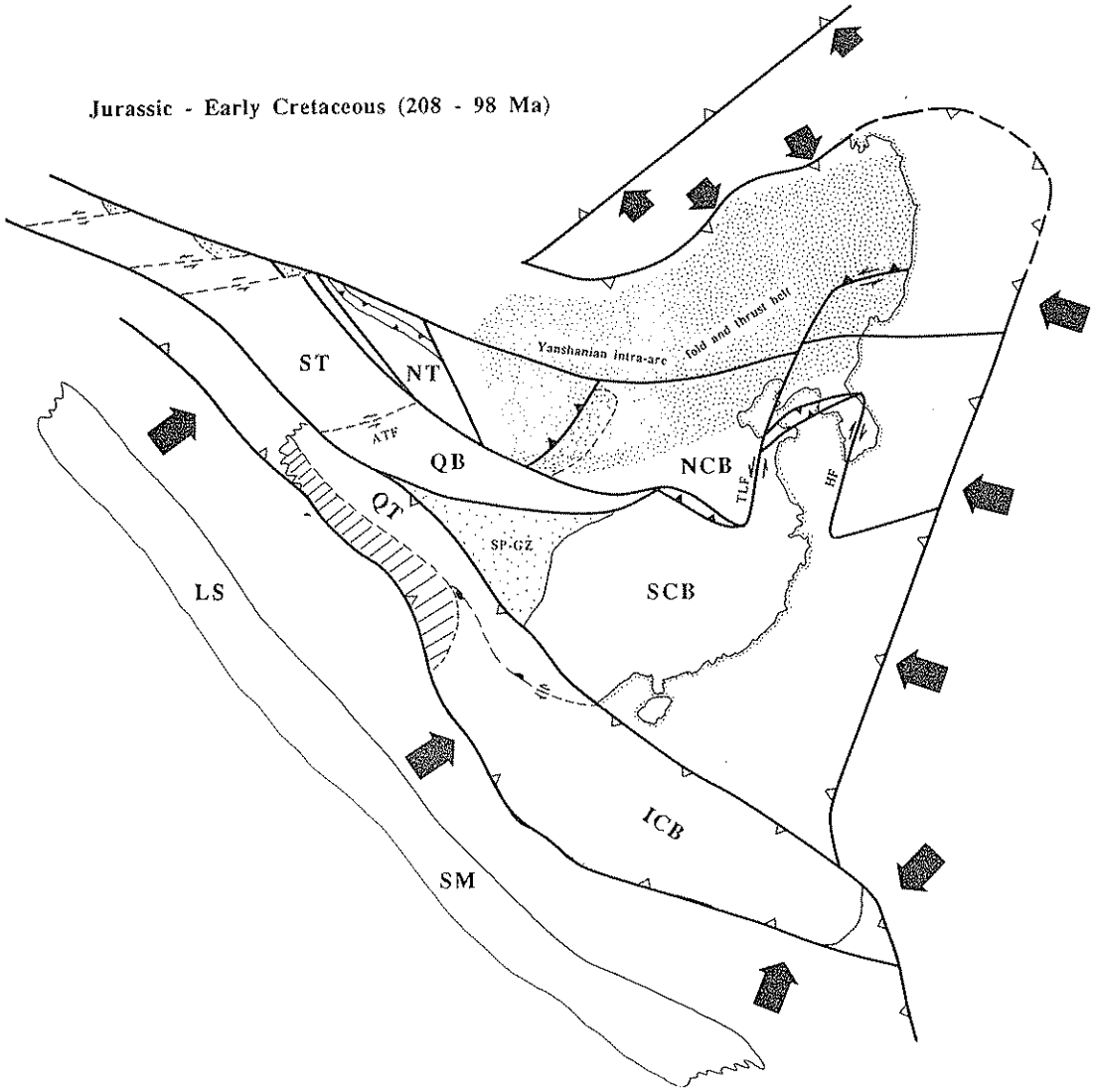

Figure 20.18 (J) Stage 10: early Jurassic–early Cretaceous (208–98 Ma). The convergence between the North and South China blocks could have been ongoing, as indicated by paleomagnetic studies (Enkin et al., 1992; Nie and Rowley, 1994) and the age of the Yangtze River fold-and-thrust belt. The late Jurassic E–W-trending fold-and-thrust belt in North China may have been generated by (1) the southward subduction of the Mongol–Okhotsk plate beneath North China or (2) the collision between North China and South China, or (3) the subduction of the Pacific plate beneath eastern Asia, or (4) a combination of the three. In addition to the closure of the Okhotsk ocean to the north, the Lhasa block was colliding with the Eurasian continent in the late Jurassic. The Lhasa block was connected with the Sibumasu block of Metcalfe (1988) in southeastern Asia. Similar to the Qiangtang–Indochina block, the Lhasa–Sibumasu block has been fragmented and bent during the Indo–Asian collision. Following the late Jurassic N–S shortening was the E–W extension in the Cretaceous (not shown).

With this proposed tectonic setting in mind (Figure 20.18I), the formation of the eastern Sichuan fold-and-thrust belt could have been the result of combined thermal weakening due to subduction of the Pacific plate beneath eastern Asia and the protracted and successive collisions of the South China block with the Qiangtang block, followed by the Lhasa block. That may explain why the eastern Sichuan thrust belt does not extend north of the Qinling suture zone.

Stage 11 (98–66 Ma): India was moving northward toward the Eurasian continent (Figure 20.18K). Eastern Asia experienced continued E–W extension that began in the late Jurassic and early Cretaceous. The extension has resulted in the development of numerous basins along the eastern margin of Asia. In contrast, Cretaceous basins in northwestern China resulted from compression related to collisional tectonics along the southern margin of the Eurasian continent (Hendrix et al., 1992).

Stage 12 (66–52 Ma): Collision between India and Asia began first in the west between 60 Ma and 50 Ma and progressively migrated to the east (Le Fort, Chapter 6, this volume) (Figure 20.18L). The ocean between India and Eurasia was completely closed by 45 Ma (Le Fort, Chapter 6, this volume). The Bohai Bay region received shallow-marine deposition in the early Tertiary (Gong, 1987).

Stage 13 (50–40 Ma): During the Paleogene, thrusts and folds began to develop in the Fenghuo Shan region of northern Tibet and southern Qaidam (Leeder et al., 1988; Qinghai BGM, 1989) and along the Indian Tethyan shelf (Ratschbacher et al., 1994). The formation of the former subsequently led to extrusion of the Indochina block eastward along the Red River fault (Figure 20.18M).

Stage 14 (40–20 Ma): The development of the Fenghuo Shan thrust belt may have lasted until the early Miocene, as indicated by continued deposition of coarse clastic rocks in the thrust-related basins (Qinghai BGM, 1989). That thrust belt would be located at the northern tip of the Indochina block if the left-lateral displacement along the Red River fault were restored.

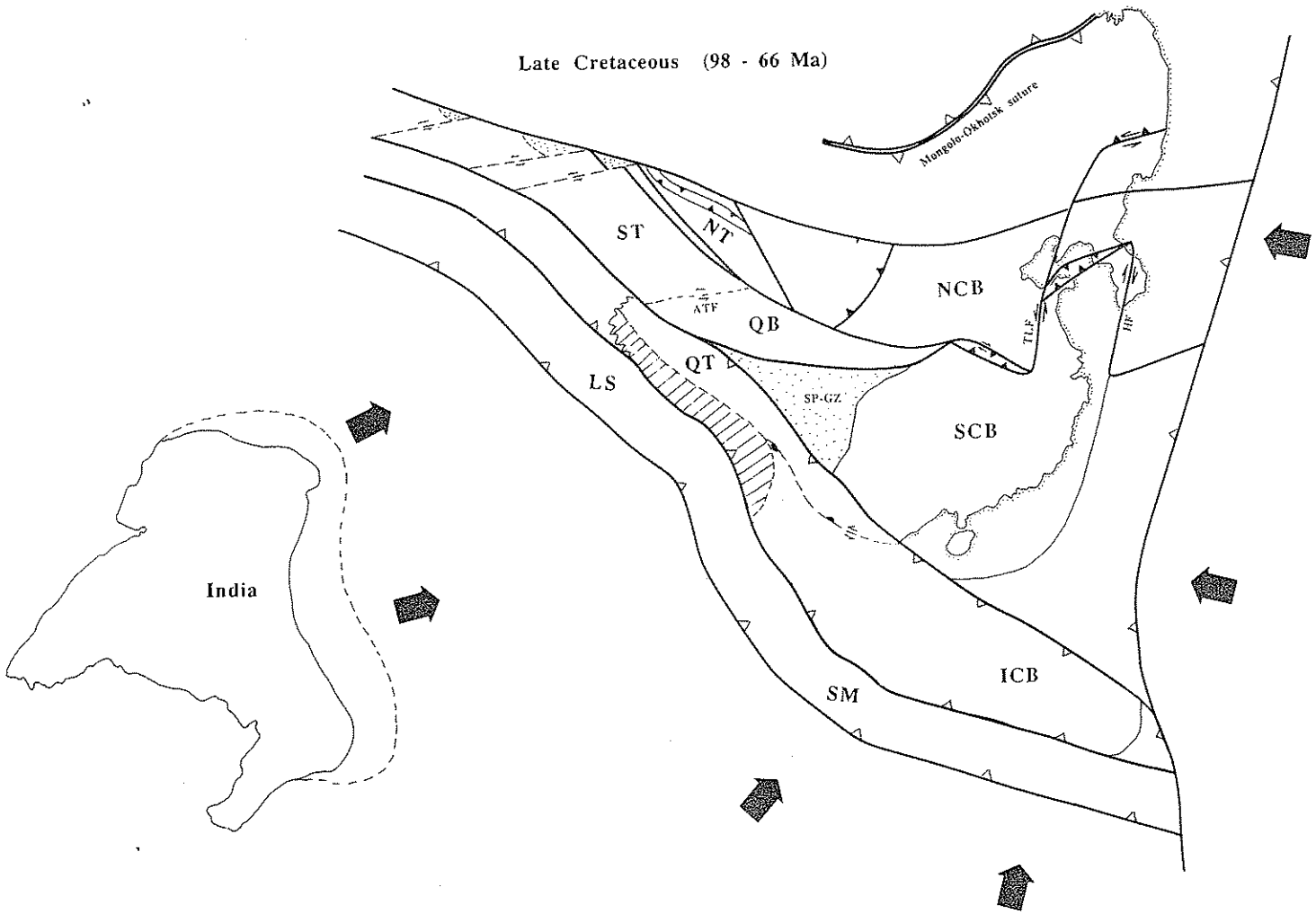

Figure 20.18 (K) Stage 11: late Cretaceous (98–66 Ma). India was moving northward toward the Eurasian continent. Eastern Asia experienced continued E–W extension that began in the early Cretaceous. The extension resulted in the development of numerous basins along the eastern margin of Asia. In contrast, Cretaceous basins in northwestern China were caused by compression related to collisional tectonics along the southern margin of the Eurasian continent (Hendrix et al., 1992).

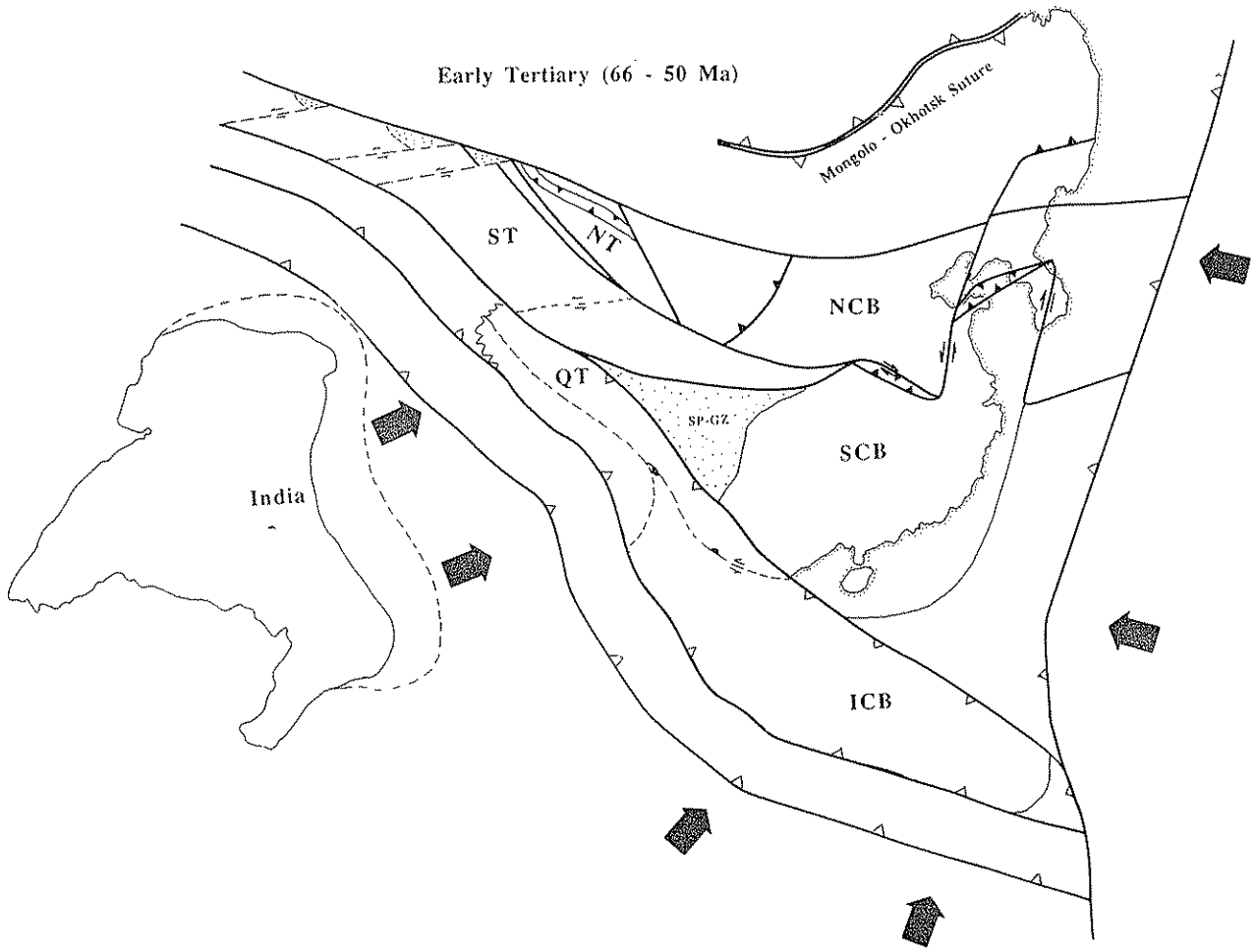

Figure 20.18 (L) Stage 12: early Tertiary (66–50 Ma). The collision between India and Asia began first in the west, between 60 Ma and 50 Ma, and progressively migrated to the east. The ocean between India and Eurasia was completely closed by 45 Ma. The Bohai Bay region received shallow-marine deposition in the early Tertiary (not shown) (Gong, 1987).

The left-slip history of the Red River fault occurred between 35 Ma and 17 Ma, broadly coeval with the development of the Fenghuo Shan thrust belt. We show the two features as kinematically related products of the early phase of the Indo–Asian collision (Figure 20.18N).

In the Himalaya and southern Tibet, the development of the Gangdese thrust system occurred first, between about 27 Ma and 23 Ma (Yin et al., 1994), followed by development of the Main Central Thrust and the Renbu–Zedong thrust at 20–18 Ma (Harrison et al., 1992; Yin et al., 1994) (Figure 20.18M). The Tethyan Himalayan thrust belt formed between 50 Ma and 18 Ma (Ratschbacher et al., 1994). Crustal thickening in the Himalaya and southern Tibet was associated with synchronous erosion. It was expressed by coeval rapid cooling in southern Tibet and rapid accumulation of a thick sedimentary pile in the Bengal Fan in the mid-Miocene (Graham et al., 1975; Curry, 1991; Harrison et al., 1992). Crustal thickening in southern Tibet was followed by E–W extension along N–S-trending normal-fault systems, which began at about 8 Ma (Yin et al., 1994; Harrison, McKegan, and Le Fort, in press-b). The E–W extension has been attributed to gravitational spreading of the Tibetan plateau when it reached its maximum elevation (Peltzer and Tapponnier, 1988; England and Houseman, 1988).

Stage 15 (20–10 Ma): Following an earlier suggestion by Yin et al. (1993), we propose that the Chaman fault, which began to develop in the mid-Miocene (Farah et al., 1984), cut through the Eurasian continent and carried a slice of its fragment to the north during the collision (Figure 20.18O). The Chaman fault may have been connected with the Altun Tagh fault through a restraining bend in the eastern Kunlun Shan. The Altun Tagh fault, in turn, transferred the left-slip farther north to the Qilian Shan thrust belt (= Nan Shan thrust belt) (Figure 20.18O). The Tien Shan fault system was initiated at about 20 Ma as a conjugate strike-slip system of the Altun Tagh fault. The central Tien Shan right-lateral strike-slip system is linked with various thrust systems (Figure 20.9). The interaction of the strike-slip and thrust systems produced numerous intermontane basins in the Tien Shan region, including the Turpan, Yili, and Boston basins, to name a few.

Stage 16 (10–0 Ma): The Altun Tagh fault was propagating

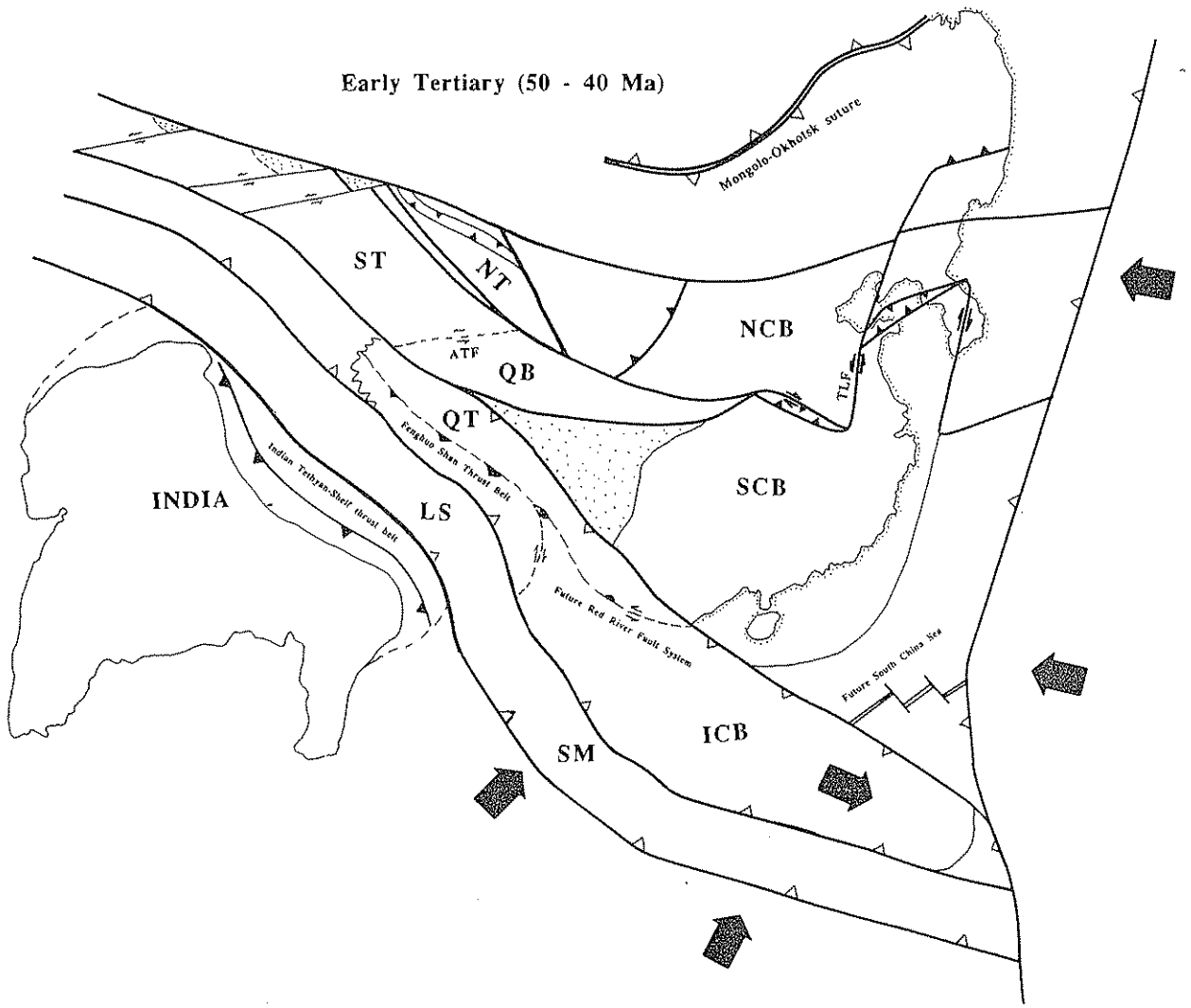

Figure 20.18 (M) Stage 13: late early Tertiary (50–40 Ma). Thrusts and folds began to develop during the Eocene in the Fenghuo Shan region of northern Tibet and southern Qaidam and along the Indian Tethyan shelf. The formation of the former subsequently led to extrusion of the Indochina block eastward along the Red River fault.

eastward along the strike and reached the Qaidam basin at about 6 Ma. The early Pliocene tectonic configuration Asia was similar to its present tectonic framework (Figure 20.16). The Red River fault rotated counterclockwise. As a result, the sense of slip reversed from left-slip to right-slip. The Karakoram–Jiali fault system began to develop to link the strike-slip faults with the N–S-trending normal faults in southern Tibet (Armijo, Tapponnier, and Han, 1989). Together, those structures have accommodated eastward extrusion of northern Tibet (Armijo et al., 1989).

Conclusions

The reconstruction presented here must be considered only preliminary, because the Cenozoic tectonics of Asia remain incompletely understood. Our poor understanding of Cenozoic tectonics is largely due to poor characterization of the geologic strain markers that formed during the Mesozoic and Paleozoic. Thus, future work should concentrate on both aspects and consider tectonic reconstructions of the Cenozoic and older tectonics in an iterative fashion, that is, using the older Paleozoic and Mesozoic geologic features to provide piercing points to quantify the Cenozoic strain. Conversely, understanding the nature of Cenozoic tectonics will provide a guide to formulate hypotheses for earlier reconstructions.

The existing geologic data from China and its neighboring regions suggest that the present configuration of eastern Asia has been strongly controlled by two major collisional events, one occurring in the early Mesozoic during the collision of North China and South China, and one in the Cenozoic during the collision of India and Asia. Both events produced large regions of crustal thickening, with the older deformation expressed by the exposure of ultra-high-pressure metamorphic rocks, and the

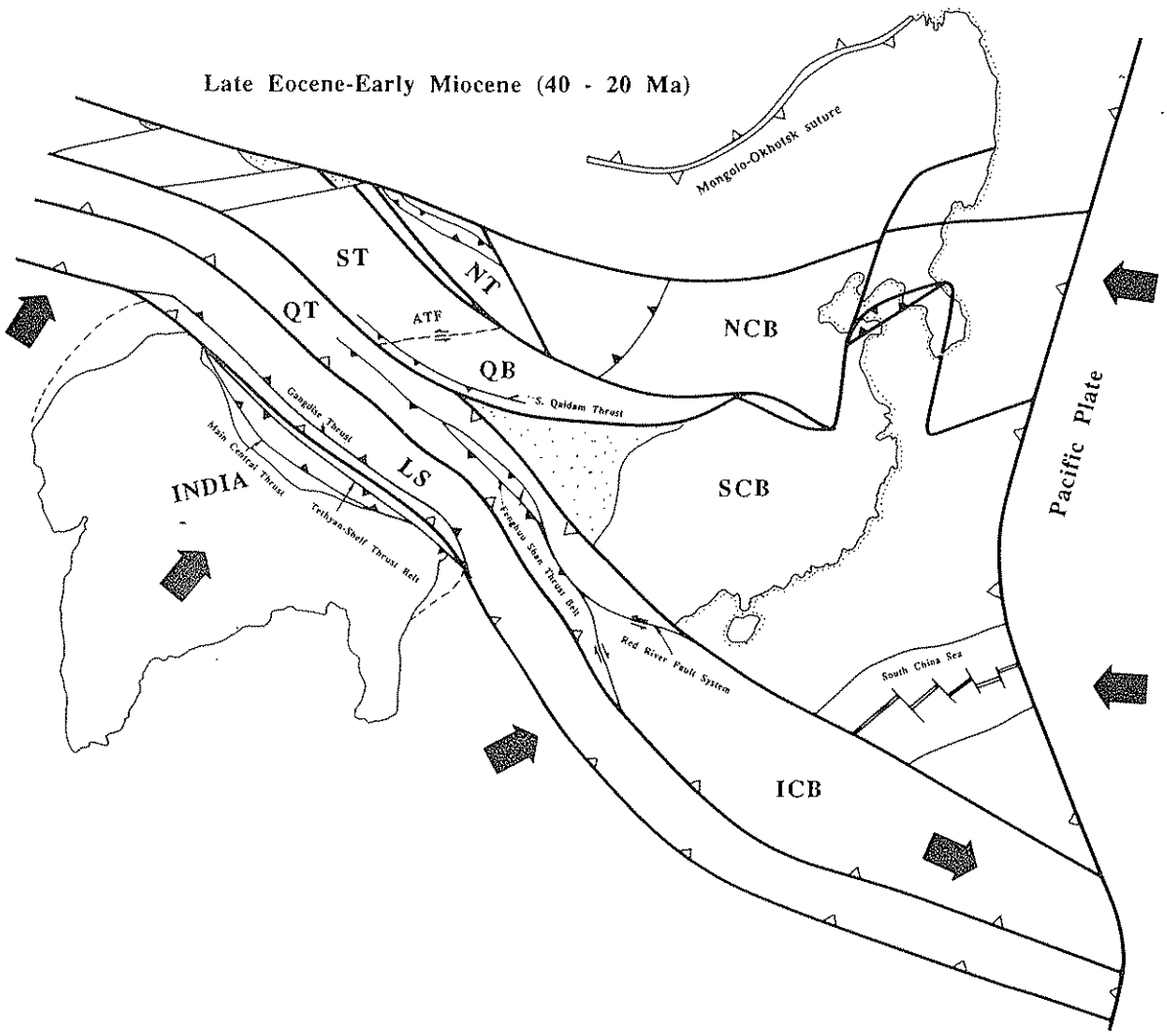

Figure 20.18 (N) Stage 14: late Eocene–early Miocene (40–20 Ma). The development of the Fenghuo Shan thrust belt led to lift-slip faulting along the Red River fault between 35 Ma and 17 Ma. Left-slip motion along the Red River fault, in turn, caused the opening of the South China Sea. In the Himalaya and southern Tibet, the development of the Gangdese thrust system occurred first between about 27 Ma and 23 Ma, followed by the development of the Main Central Thrust and the Renbu–Zedong thrust 20–18 Ma. The Tethyan Himalayan thrust belt appears to have developed between 50 Ma and 18 Ma. The crustal-thickening event in the Himalaya and southern Tibet was associated with erosion. It was expressed by coeval rapid cooling in southern Tibet and rapid accumulation of a thick sedimentary pile in the Bengal fan in the mid-Miocene.

younger deformation expressed by high mountain ranges and plateaus. Great magnitudes of strike-slip faulting were involved in both events, displacing magmatic arcs, suture zones, and older sedimentary facies for hundreds of kilometers.

The following summarizes significant events in the Phanerozoic development of China:

1. A collision between the North Tarim–North China block and the South Tarim–Qaidam block occurred during the Devonian, following early Paleozoic subduction of the South Tarim–Qaidam plate underneath the North Tarim–North China block.

2. The Permo–Triassic collision between the North Tarim–North China–Qaidam block and the South China block caused westward extrusion of the Qaidam block, which was located between the two at the time of initial collision.

3. The middle Paleozoic extrusion of the Qaidam block was accommodated by a left-slip fault system in the eastern Kunlun Shan–Qinling region, along its southern margin, and by a right-slip fault system in the Qilian Shan region, along its northern margin.

4. The middle Paleozoic suture system between the North Tarim–North China and South Tarim–Qaidam has been offset by the late Cenozoic Altun Tagh fault for about 500 km left-laterally.

5. Two regional uplift events in North China in the Ordovician and late Carboniferous were caused by heating from below, related to subduction of the Qaidam and South China plates

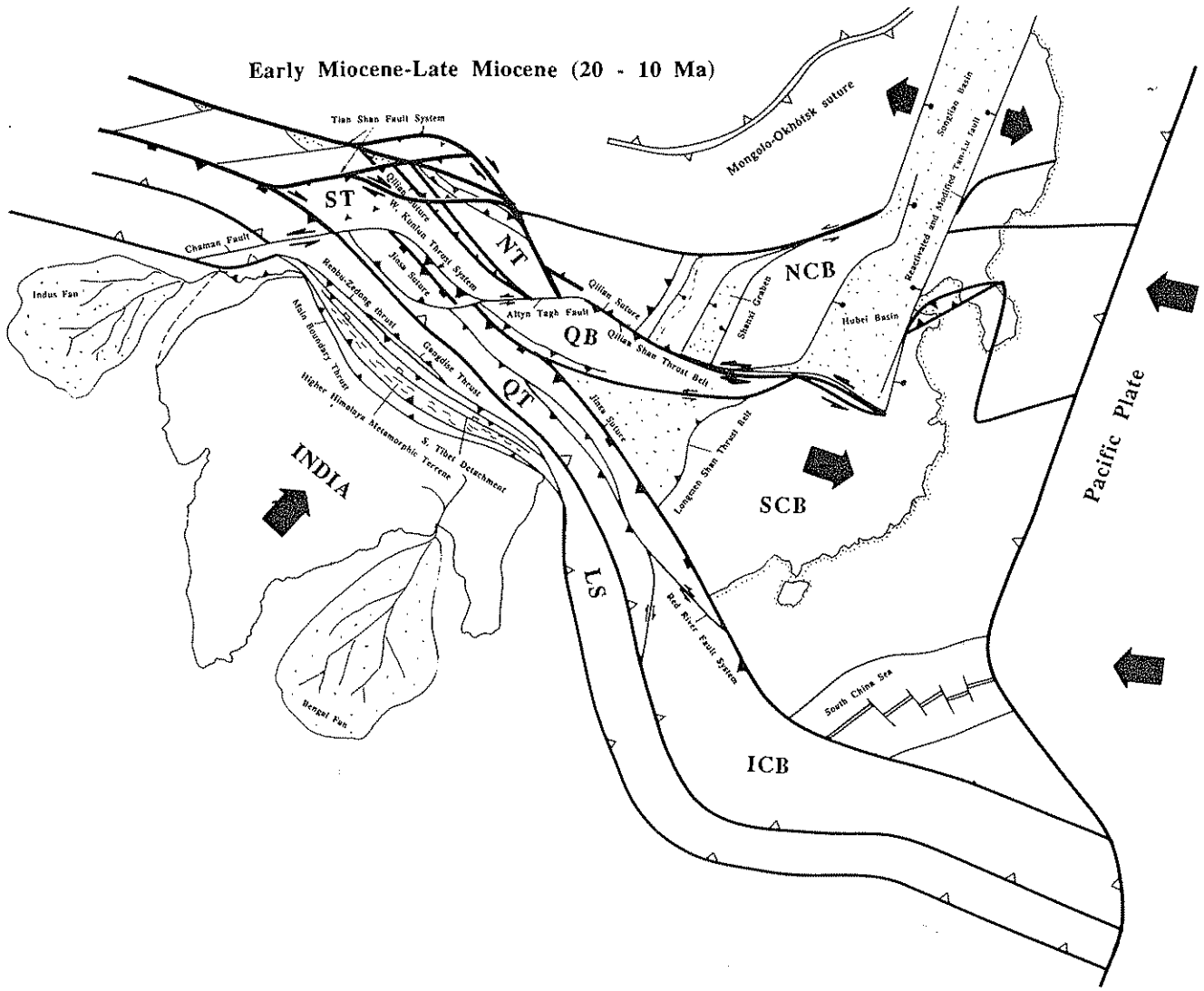

Figure 20.18 (O) Stage 15: early Miocene–late Miocene (20–10 Ma). In central Asia, the Chaman fault system began to develop, cutting into the Eurasian continent and carrying a slice of its fragment to the north during the collision. The Chaman fault connected with the Altun Tagh fault through a restraining band in the eastern Kunlun Shan, Karakoram, and Pamir regions. The Altun Tagh fault, in turn, transferred the left-slip farther north to the Qilian Shan thrust belt (i.e., Nan Shan thrust belt) region. The Tien Shan fault system was initiated at about 20 Ma as a conjugate strike-slip system of the Altun Tagh fault. The central Tien Shan right-lateral strike-slip system was linked with several thrust systems. That complex interaction of strike-slip and thrust faults produced the intermontane basins, such as the Turpan, Boston, aud Yili basins in central Asia.

beneath the North China block, from the south, and subduction of an oceanic plate below the North China block, from the north, respectively.

6. The available geochronologic constraints suggest that Cenozoic deformation in Asia did not progress uniformly from south to north. Instead, the northern edge of the Tibetan plateau and the southern margin of the Qaidam basin were first affected by crustal thickening in the late Paleogene and early Eocene, which could have been related to the coeval or subsequent eastward extrusion and/or rotation of the Indochina block between 35 Ma and 17 Ma in the Oligocene and Miocene. Deformation then shifted southward to southern Tibet and the Himalaya in the late Oligocene, at about 27 Ma, and lasted until about 20 Ma. Crustal thickening in southern Tibet was replaced by E–W extension initiated at about 20–18 Ma and peaking at about 8 Ma. Simultaneously, development of the Chaman–Altun Tagh–Tien Shan system led to enlargement of the Tibetan plateau to the north and formation of large intracontinental basins, such as the Tarim, Junggar, Turpan, and Qaidam.

Acknowledgments

Our research in eastern Asia has been supported by the U.S. National Science Foundation and the Chinese Natural Sciences Foundation. Mark Harrison and Marty Grove are particularly thanked for their help in preparing, analyzing, and interpreting

the $^{40}Ar/^{39}Ar$ data presented in this study. A critical review by Mark Harrison significantly improved the manuscript. We are very grateful to Dr. Catherine Flack for her continuing encouragement during preparation of this manuscript. We thank Peter Rumelhart for stimulating discussions, a critical review of the manuscript, and aid in drafting some of the figures. Constructive reviews by Steve Graham and Ray Ingersoll are greatly appreciated. Steve Graham shared many ideas with us on Asian tectonics and provided preprints of his work that helped in writing this chapter. We are especially thankful to Professor Wang Xiao-Feng and Mr. Zhang Qing from the Institute of Geomechanics, Chinese Academy of Geological Sciences, administered by the Chinese Ministry of Geology, for providing $^{40}Ar/^{39}Ar$ samples from the southern Anhui region. We also thank them for guiding us in the field in eastern China and offering insightful interpretations of the Tan Lu fault system.

References

Allègre, C. J., et al. 1984. Structure and evolution of the Himalaya–Tibet orogenic belt. *Nature* 307:17–22.

Allen, C. R., Gillespie, A., Han, Y., Sieh, K. E., Zhang, B., and Zhu, C. 1984. Red River and associated faults, Yunnan Province, China: Quaternary geology, slip rates and seismic hazard. *Geol. Soc. Am. Bull.* 95:686–700.

Allen, M. B., Şengör, A. M. C., and Natal'in, B. A. 1994. Junggar, Turfan and Alakol basins as late Permian to ?Early Triassic extensional structures in a sinistral shear zone in the Altaid orogenic collage, central Asia. *J. Geol. Soc. London* 150:1–11.

Altun Tagh Working Group. 1992. *Altun Tagh Active Fault Zone* in Chinese, with English abstract. Beijing: Seismological Publishing House.

Ames, L. 1994. Geochronology and geochemistry of ultrahigh-pressure metamorphism with implications for collision of the Sino–Korean and Yangtze cratons, central China *EOS, Trans. Am. Geophys. Union* 75:691.

Ames, L., Tilton, G. R., and Zhou, G. Z. 1993. Timing of collision of the Sino–Korean and Yangtse cratons: U-Pb zircon dating of coesite-bearing eclogites. *Geology* 21: 339–42.

Anhui BGM (Anhui Bureau of Geology and Mineral Resources). 1987. *Regional Geology of Anhui Province* (in Chinese, with English summary). Beijing: Geological Publishing House.

Armijo, R., Tapponnier, P., and Han, T. 1989. Late Cenozoic right-lateral strike-slip faulting in southern Tibet, *J. Geophys. Res.* 94:2787–838.

Arnaud, N. O., Vidal, P., Tapponnier, P., Mate, P., and Deng, W. M. 1992. The high K_2O volcanism of northwestern Tibet: geochemistry and tectonic implications. *Earth Planet. Sci. Lett.* 111:351–67.

Avouac, J.-P., and Peltzer, G. 1993. Active tectonics in southern Xinjiang, China: analysis of terrace rises and normal fault scarp degradation along the Hotan–Qira fault system. *J. Geophys. Res.* 98:21,773–807.

Bird, P. 1991. Lateral extrusion of lower crust from under high topography, in the isostatic limit. *J. Geophys. Res.* 96:10,275–86.

Bond, G. C., Nickerson, P. A., and Kominz, M. A. 1984. Breakup of a supercontinent between 625–555 Ma: new evidence and implications for continental histories. *Earth Planet. Sci. Lett.* 70:325–45.

Briais, A. E., Patriat, P., and Tapponnier, P. 1993. Updated interpretation of magnetic anomalies and sea-floor spreading stages in the South China Sea: implications for the Tertiary tectonics of SE Asia. *J. Geophys. Res.* 98:6299–328.

Burchfiel, B. C., Chen, Z., Hodges, K. V., Liu, Y., Royden, L. H., Deng, C., and Xu, J. 1992. The South Tibetan Detachment System, Himalayan orogen: extension contemporaneous with and parallel to shortening in a collisional mountain belt. *Geol. Soc. Am. Special Papers* 269:1–41.

Burchfiel, B. C., Deng, Q., Molnar, P., Royden, L. H., Wang, Y., Zhang, P., and Zhang, W. 1989. Intracrustal detachment with zones of continental deformation. *Geology* 17:748–52.

Burchfiel, B. C., Molnar, P., Deng, Q., Wu, Z., Feng, X., Li, J., and You, H. 1994. Latest Cenozoic rates of shortening across the margins of Tian Shan, Xinjiang, China. *Geol. Soc. Am. Abstr. Prog.* 26:462.

Burchfiel, B. C., and Royden, L. H. 1991. Tectonics of Asia 50 years after the death of Emile Argand. *Eclogae Geol. Helv.* 84:599–629.

Burchfiel, B. C., et al. 1991. Geology of the Haiyuan fault zone, Ningxia–Hui Autonomous Region, China, and its relation to the evolution of the northeastern margin of the Tibetan Plateau. *Tectonics* 6:1091–110.

Burg, J. P. (ed.) 1983. *Carte geologique du sud du Tibet, scale 1 : 500,000.* Paris: CNRS.

Burtman, V. S. 1975. Structural geology of the Variscan Tien Shan, USSR. *Am. J. Sci.* 272A:157–86.

Burtman, V. S., and Molnar, P. 1993. Geological and geophysical evidence for deep subduction of continental crust beneath the Pamir. *Geol. Soc. Am. Special Papers* 281:1–76.

Carroll, A. R., Graham, S. A., Hendrix, M. A., Yang, D., and Zhou, D. 1995. Late Paleozoic tectonic amalgamation of northwestern China: sedimentary record of the northern Tarim, northwestern Turpan, and southern Junggar basins. *Bull. Geol. Soc. Am.* 107:571–94.

Carroll, A. R., Liang, Y., Graham, S. A., Xiao, X., Hendrix, M. S., Chu, J., and McKnight, C. L. 1990. Junggar basin, northwest China: trapped late Paleozoic ocean. *Tectonophysics* 181:1–14.

Chang, C., et al. 1986. Preliminary conclusions of the Royal Society–Academia Sinica 1985 geotraverse of Tibet. *Nature* 323:501–7.

Chen, W. J., Harrison, T. M., Heizler, M. T., Liu, T. X., Ma, B. L., and Li, J. L. 1992. The tectonic history of mélange zone in north Jiangsu–South Shandong region: evidence from multiple diffusion domain $^{40}Ar/^{39}Ar$ thermal geochronology. *Acta Petrol. Sinica* 8:1–17.

Chen, W. J., Li, Q., Li, D., and Wang, X. 1988. Geochronological implications of K/Ar isotope system of fault gouge – a preliminary study. *Phys. Chem. Earth* 17:17–23.

Chen, Z. (ed.) 1985. *1 : 2000000 Geologic Map of Xinjiang Uygur Autonomous Region, China.* Beijing: Geological Publishing House.

Chen, Y. Q. 1989. *Geologic Map of China at a scale of 1 : 5000000.* Beijing: Geological Publishing House.

Choi, D. K. 1994. Late Cambrian to Tremadocian trilobite faunal successions of the Josen Supergroup in the Yeongweol area and their paleobiogeographic implications. In *IGCP 321 – Gondwana Dispersion and Asian Accretion.* Fourth international symposium and field excursion, Seoul, p. 18. Seoul National University.

Choo, S. H., and Chi, S. J. 1990. A study of Rb-Sr age determination on the Kwangju granite. *Korean Inst. Energy and Res. Reports* 90-1B2:3–54.

Choo, S. H., and Kim, S. J. 1986. A study of Rb-Sr age determinations in the Ryeongnam massif (I): Ryeonghae, Buncheon and Kimcheon granite gneisses and gneissose granites in the south-western Jirisan region. *Korean Inst. Energy and Res. Reports* 86–7:7–29.

Cluzel, D., Cadet, J.-P., and Lapierre, H. 1990. Geodynamics of the Ogcheon belt (South Korea). *Tectonophysics* 193:41–56.

Cobbold, P. R., and Davey, P. 1988. Indentation tectonics in nature and experiments. 2. Central Asia. *Bull. Geol. Inst. Univ. Uppsala* 14:143–62.

Copeland, P., Harrison, T. M., and Le Fort, P. 1990. Age and cooling history of the Manaslu granite: implications for Himalayan tectonics. *J. Volcanol. Geotherm. Res.* 96: 8475–500.

Coward, M. P., and Burtler, R. W. H. 1985. Thrust tectonics and the deep structures of the Pakistan Himalaya. *Geology* 13:417–20.

Coward, N. P., Kidd, W. S. F., Pan, Y., Shackleton, R. M., and Zhang, H. 1988. The structure of the 1985 Tibet Geotraverse, Lhasa to Golmud. *Phil. Trans. R. Soc. Lond.* A327:307–36.

Craig, P., Yin, A., and Nie, S. 1994. Reconstruction of Cenozoic depositional systems in the southern Tian Shan, NW China: implications for timing of deformation. *Geol. Soc. Am. Abstr. Prog.* 26:462.

Curry, J. R. 1991. Possible greenschist metamorphism at the base of a 22-km sediment section, Bay of Bengal. *Geology* 19:1097–100.

Dalziel, I. W. D. 1991. Pacific margins of Laurentia and East Antarctica–Australia as a conjugate rift pair: evidence and implications for an Eocambrian supercontinent. *Geology* 19:598–601.

Dewey, J. F., Shackleton, R. M., Chang, C., and Sun, Y. 1988. Tectonic evolution of the Tibetan plateau. *Phil. Trans. R. Soc. Lond.* A327:379–413.

England, P., and Houseman, G. 1988. The mechanics of the Tibetan plateau. *Phil. Trans. R. Soc. Lond.* A326:301–20.

England, P., and Molnar, P. 1990. Right-lateral shear and rotation as the explanation for strike-slip faulting in eastern Tibet. *Nature* 344:140–2.

Enkin, R. J., Yang, Z. Y., Chen, Y., and Courtillot, V. 1992. Paleomagnetic constraints on the geodynamic history of China from the Permian to the present. *J. Geophys. Res.* 97:13953–89.

Ernst, W. G. (ed.) 1988. *Metamorphic and Tectonic Evolution of the Western Cordillera, Conterminous United States.* Englewood Cliffs, NJ: Prentice-Hall.

Ernst, W. G., Cao, R. L., Jiang, J. Y. 1988. Reconnaissance study of Precambrian metamorphic rocks, northeastern Sino–Korean shield, People's Republic of China. *Geol. Soc. Am. Bull.* 100:692–701.

Farah, A., Ghazanfar, A., DeJong, K. S., and Lawrence, R. 1984. Evolution of the lithosphere in Pakistan. *Tectonophysics* 105:207–27.

Gansser, A. 1964. *The Geology of the Himalayas.* New York: Wiley-Interscience.

Gansu BGM (Gansu Bureau of Geology and Mineral Resources). 1989. *Regional Geology of Gansu Province* (in Chinese, with English summary). Beijing: Geological Publishing House.

Gong, Z. S. (ed.) 1987. *Oil- and Gas-bearing Areas on the Continental Shelf and Its Neighboring Regions. Petroleum Geology of China,* vol. 16. Beijing: Petroleum Industry Publishing House.

Graham, S. A., Brassell, S., Carroll, A. R., Xian, X., Demaison, G., McKnight, C. L., Liang, Y., Chu, J., and Hendrix, M. A. 1991. Characteristics of selected petroleum source rocks, Xinjiang Uygur Autonomous Region, northwest China. *Am. Assoc. Pet. Geol. Bull.* 74:493–512.

Graham, S. A., Dickinson, W. R., and Ingersoll, R. V. 1975. Himalayan–Bengal model for flysch dispersal in Appalachian–Ouachita system. *Geol. Soc. Am. Bull.* 86:273–86.

Hallam, A. 1992. *Phanerozoic Sea-Level Changes.* New York: Columbia University Press.

Hao, Y. C. (ed.) 1983. *The Cretaceous System of China. The Stratigraphy of China,* vol. 12. Beijing: Geological Publishing House.

Harland, W. B., Armstrong, R. L., Cox, A. V., Craig, L. E., and Smith, A. 1990. *Geologic Time Scale.* Cambridge University Press.

Harrison, T. M., Copeland, P., Kidd, W. S. F., and Yin, A. 1992. Raising Tibet. *Science* 255:1663–70.

Harrison, T. M., Copeland, P., Pan, Y., Kidd, W. S. F., and Lovera, O. in press-a. The Nyainquentanghla shear zone: implications for Tibetan plateau uplift and onset of the Asian monsoon. *Tectonics*

Harrison, T. M., McKegan, K., and Le Fort, P. in press-b. Detection of inherited monazite in the Manaslu leucogranite by $^{208}Pb/^{232}Th$ ion microprobe dating: crystallization age and tectonic implications. *Earth Planet. Sci. Lett.*

Hebe; BGM (Hebei Bureau of Geology and Mineral Resources). 1989. *Regional Geology of Hebei Province* (in Chinese, with English summary). Beijing: Geological Publishing House.

Henan BGM (Henan Bureau of Geology and Mineral Resources). 1989. *Regional Geology of Henan Province* (in Chinese, with English summary). Beijing: Geological Publishing House.

Hendrix, M. A., Dumitra, T. A., and Graham, S. A. 1994. Late Oligocene–early Miocene unroofing in the Chinese Tian Shan: An early effect of the India–Asia collision. *Geology* 22:487–90.

Hsü, K. J. 1988. Relict back-arc basins: principles of recognition and possible new examples from China. In *New Perspective in Basin Analysis*, ed. K. L., Kleinspehn and C. Paola, pp. 345–63. Berlin: Springer-Verlag.

Hsü, K. J., Li, J., Chen, H., Wang, Q., Sun, S., and Şengör, A. M. C. 1990. Tectonics of south China: key to understanding West Pacific. *Tectonophysics* 183:9–39.

Hsü, K. J., Wang, Q., Li, J., Zhou, D., and Sun, S. 1987. Tectonic evolution of Qinling Mountains, China. *Eclogae Geol. Helv.* 80:735–52.

Huang, T. K., Jen, C. S., Jiang, C. F., Chang, C. M., and Chin, Z. Q. 1980. *The Geologic Evolution of China.* Beijing: Publishing House of Geology.

Huang, T. K., Jen, C. S., Jian, C. F., Chang, C. M., and Xu, Z. Q. 1977. An outline of the tectonic characteristics of China. *Acta Geol. Sinica* 1:36–52.

Hubbard, M. S., and Harrison, T. M. 1989. $^{40}Ar/^{39}Ar$ constraints on deformation and metamorphism in the MVT zone and Tibetan slab, eastern Nepal Himalaya. *Tectonics* 8:865–80.

Ingersoll, R. V., Graham, S. A., and Dickinson, W. R. 1995. Remnant ocean basins. In *Tectonics of Sedimentary Basins,* ed. C. J. Busby and R. V. Ingersoll, pp. 1–51. London: Blackwell.

Ji, X., and Coney, P. J. 1985. Accreted terranes of China. In *Tectonostratigraphic Terranes of the Circum-Pacific Region,* ed. D. F. Howell, pp. 349–62. Houston: Circum-Pacific Council for Energy and Mineral Resources.

Ji, F. J., and Fang, Z. J. 1987. Regional tectonic framework of the Tan-Lu fault. In *The Tan-Lu Fault,* ed.H.-X. Jiang, pp. 12–22. Beijing: Seimological Publishing Company.

Jia, C., Yao, H., Wi, G., and Li, L. 1991. Plate tectonic evolution and characteristics of major tectonic units of the Tarim basin. In *The Tarim Basin,* ed. X. Tong and D. Liang, pp. 207–55. Urumugi: Xinjiang Scientific Publishing House.

Jiangsu BMG (Jiangsu Bureau of Geology and Mineral Resources). 1984. *Regional Geology of Jiangsu Province* (in Chinese, with English summary). Beijing: Geological Publishing House.

Khain, V. E. 1993. *Geology of Northern Eurasia.* Berlin: Gebruder Borntraeger.

Kim, Y. J., Park, Y. S., and Kang, S. W. 1994. The study of geochronology and petrogenesis of foliated granites in the Honam shear zone, South Korea. *Econ. Environ. Geol.* 27:247–61.

Klimetz, M. P. 1983. Speculations on the Mesozoic plate tectonic evolution of eastern China. *Tectonics* 2:139–66.

Kobayashi, T. 1966. Stratigraphy of the Chosen Group in Korea and South Manchuria and its relations to the Cambro–Ordovician formations of other areas. *J. Fac. Sci. Univ. Tokyo* 6:381–535.

Kröner, A., Zhang, G. W., and Sun, Y. 1993. Granulites in the the Tongbai area, Qinling belt, China: geochemistry, petrology, single zircon geochronology, and implications for the tectonic evolution of eastern Asia. *Tectonics* 12:245–55.

Lacassin, R., Leloup, P. H., and Tapponnier, P. 1993. Bounds on strain in large Tertiary shear zones of SE Asia from boundinage restoration. *J. Struct. Geol.* 15:677–92.

Lan, C. Y., Lee, T., Zhou, X. H., and Kwon, S. T. 1995. Archean basement under South China? Nd isotopic evidence from South Korea. *Geology* 23:249–52.

Lee, D. S. 1987. *Geology of Korea.* Seoul: Kyohak-Sa Publishing Co.

Lee, S. R., Cho, M. S., and Kwon, S. T. 1994. Tectonometamorphic evolution of the Chuncheon amphibolite, central Gyeonggi Massif, Korea. *EOS, Trans. Am. Geophys. Union* 75:99.

Leeder, M. R., Smith, A. B., and Yin, J. 1988. Sedimentology, paleoecology and paleoenvironmental evolution of the 1985 Lhasa to Golmud Geotraverse. *Phil. Trans. R. Soc. Lond.* A327:107–43.

Leloup, P. H., Harrison, T. M., Ryerson, F. J., Wenji, C., Qi, L., Tapponnier, P., and Lacassin, R. 1993. Structural, petrological and termal evolution of a Tertiary ductile strike-slip shear zone, Diancan Shan (Yunnan, PRC). *J. Geophys. Res.* 98:6715–43.

Li, C. Y. 1975. Analysis of regional tectonic development of China in the framework of plate tectonics. *Acta Geophys. Sinica* 18:52–76.

Li, C. Y. Liu, Y., Zhu, B. C., Feng, Y. M., and Wu, H. C. 1978. Structural evolution of Qinling and Qilian Shan. In *Scientific Papers on Geology and International Exchange,* pp. 174–97. Beijing: Publishing House of Geology.

Li, S. G., Hart, S. R., Zheng, S. G., Liu, D. L., Zhang, G. W., and Guo, A. L. 1989. Timing of collision between the North and South China Blocks – The Sm-Nd isotopic age evidence. *Acta Sci. Sinica Ser. B* 32:1393–400.

Li, S. G., Xiao, Y., Liou, D., Chen, Y., Ge, N., Zhang, Z., Sun, S. S., Cong, B., Zhang, R., Hart, S., and Wang, S. 1993. Collision of the North China and Yangtze blocks and formation of coesite-bearing ecologites: timing and processes. *Geochem. Geol.* 109:89–111.

Liaoning BGM (Liaoning Bureau of Geology and Mineral Resources). 1989. *Geologic Map of Liaoning Province, P.R.C., at a scale of 1 : 400000.* Beijing: Geological Publishing House.

Lin, J. L., and Fuller, M. 1990. Paleomagnetism, north China and south China collision, and the Tan-Lu fault. In *Allochthonous Terranes,* ed. J. F. Dewey, I. G. Gas, G. B. Gass, N. B. W. Harris, and A. M. C. Şengör, pp. 133–42. Cambridge University Press.

Lin, J. L., Fuller, M., and Zhang, W. Y. 1985. Preliminary Phanerozoic polar wander paths for the North and South China Blocks. *Nature* 313:444–9.

Liu, D. Y., Nutman, A. P., Compton, W., Wu, J. S., and Shen, Q. H. 1992. Remnants of >3800 Ma crust in the Chinese part of the Sino–Korean craton. *Geology* 20:339–42.

Liu, H. Y. 1991. Tectonic, paleogeographic and sedimentary evolution of late Precambrian in China (in Chinese, with English abstract). *Sci. Geol. Sinica* 1991: 309–16.

Liu, X. H., and Hao, J. 1989. Structure and tectonic evolution of the Tongbai–Dabie range in the eastern Qinling collisional belt, China. *Tectonics* 8:639–45.

Liu, Z. Q. (ed.) 1988. *Geologic Map of Qinghai–Xizang Plateau and Its Neighboring Regions scale 1: 500000* (in Chinese). Beijing: Geological Publishing House.

Lovera, O. M., Richter, F. M., and Harrison, T. M. 1989. $^{40}Ar/^{39}Ar$ geothermometry for slowly cooled samples having a distribution of diffusion domain sizes. *J. Geophys. Res.* 94:17917–35.

Lovera, O. M., Richter, F. M., and Harrison, T. M. 1991. Diffusion domains determined by ^{39}Ar release during step heating. *J. Geophys. Res.* 96:2057–69.

Lyon-Caen, H., and Molnar, P. 1983. Constraints on the structure of the Himalaya from an analysis of gravity anomalies and a flexural model of the lithosphere. *J. Geophys. Res.* 88:8171–91.

Lyon-Caen, H., and Molnar, P. 1985. Gravity anomalies, flexure of the Indian plate, and the structure, support and evolution of the Himalaya and Ganga Basin. *Tectonics* 4:513–38.

Ma, X. Y. 1986, *Geodynamic Map of China at scale of 1 : 4000000.* Beijing: Geological Publishing House.

McElhinny, M. W., Embleton, B. J., Ma, X. H., and Zhang, Z. K. 1981. Fragmentation of Asia in the Permian. *Nature* 293:212–16.

McKnight, C. L., and Graham, S. A. 1994. Compressional episodes, structural styles, and shortening estimates, southern Tian Shan foreland, NW China. *Geol. Soc. Am. Abstr. Prog.* 26:463.

Mattauer, M., Matte, P., Malavieille, J., Tapponnier, P., Maluski, H., Xu, Z. Q., Lu, Y. L., and Tang, Y. Q. 1985. Tectonics of the Qinling belt: build-up and evolution of eastern Asia. *Nature* 317:496–500.

Mattauer, M., Matte, P., Maluski, H., Xu, Z., Zhang, Q. W., and Qiang, Y. M. 1991. Paleozoic and Triassic plate boundary between North and South China; new structural and radiometric data on the Dabie Shan (eastern China), *C. R. Acad. Sci., Ser. II* 312:1227–33.

Metcalfe, I. 1983. Southeast Asia. In *The Carboniferous of the World, vol. 1,* ed. P. H. Wagner, C. F. Winkler Prins, and L. F. Granados, pp. 213–43. IUGS publication no. 16.

Metcalfe, I. 1988. Origin and assemblage of south-east Asian continental terranes. In *Gondwana and Tethys*, ed. M. G. Audley-Charles and A. Hallam, pp. 101–18. Geological Society of America special publication no. 37.

Molnar, P., Burchfiel, B. C., Zhao, Z. Y., Lian, K., Wang, S., and Huang, M. 1987. Geologic evolution of northern Tibet: results of an expedition to Ulugh Muztagh. *Science* 234:299–305.

Molnar, P., England, P., and Maritinod, J. 1993. Mantle dynamics, uplift of the Tibetan plateau, and the Indian monsoon. *Rev. Geophys.* 31:357–96.

Molnar, P., and Tapponnier, P. 1975. Cenozoic tectonics of Asia: effects of a continental collision. *Science* 189:419–26.

Molnar, P., et al. 1994. Quaternary climate change and the formation of river terraces across growing anticlines on the north flank of the Tien Shan, China. *J. Geol.* 102:583–602.

Moors, E. M. 1991. Southwest U.S.–East Antarctica (SWEAT) connection: a hypothesis. *Geology* 19:425–8.

Nie, S. Y. 1991. Paleoclimatic and Paleomagnetic constraints on the paleozoic reconstruction of south China, north China and Tarim. *Tectonophysics* 196:279–308.

Nie, S., and Rowley, D. 1994. Comment of "Paleomagnetic constraints on the geodynamic history of the major blocks of China from the Permian to the present" by Enkins et al. *J. Geophys. Res.* 99:18035–42.

Nie, S. Y., Rowley, D. B., and Ziegler, A. M. 1990. Constraints on the locations of Asian microcontinents in Paleo-Tethys during the late Paleozoic. In *Paleozoic Paleogeography and Biogeography*, ed. W. S. McKerrow and C R. Scotese, pp. 397–408. Memoirs of the Geological Society of London, no. 12.

Nie, S., Yin, A., Craig, P., Yang, G., and Qian, X. 1994a. Tertiary structural evolution of the Kuche thrust system in the southern Tian Shan region. *Geol. Soc Am. Abstr. Prog.* 26:462.

Nie, S., Yin, A., Rowley, D. B., and Jin, Y. 1994b. Exhumation of the Dabie Shan ultrahigh-pressure rocks and accumulation of the Songpan–Ganzi flysch sequence, central China. *Geology* 22:999–1002.

Ningxia BGM (Ningxia Bureau of Geology and Mineral Resources). 1989. *Regional Geology of Ningxia Hui Autonomous Region* (in Chinese, with English summary). Beijing: Geological Publishing House.

Okay, A. I., and Şengör, A. M. C. 1992. Evidence for intracontinental thrust-related exhumation of the ultrahigh-pressure rocks in China. *Geology* 20:411–14.

Okay, A. I., Şengör, A. M. C., and Satir, M. 1993. Tectonics of an ultrahigh-pressure metamorphic terrane: the Dabie Shan Tongbai Shan orogen, China. *Tectonics* 12:1320–34.

Peltzer, G., and Tapponnier, P. 1988. Formation and evolution of strike-slip faults, rifts, and basins during the India–Asia collision: an experimental approach. *J. Geophys. Res.* 93:15085–117.

Peltzer, G., Tapponnier, P., and Armijo, R. 1989. Magnitude of late Quaternary left-lateral displacements along the northern edge of Tibet. *Science* 246:1285–9.

Peltzer, G., Tapponnier, P., Zhang, Z., and Xu, Z. Q. 1985. Neogene and Quaternary faulting in and along the Qinling Shan. *Nature* 317:500–5.

Qinghai BGM (Qinghai Bureau of Geology and Mineral Resource). 1989. *Geologic History of the Qinghai Region* Beijing: Geological Publishing House.

Ratschbacher, L., Frisch, W., Liu, G., and Chen, C. S. 1994. Distributed deformation in southern and western Tibet during and after the the India–Asia collision. *J. Geophys. Res.* 99:19917–45.

Ree, J. H., Cho, M., Kwon, S. T., Chi, K. H., and Nakamura, E. 1994. The Imijingang belt in South Korea: a preliminary result. In *IGCP 321 – Gondwana Dispersion and Asian Accretion.* Fourth International Symposium and Field Excursion, Seoul, p. 103. Seoul National University.

Reedman, A. J., and Um, S. H. 1975. *Geology of Korea.* Seoul: Korean Institute of Energy and Resources.

Reischmann, T., Altenberger, U., Kröner, A., Zhang, G., Sun, Y., and Yu, Z. 1990. Mechanism and time of deformation and metamorphism of mylonitic orthogneisses from the Shagou shear zone, Qinling belt, China. *Tectonophysics* 185:91–109.

Scotese, C. R., and McKerrow, W. S. 1990. Revised world maps and introduction. In *Paleozoic Paleogeography and Biogeography*, ed. W. S. McKerrow and C. R. Scotese, pp. 1–12. Memoirs of the Geological Society of America, no. 12.

Şengör, A. M. C. 1985. East Asia tectonic collage. *Nature* 318:16–17.

Şengör, A. M. C. 1987. Tectonic subdivision and evolution of Asia. *Bull. Tech. Univ. Istanbul* 40:355–435.

Şengör, A. M. C., Altiuner, D., Cin, A., Ustaömer, T., and Hsü, K. J. 1988. Origin and assembly of the Tethyan orogenic collage at the expense of Gondwana Land. In *Gondwana and Tethys*, ed. M. G. Audley-Charles and A. Hallam. *Geol. Soc. Am. Special Papers* 37:119–81.

Şengör, A. M. C., Natal'in, B. A., and Burtman, B. S. 1993. Evolution of the Altaid tectonic collage and Paleozoic crustal growth in Eurasia. *Nature* 364:299–307.

Shaanxi BGM (Shaanxi Bureau of Geology and Mineral Resources). 1989. *Regional Geology of Shaanxi Province* (in Chinese, with English summary). Beijing: Geological Publishing House.

Shandong BGM (Shandong Bureau of Geology and Mineral Resources). 1989. *Regional Geology of Shandong Province* (in Chinese, with English summary). Beijing: Geological Publishing House.

Song, T., and Wang, X. 1993. Structural styles and stratigraphic patterns of syndepositional faults in a contractional setting: example from Quaidam basin, northwestern China. *Am. Assoc. Pet. Geol. Bull.* 77:102–17.

Sun, J. X., Chen, F. S., Wang, G. P., and Jin, Y. N. 1993. Correlation between the Subei–Jiaonan and Dabie blocks and horizontal displacement of the Tancheng–Lujiang fault zone. In *The Tancheng–Lujiang Wrench Fault System*, ed. J. W., Xu, pp. 97–104. New York: Wiley.

Sun, Z., Xie, Q., and Yang, J. 1989. Ordos basin – a typical example of an unstable cratonic interior superimposed basin. In *Chinese Sedimentary Basins*, ed. X. Zhu, pp. 63–75. New York: Elsevier.

Tang, T. F. (ed.) 1990. *Late Cretaceous–Early Tertiary Sedimentary Evolution of Tarim*, Beijing: Science Press.

Tan-Lu Fault Working Group. 1987. *The Tan-Lu Fault.* Beijing: Seismological Publishing Company.

Tapponnier, P., and Molnar, P. 1977. Active faulting and Cenozoic tectonics of China. *J. Geophys. Res.* 82:2905–30.

Tapponnier, P., and Molnar, P. 1979. Active faulting and Cenozoic tectonics of the Tien Shan, Mongolia and Baykal regions. *J. Geophys. Res.* 84:3425–59.

Tapponnier, P., Mattauer, M., Proust, F., and Cassaigneau, C. 1981. Mesozoic ophiolites, sutures, and large-scale tectonic movements in Afghanistan. *Earth Planet. Sci. Lett.* 52:355–71.

Tapponnier, P., Meyer, B., Avouac, J. P., Peltzer, G., Gaudemer, Y. S., Guo, H. X., Yin, K., Chen, Z., Cai, S., and Dai, H. 1990. Active thrusting and folding in the Qilian Shan, and decoupling between upper crust and mantle in northeastern Tibet. *Earth Planet. Sci. Lett.* 97:382–403.

Tapponnier, P., Peltzer, G., Le Dain, A. Y., Armijo, R., and Cobbold, P. 1982. Propagating extrusion tectonics in Asia. *Geology* 10:611–16.

Turner, S., Hawkesworth, C., Liu, J., Rogers, N., Kelley, S., and van Calsteren, P. 1993. Timing of Tibetan uplift constrained by analysis of volcanic rocks. *Nature* 364:50–4.

Wang, H. Z. (ed.) 1985. *Atlas of the Palaeogeography of China* (in Chinese and English). Beijing: Cartographic Publishing House.

Wang, H. Z., Xu, C. Y., and Zhou, Z. G. 1982. Tectonic development of the continental margins on both sides of the Qinling marine realm (in Chinese, with English abstract). *Acta. Geol. Sinica* 63:270–80.

Wang, X., Zhang, Q., Yin, A., and Nie, S. 1994. Evolution of the Tan-Lu fault system: implications for geologic development in its adjacent area, eastern China. *EOS, Trans. Am. Geophys. Union* 75:630.

Watson, M. P., Hayward, A. B., Parkinson, D. N., and Zhang, Z. M. 1987. Plate tectonic history, basin development and petroleum source rock deposition onshore China. *Marine Petrol. Geol.* 4:205–25.

Windley, B. F., Allen, M. B., Zhang, C., Zhao, Z. Y., and Wang, G. R. 1990. Paleozoic accretion and Cenozoic redeformation of the Chinese Tien Shan Range, central Asia. *Geology* 18:128–31.

Winston, D. 1986. Middle Proterozoic tectonics of the Belt basin, western Montana and northern Idaho. In *Belt Super Group: A Guide to Proterozoic Rocks of Western Montana and Adjacent Areas,* ed. S. M. Roberts, pp. 245–58. Montana Bureau of Mines and Geology Special Publication 94.

Xinjiang BGM (Xinjiang Bureau of Geology and Mineral Resources). 1993. *Regional Geology of Xinjiang Uiguer Autonomous Region* (in Chinese, with English summary). Beijing: Geological Publishing House.

Xu, J. W. 1993. Basic characteristics and tectonic evolution of the Tancheng–Lujiang fault zone. In *The Tancheng–Lujiang Wrench Fault System,* ed. J. W. Xu, pp. 17–50. New York: Wiley.

Xu, J. W., Ma, X. H., Tong, W., Zhu, G., and Lin, S. 1993. Displacement of the Tancheng–Lujiang wrench fault system and its geodynamic setting in the northwestern circum-Pacific. In *The Tancheng–Lujiang Wrench Fault System,* ed. J. W. Xu, pp. 51–73. New York: Wiley.

Xu, J. W., Zhu, G., Tong, W., Cui, K., and Liu, Q. 1987. Formation and evolution of the Tancheng–Lujiang wrench fault system: a major shear system to the northwest of the Pacific ocean. *Tectonophysics* 134:273–310.

Xu, Z. Q. 1985. General features of the Tangcheng–Lujiang rift system (in Chinese, with English abstract). *Collect. Struct. Geol.* 3:39–46.

Yan, L. 1991. Three important structural patterns in the Tarim basin: "Y"-shaped fault systems, hangingwall anticlines, and anticlines. In *The Tarim Basin,* ed. X. Tong and D. Liang, pp. 195–206. Urumuqi: Xinjiang Scientific Publishing House.

Yanai, S., Park, B. S., and Otah, S. 1985. The Honam shear zone (South Korea): deformation and tectonic implications in the Far East. *Sci. Papers College Arts Sci., Univ. Tokyo* 32:181–210.

Yang, Z. Y, Cheng, Y. Q., and Wang, H. Z. 1986. *The Geology of China.* Oxford: Clarendon Press.

Ye, C. H., and Huang, R. J. 1992. The Tertiary (in Chinese). In *Stratigraphy of Tarim,* pp. 308–63. Beijing: Science Press.

Yin, A., Harrison, T. M., Ryerson, F. J., Chen, W., Kidd, W. S. F., and Copeland, P. 1994. Tertiary structural evolution of the Gangdese thrust system, southeastern Tibet. *J. Geophys. Res.* 99:18175–201.

Yin, A., and Nie, S. Y. 1993. An indentation model for North and South China collision and the development of the Tan-Lu and Honam fault systems, eastern Asia. *Tectonics* 12:801–13.

Yin, A., Nie, S. Y., Fillipone, J. A., Harrison, T. M., Qian, X. L., and Li, M. S. 1993. A kinematic model for the Tertiary development of the Tian Shan, Altyn Tagh, and Chaman fault system in central Asia during the Indo–Asian collision. *Geol. Soc. Am. Abst. Prog.* 26:463.

Zai, G. M. (ed.) 1987. *Petroleum Geology of China,* 16 vols. Beijing: Petroleum Industry Publishing House.

Zhang, G. W., Yu, Z. P., Sun, Y., Cheng, S. Y., Li, T. H., Xue, F., and Zhang, C. L. 1989. The major suture zone of the Qinling orogenic belt. *J. Southeast Asian Earth Sci.* 3:63–7.

Zhang, P., et al. 1991. Amount and style of late Cenozoic deformation in the Liupan Shan area, Ningxia autonomous region, China. *Tectonics* 10:1111–29.

Zhang, Q., Wang, X., Yin, A., and Nie, S. 1994. The relationship between Zhangbaling ductile–brittle structure and the development of the Tan-Lu fault system, eastern China. *EOS Trans. Am. Geophys. Union* 75:630.

Zhang, Z. H., Liou, J. G., and Coleman, R. G. 1984. An outline of the plate tectonics of China. *Geol. Soc. Am. Bull.* 95:295–312.

Zhao, X., and Coe, R. S. 1987. Paleomagnetic constraints on the collision and rotation of North and South China. *Nature* 327:141–4.

Zhao, X. X., Coe, R., Zhou, Y., Wu, H., and Wang, J. 1990. New paleomagnetic results from northern China: collision and suturing with Siberia and Kazakhstan. *Tectonophysics* 181:43–81.

Zhao, Z. Y., and Zhu, S. D. 1980. Kuyak rift obliquely cross-cutting the Kunlun Shan. *Kexuetongbao* 24:1131–3.

Zheng, Y. D., Wang, S. Z., and Wang, Y. F. 1991. An enormous thrust nappe and extensional metamorphic core complex newly discovered in the Sino–Mongolian boundary area. *Science in China, Ser. B* 34:1145–52.

Zhou, Q., and Zheng, J. 1990. *Structural Analysis of the Tarim Region.* Beijing: Science Press.

Zhou, X. H. 1994. Geochemical constraints on tectonic evolution of South China. In *Isotopic Geochemistry of China,* ed. J. S. Yu, pp. 98–117. Beijing: Science Press.

Zhou, Z., and Chen, P. 1990. *Paleontology, Stratigraphy, and Geologic Evolution of the Tarim Basin.* Beijing: Science Publishing House.

Zonenshain, L. P., Kuz'min, M. I., and Natapov, L. M. 1990. *Geology of the USSR: A Plate-Tectonic Synthesis.* Washington, DC: American Geophysical Union.